Hungarian Academy of Sciences
KFKI Atomic Energy Research Institute

EXPERIMENTAL DATABASE OF E110 CLADDINGS UNDER ACCIDENT CONDITIONS

E. Perez-Feró, Cs. Győri, L. Matus, L. Vasáros, Z. Hózer, P. Windberg,
L. Maróti, M. Horváth, I. Nagy, A. Pintér-Csordás, T. Novotny

AEKI-FRL-2007-123-01/01

Budapest, November 2007

Project:	**COHYRA - Zr Cladding Oxidation In Hydrogen Rich Atmosphere**
Title:	**Experimental database of E110 claddings under accident conditions**
Authors:	E. Perez-Feró, Cs. Győri, L. Matus, L. Vasáros, Z. Hózer, P. Windberg, L. Maróti, M. Horváth, I. Nagy, A. Pintér-Csordás, T. Novotny
Type of the document:	**Database report**
Registry number:	**AEKI-FRL-2007-123-01/01**

Revision	Date	Signatures		
		Authors	Reviewed by	Approved by
0.	28.11.2007	E. Perez-Feró	Z. Hózer	I. Vidovszky
1.				
2.				
3.				

Revision Date	Short description of the revision
1.	
2.	
3.	

TABLE OF CONTENTS

1. INTRODUCTION

The zirconium-steam reaction under accident conditions results in the oxidation of the fuel cladding and hydrogen production as an accompaniment. The oxidation causes mechanical deterioration and embrittlement of the cladding. The formed hydrogen is partly absorbed by the Zr alloy and it contributes to the cladding brittleness, which can lead to the fragmentation of the fuel rods under thermal and mechanical loads.

Since the beginning of the 90s', several experimental series have been performed at the AEKI with Zr1%Nb (E110) and Zircaloy claddings. The aims of these experiments were to study and to compare the mechanical properties of the cladding materials in the temperature range of 20-1200 ^{o}C and to investigate the effect of oxidation and hydrogen uptake on the mechanical performance of the claddings. The objectives have been achieved through separate effect tests with well defined conditions.

Due to the Zr-steam reaction, in accidental conditions a hydrogen-rich steam atmosphere may evolve, as well. In 2004 a new experimental programme (COHYRA) started at the AEKI in order to investigate the combined effects of steam and H-contents on the mechanical properties of the VVER fuel cladding.

This report gives an overview of the experiments involved in the database, the test facilities and conditions. It presents the most important results and consequences.

2. CONTENTS OF THE DATABASE

The *Experimental Database of E110 Claddings under Accident Conditions* involves the data of oxidation and mechanical tests performed at the AEKI with E110 claddings, the results of post-test investigations, photos, figures, information concerning the test conditions and the corresponding English-language publications.

The experimental database contains the results of some tests performed at the AEKI (from 1994 to 2004) with Zircaloy-4 claddings, as well.

The involved separate effect tests were grouped as follows:

1. Cladding ballooning tests

- 7-rod bundle tests to investigate the hazard of coolant flow blockage
- isothermal burst tests with as-received and pre-oxidized Zr1%Nb tube specimens
- isothermal burst tests with as-received Zircaloy-4 tube specimens
- isothermal burst tests with Zr1%Nb tube specimens to investigate the effect of pressurization rate
- burst tests on pre-pressurized Zr1%Nb rods with linear temperature increase
- Isothermal burst tests with as-received and pre-oxidized Zr1%Nb tube specimens in argon atmosphere
- Isothermal burst tests with as-received Zr1%Nb tubes in argon-hydrogen atmosphere

2. Tensile tests

- tests with Zr1%Nb sheet specimens
- tests with Zr1%Nb tube specimens
- tests with Zircaly-4 sheet specimens
- tests with Zircaloy-4 tube specimens
- tests with pre-oxidized Zr1%Nb rings specimens

3. Oxidation tests

- one-side steam oxidation of Zr1%Nb tubes at 900 ^{o}C (Pre-oxidation for ballooning tests in 1995)
- double-side steam oxidation of Zr1%Nb rings at 900 – 1200 ^{o}C (PECO Project 1995)
- double-side steam oxidation of Zr1%Nb rings at 500 – 900 ^{o}C (IAEA CRP 1995)
- double-side steam oxidation of Zr1%Nb and Zircaloy-4 rings at 900-1200 ^{o}C (1997)
- double-side steam oxidation of Zr1%Nb rings at 800 – 1100 ^{o}C (2000)
- double-side steam oxidation of Zr1%Nb rings at 1010 ^{o}C (OMFB 1994)
- double-side oxidation of Zr1%Nb rings in hydrogen-steam mixture at 900 - 1100 ^{o}C (pre-oxidation for ring compression tests)
- double-side oxidation of Zr1%Nb rings in hydrogen-steam mixture at 900 - 1100 ^{o}C (pre-oxidation for ring tensile tests)
- one-side oxidation of Zr1%Nb tubes in hydrogen-steam mixture at 900 - 1100 ^{o}C (pre-oxidation for first test series ballooning tests)

4. Ring compression tests

- tests with Zr1%Nb tube specimens
- tests with Zircaloy-4 tube specimens
- tests with pre-oxidized Zr1%Nb rings specimens to study ductile-brittle transition

5. Post-test investigations

- visual observations
- metallographic analysis
- SEM analysis

3. BALLOONING TESTS

Cladding ballooning tests at the AEKI comprised both single rod and rod bundle experiments to evaluate the strength and deformation of the VVER fuel rods as well as the hazard of coolant flow blockage under LOCA conditions. The pressure histories and the residual deformations of more than 170 rods are available in the database.

3.1. 7-rod bundle tests

To investigate cladding tube deformation and flow blockage phenomenon in VVER bundle were the main objectives of the test. The experiments were performed in a domestic project supported by the National Committee for Technological Development (OMFB) [2].

3.1.1. Description of the tests

This test series was performed with short (150 mm) 7-rod bundles in order to investigate the possible flow blockage rate in a VVER core under LOCA conditions. The experimental facility contained a high temperature furnace with temperature control system, a steam generator with a super heater, a pre-pressurization system to set the initial pressure of the rods and a computerized measurement and data acquisition system. (Figure 1).

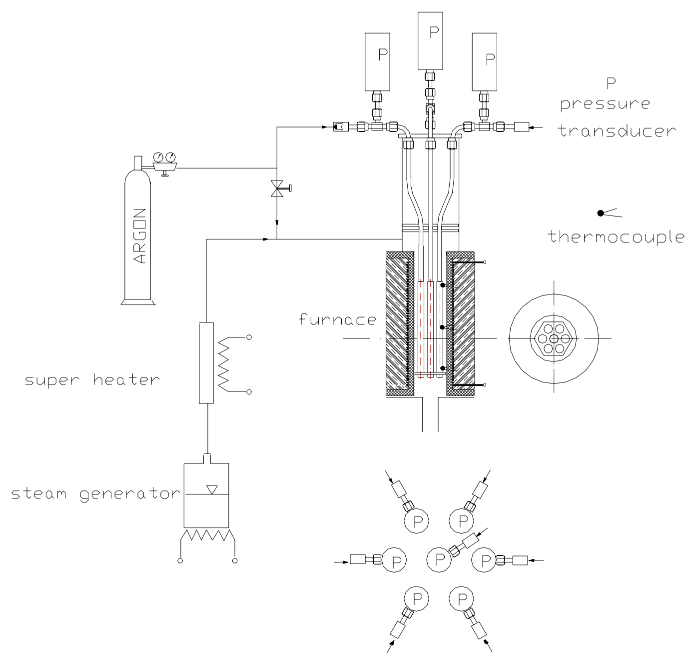

Figure 1. Schematic view of the test facility for bundle blockage tests

Each test bundle contained seven Zr1%Nb cladding tubes arranged in hexagonal geometry with the pitch of 12.2 mm characterizing the VVER-440 reactor core. The lower and upper grid plates were prepared from Zr2%Nb plates with 2 mm thickness. The cladding tubes were connected to the pre-pressurization system mounted with check valves and pressure transducers. On the other end the tubes were closed with Zr2%Nb plugs. The test assembly was placed in an Al_2O_3 ceramic tube with hexagonal inner hole. (Test characteristics are summarized below.)

<u>Characterization of the test</u>

- Cladding tube:
  - alloy: Zr1%Nb
  - geometry: ∅9.1 x 0.65 length=150 mm
  - end plugs: Zr2%Nb
  - ZrO_2 layer: 0-200 μm
- Pressurization tube:
  - alloy: Zry-4
  - geometry: ∅ 6.0 x 1.0
- Grid plates:
  - alloy: Zr2%Nb
  - geometry: hexagonal (plate distance=34 mm, pitch=12.2 mm)
  - number: two (150 mm distance between the spacers)
- Test pressure: 60 bar
- Instrumentation: pressure transducer for each tube
  thermocouples at three axial locations (middle ± 70 mm)
- Temperature range: 20-1300°C
- Temp. increase rate: 1 K/s
- Pressure range: 7-55 bar (maximum pressure in cold state)
- Atmosphere: argon / steam
- Data acquisition: 1 record/s
- Number of specimens 9 x 7 rods

There were nine successful experiments performed at linear temperature increase of 1K/s. The initial pressure of the rods varied between 3 and 30 bars. The individual pressure history of each rod was measured on-line and the temperature was detected in three different axial positions. The data acquisition frequency was 1 record/s. Tests in argon (bundles 1-5) and steam atmosphere (bundles 6-9) were compared to investigate the effect of cladding oxidation on flow blockage.

The main steps of the experiments were as follows:

1. pre-pressurization of the test tubes (3-30 bar)
2. activating Ar or steam injection into the furnace
3. heat-up of the furnace (1 K/s)
4. on-line detection of the pressure and temperature histories
5. stop of the experiment after the burst of all the seven rods of the bundle

Post-test examinations

In order to measure the deformations and the flow blockage rate after the test the bundles were filled with epoxy and horizontal cuts were prepared at different elevations. (Photos of the cuts are involved in file '*cuts.pdf*'). The elevations of the cuts corresponded to 0, ±10 and ±20 mm measured from the axial position of the bursts. (The axial location of the claddings' blow was identical in the bundle and generally corresponded to the hottest point.) The flow blockage rate was calculated on the basis of the measured total cross section area of the deformed rods. The considered flow channel is represented in Figure 2. The ZrO_2 layer thicknesses were measured, as well.

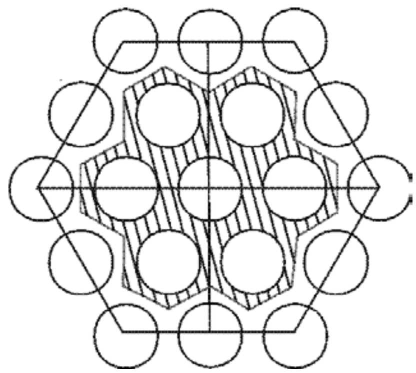

Figure 2. Flow channel considered to calculate the blockage rate in the test bundle

3.1.2. Test results and conclusions

The performed tests represented the ballooning of the cladding tubes, and the measured parameters provided adequate information for comparative analyses. The most important experimental data are summarized in Table 1 (See Appendix 1, too). The measured pressure and temperature histories for all the 9 bundles are figured in file '*graphs.pdf*'. (Figure 3 represents the data of test bundle 5). The data files of the histories are stored in separated files for all the nine experiments (*'test01.prn' – 'test09.prn'*)

No.	Atmos-phere	Initial pressure	Max. pressure	Temperature at the failure of the 1st rod	Max. temperature	Blockage rate
1	Argon	10 bar	23 bar	800 ^oC	1000 ^oC	72 %
2	Argon	3 bar	7.5 bar	1100 ^oC	1200 ^oC	57 %
3	Argon	20 bar	35 bar	900 ^oC	900 ^oC	59 %
4	Argon	30 bar	46 bar	800 ^oC	900 ^oC	-
5	Argon	30 bar	53 bar	800 ^oC	900 ^oC	76 %
6	Steam	30 bar	55 bar	900 ^oC	900 ^oC	43 %
7	Steam	20 bar	36 bar	800 ^oC	900 ^oC	55 %
8	Steam	10 bar	20 bar	900 ^oC	900 ^oC	57 %
9	Steam	3 bar	7 bar	-	1300 ^oC	34 %

Table 1. Summary of 7-rod ballooning test parameters [3]

Figures of the measured cross section areas are presented in file '*csa.pdf*'. The data are printed in Appendix 1. On the basis of the measured data the following conclusions were drawn:

- Lower initial pressure resulted in higher failure temperature.
- Ballooning always occurred at the elevation of the maximum temperature.
- Each rod of the test bundle burst at the same axial elevation.
- Oxidation due to steam atmosphere resulted in smaller deformation.
- High initial pressure resulted in larger crack.
- The typical blockage rate was 40-50%.
- The maximum blockage rate was below 80%. The largest cladding deformation was observed in test 5. The temperature and pressure histories of this bundle are presented in Figure 3. The measured cross section areas and the flow blockage rate are presented in Figures 4 and 5, respectively.

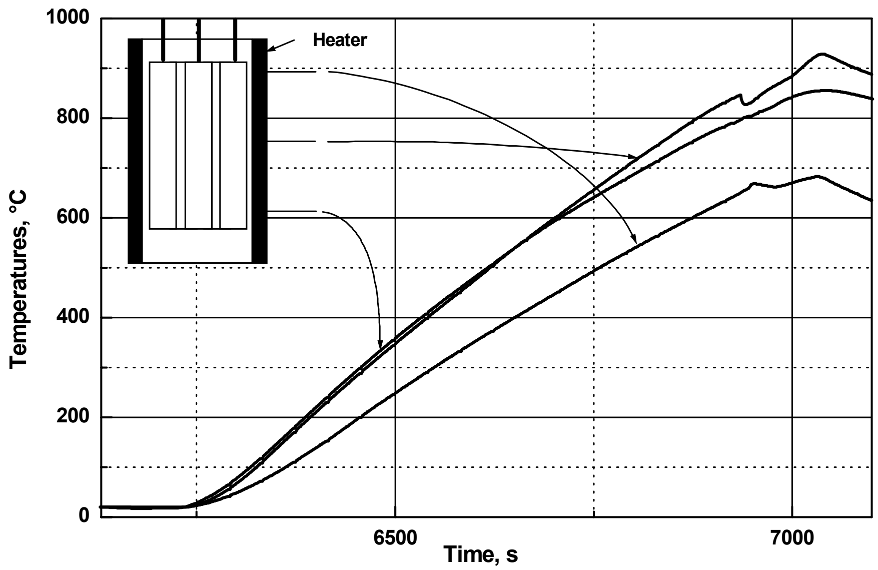

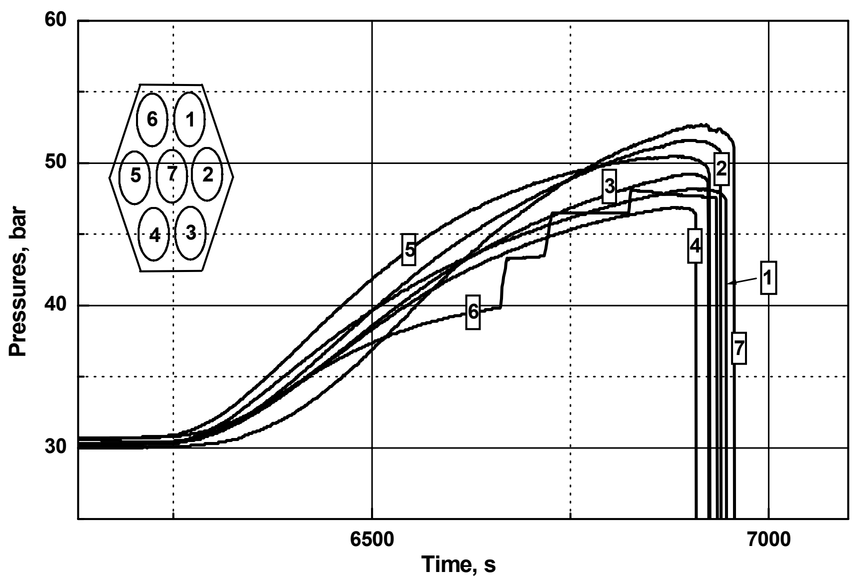

Ballooning Test N° 5
Initial Pressure: 30 bar
Environment: Argon

Figure 3. Measured temperature and pressure histories of test bundle 5

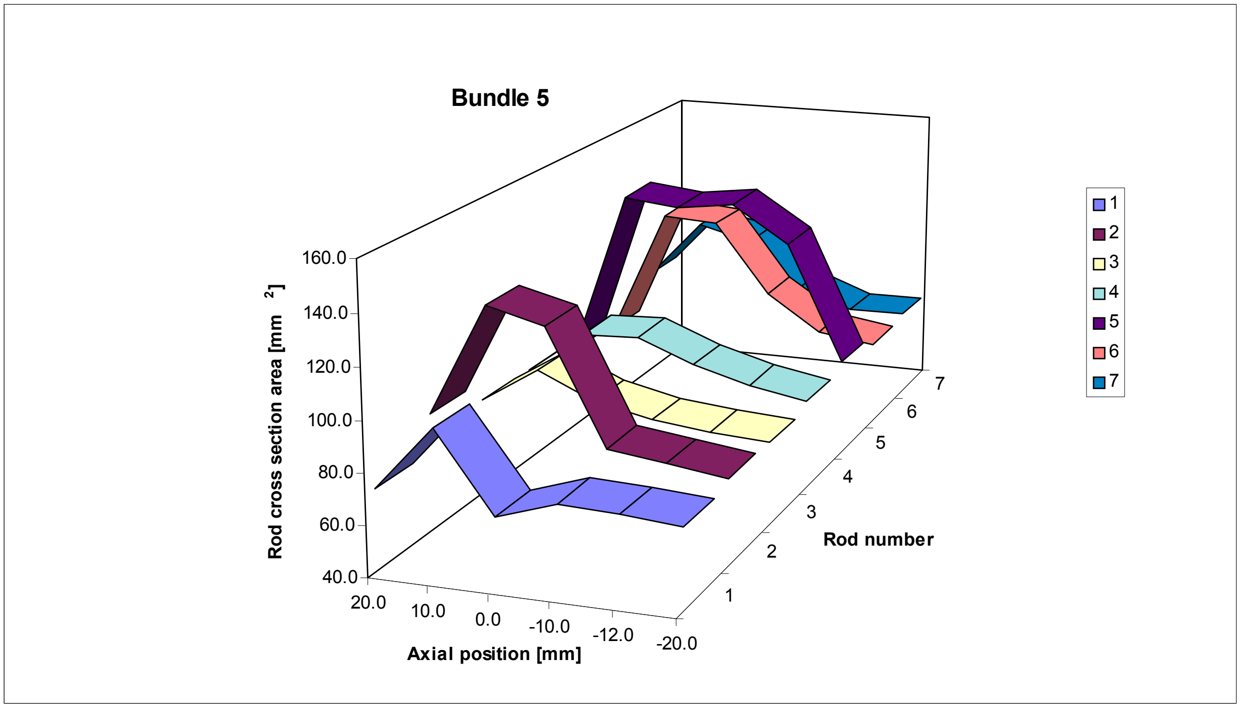

Figure 4. Rod cross section areas in test bundle 5 after the ballooning experiment

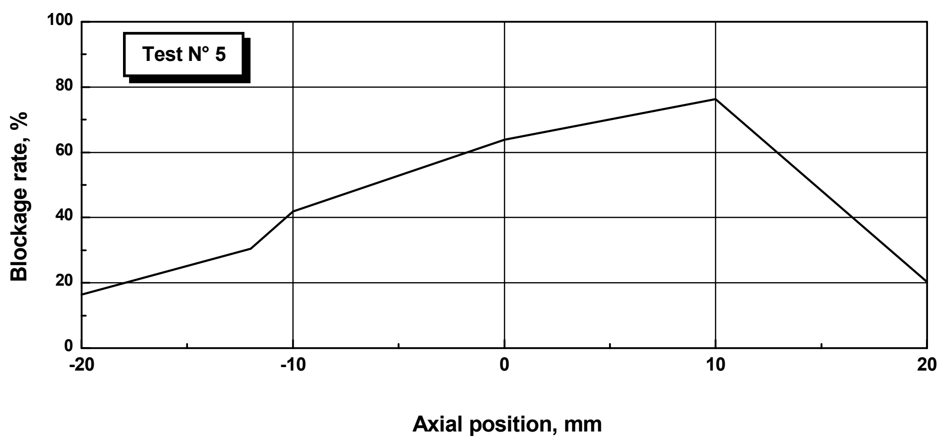

Figure 5. Flow blockage rate in test bundle 5 as a function of the axial elevation measured from the cracked part

3.2. Single rod ballooning tests

3.2.1. Test series in steam atmosphere

Altogether three test series were performed to investigate the mechanical behaviour and strength of VVER cladding tubes and to provide adequate data for model validation. The effects of temperature, pressurization rate oxidation and iodine absorption produced on the deformation and the burst pressure were investigated in more than 100 biaxial tests [4, 5].

3.2.1.1. Description of the tests

Test series PUKI

The first test series (experiments PUKI) was initiated in 1995 under the support of the National Committee for Technological Development (OMFB). Fifty-four short Zr1%Nb tube samples were investigated in a resistance furnace providing isothermal conditions in the temperature range of 650-1200 ^{o}C. The inner pressure of the test tube was increased linearly until the burst of the sample. The pressure history was monitored on-line by a computerized data acquisition system. The residual deformation of the samples was measured after the test.

The schematic view of the test facility is presented in Figure 6. The specimen was placed in a quartz test tube filled with inert gas (Ar), and heated up in an electrical furnace. The pressure of the inert gas in the quartz tube was kept at constant 1 bar by means of a buffer volume. After an approximately 1000 s heat-up period the sample was pressurized with argon gas at a constant pressure gradient provided by choking with a capillary tube. Different pressurization rates between 0.01-0.1 bar/s could be achieved by using capillary tubes with different diameters. The temperature in the furnace and the cladding inner pressure were recorded by a PC with the data acquisition frequency of 10 records/s.

The specimens were 50 mm long pieces of original VVER claddings with the inner / outer diameters of 7.8 / 9.1 mm respectively. The samples were closed with Zircaloy end-plugs welded to the cladding in argon atmosphere. The pressurization was performed through a Zircaloy-4 pipe (∅2.15 x 0.25) attached to one end of the specimen. (Figure 7) In order to investigate the effect of corrosion on the mechanical strength of Zr1%Nb some samples were treated in steam or iodine atmosphere before the ballooning tests. Pre-oxidation was performed in steam at 900 ^{o}C for different time periods between 50 and 3600 s. Iodine treatment was carried out for 1200 s at 700 ^{o}C in special argon-filled ampoules containing iodine in the concentration of 10 mg/cm^3. These treatments issued in samples with outer oxide layer of 14-57 μm or iodine concentration of 1.7-2.6 mg/cm^2.

The experimental data involved in the summary file *'pukizrnb.prn'* are tabulated in Appendix 2, as well.

Characterization of the test:

- Cladding tube:
  - alloy: Zr1%Nb
  - geometry: ∅9.1 x 0.65 length=50 mm
  - end plugs: Zircaloy-4
  - ZrO_2 layer: 0-57μm
- Pressurization tube:
  - alloy: Zry-4
  - geometry: ∅ 2.15 x 0.25
- Instrumentation: pressure sensor, temperature sensor
- Temperature range: 650-1200°C
- Temperature increase rate: isothermal tests
- Pressure range: 0-140 bar
- Pressurization rate: 0.007-0.17 bar/s
- Atmosphere: argon
- Data acquisition: 10 records/s
- Number of specimens tested successfully: 54

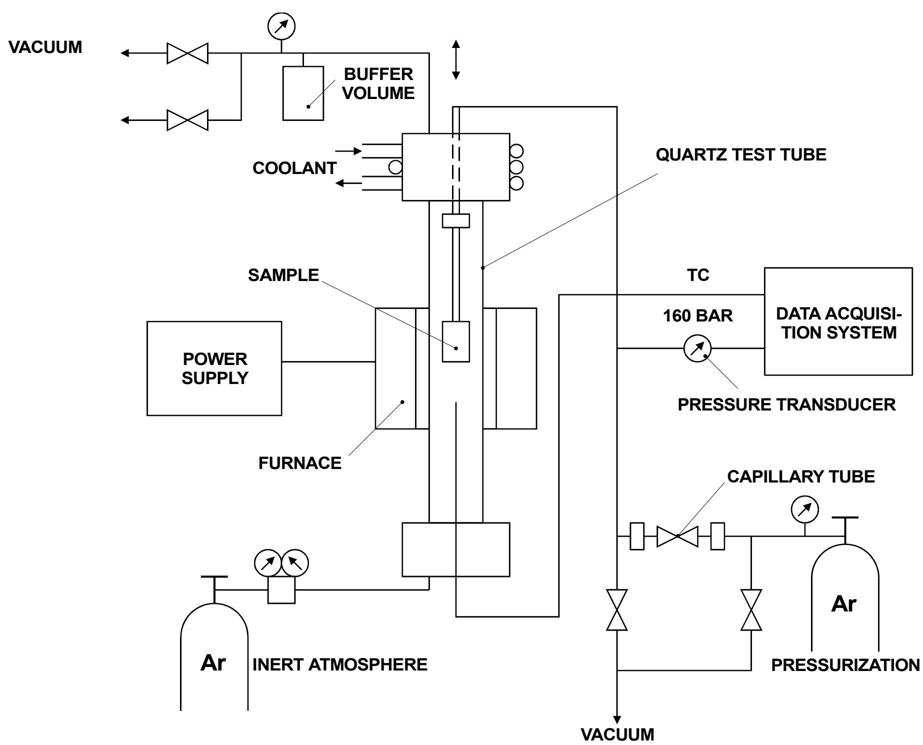

Figure 6. Schematic view of the test facility for single rod ballooning test

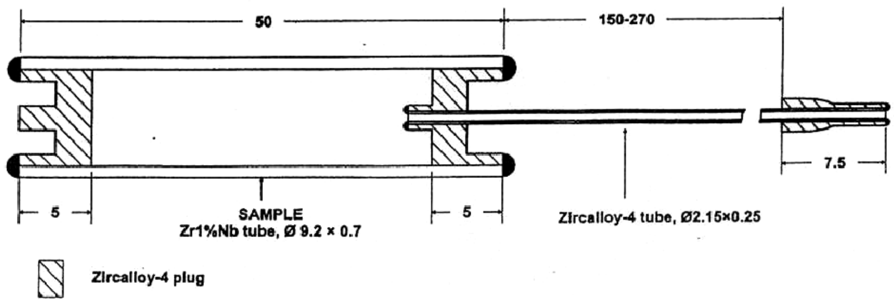

Figure 7. Drawing of the Zr1%Nb tube specimen for ballooning test

Test series PUZRY

The second test series (experiments PUZRY) was performed in the same test facility with thirty-one Zircaloy-4 tube specimens in order to provide data for comparative analyses too [4, 5]. The specimens' inner / outer diameters of 9.3 / 10.75 mm corresponded to the parameters of PWR fuel claddings. The test conditions were very similar to that of the first test series: linear pressure increase under isothermal conditions in the range of 700-1200 ^{o}C. The effect of corrosion on the mechanical performance of Zircaloy-4 cladding was not investigated. (The experimental data can be found in Appendix 3.)

Characterization of the test:

- Isothermal tests with linear pressure increase
- Cladding tube:
  - alloy: Zircaloy-4
  - geometry: ∅10.75 x 0.725 length=50 mm
  - end plugs: Zircaloy-4
  - ZrO_2 layer: 0 μm
- Pressurization tube:
  - alloy: Zry-4
  - geometry: ∅ 2.15 x 0.25
- Instrumentation: pressure sensor, temperature sensor
- Temperature range: 700-1200^{o}C
- Temperature increase rate: isothermal tests
- Pressure range: 0-106 bar
- Pressurization rate: 0.007-0.26 bar/s
- Atmosphere: argon
- Data acquisition: 10 records/s
- Number of specimens tested successfully: 31

Test series BALL

The third test series (experiments BALL) was performed in 2000 in order to investigate the effect of pressurization and temperature increase rate produced on the burst pressure of Zr1%Nb cladding tubes. Twenty-five experiments in two groups were performed in an interim project of the AEKI. New test facility was constructed to provide higher pressurization rates and steam atmosphere, as well.

In the first group of this test series 150 mm long, pre-pressurized Zr1%Nb tube samples were investigated at linear temperature increase. The initial pressure of the samples and the temperature increase rate were varied between 10-40 bars and 6.4-13.5 K/s, respectively.

In the second group of the test series the Zr1%Nb tube samples were investigated at different linear pressure increase rates (0.6-6.6 bar/s) under isothermal conditions in the temperature range of 800-1200 ^oC.

Appendix 4 contains the summary of the experimental data.

Characterization of the test:

- Cladding tube:
  - alloy: Zr1%Nb
  - geometry: ∅9.1 x 0.65 length=150 mm
  - end plugs: Zircaloy-4
  - ZrO_2 layer: 0
- Instrumentation: pressure sensor
  thermocouples at three different elevations
- Temperature range: 800-1200^{o}C
- Temperature increase rate: 6.4-13.5 K/s
- Pressure range: 10-40 bar
- Pressurization rate: 0.6-6.6 bar/s
- Atmosphere: argon / steam
- Data acquisition: 2 records/s
- Number of specimens tested successfully: 25

3.2.1.2. Test results and conclusions

On the basis of the ballooning tests, performed with 110 (79 Zr1%Nb + 31 Zircaloy-4) cladding tube samples the following main conclusions were drawn:

1. The mechanical behaviour of the PWR and VVER claddings are similar. However, the experiments revealed that in the temperature range of 800-1000 ^oC the mechanical strength of the Zr-1%Nb cladding is lower than that of the Zircaloy-4 tube, since the α-β phase transition temperature is different for Zr1%Nb and Zircaloy-4 (Figure 8).

2. The coolant side oxidation had a significant effect on the mechanical strength of the cladding. The strength of Zr-1%Nb increased up to 10 µm oxide layer thickness, but decreased with further oxidation (Figure 9). Decreasing deformation with an increasing ZrO_2 layer was also observed. At the oxide layer thickness of 10-40 µm the tangential strain decreased to the 40-30% of the oxide-free samples' strain.

3. The iodine treatment did not influence the mechanical behaviour significantly: only a small increase of the Zr1%Nb cladding's high temperature strength and a small decrease of deformation were observed.

4. Larger pressure increase rate resulted in higher burst pressure (Figure 10). On the other hand, no influence of the temperature increase rate was experienced.

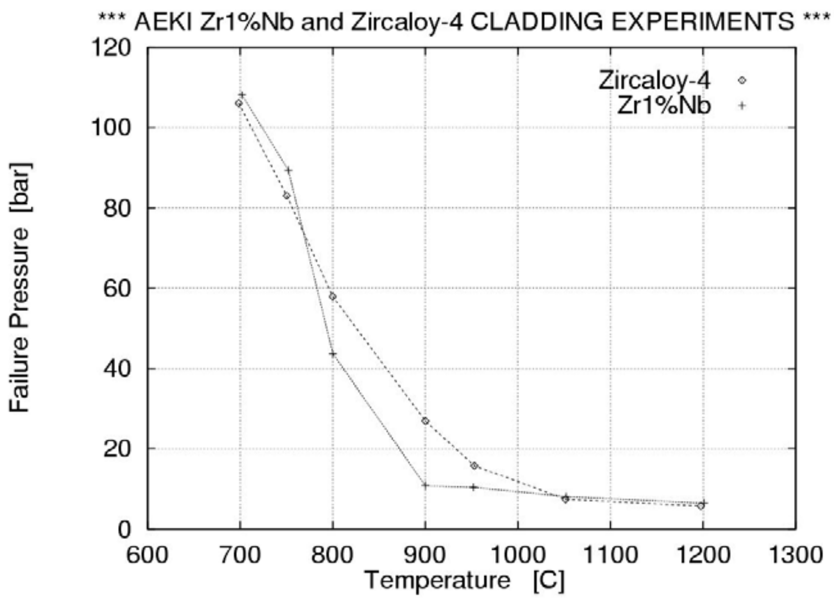

Figure 8. Comparison of the failure pressures measured in biaxial tests for Zr1%Nb and Zircaloy-4 cladding specimens

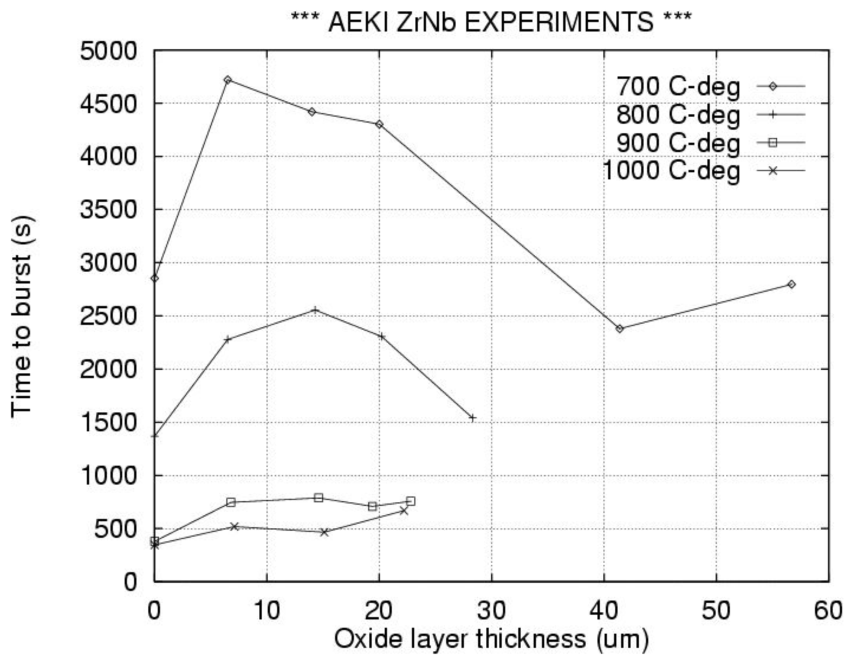

Figure 9. Measured time to burst at constant pressurization rate in biaxial tests as a function of the ZrO_2 layer thickness on pre-oxidized Zr1%Nb cladding samples

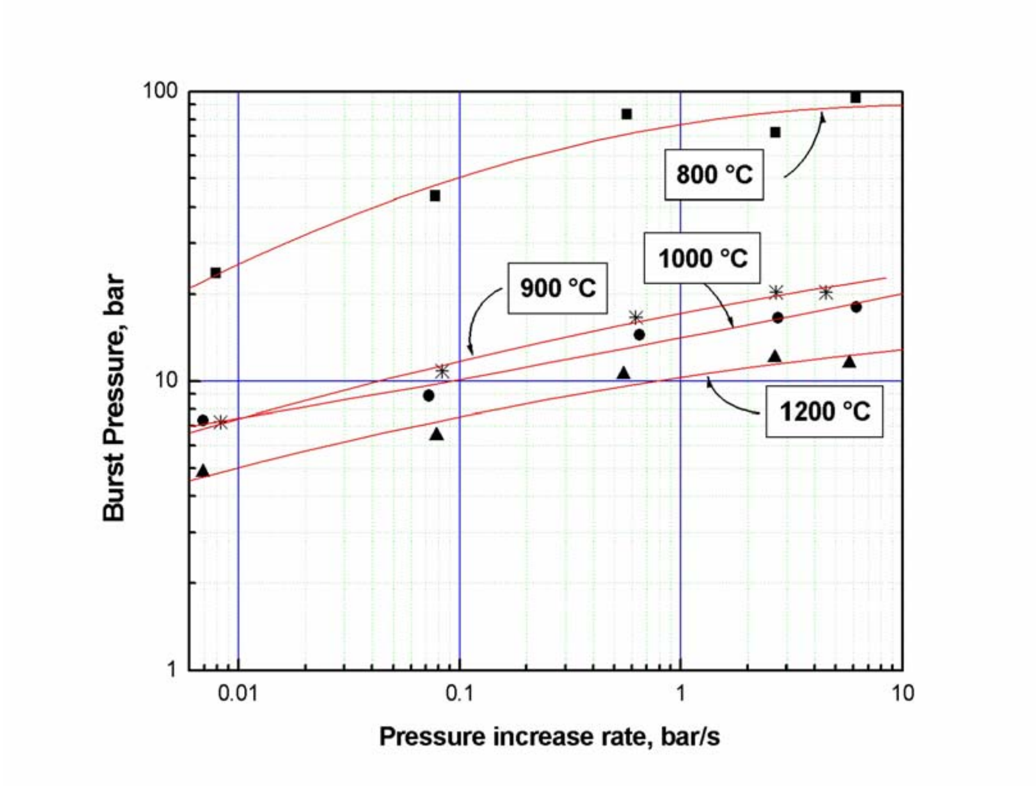

Figure 10. Burst pressure of Zr1%Nb tube specimens as a function of the pressurization rate

Evaluation of high temperature cladding creep

Considering the Norton creep equation as

$$\dot{\varepsilon} = k \cdot \sigma^n \tag{1}$$

where:

$\dot{\varepsilon}$	hoop strain rate
σ	hoop stress
k	$A \cdot \exp(-Q/RT)$
A	constant
Q	heat production rate
T	cladding temperature
n	stress exponent, metallurgy parameter

k and n parameters were derived on the basis of the first and second test series' data following the methodology below [4]:

Since hoop stress can be calculated as

$$\sigma = p \cdot \frac{r}{s} = \frac{p}{p_0}\sigma_0(1+\varepsilon)^2 \tag{2}$$

where

p over pressure; linear function of the time (t):

$$p(t) = b \cdot t \tag{3}$$

r cladding mean radius
s cladding wall thickness
p_0 over pressure at $t=t_0$
σ_0 hoop stress at $t=t_0$;
ε hoop strain

The Norton equation can be integrated as follows:

$$\int_0^{\varepsilon_R} \frac{d\varepsilon}{(1+\varepsilon)^{2n}} = \int_0^{t_R} k \cdot \left(\frac{\sigma_0}{p_0}\right)^n p(t)^n \, dt \tag{4}$$

Where:

ε_R	hoop strain at rupture
t_R	time to rupture

Considering two different pressurization rates (b_1 and b_2) resulting in different rupture pressures (p_{R1} and p_{R2}) parameters n and k can be easily derived after performing the integration of the equation above:

$$n = \frac{\ln \frac{t_{R2}}{t_{R1}}}{\ln \frac{p_{R1}}{p_{R2}}} \tag{5}$$

In view of n and using the relation $$\frac{\sigma_0}{p_0} = \frac{r_0}{s_0} \tag{6}$$

$$k = \left(1 - \frac{1}{(1+\varepsilon_{R1})^{2n-1}}\right)\frac{n+1}{2n-1}\left(\frac{s_0}{r_0}\right)^n \frac{1}{p_{R1}{}^n t_{R1}} \tag{7}$$

The calculated *n* and *k* parameters for Zr1%Nb and Zircaloy-4 are presented in Tables 2 - 4 and Figures 11 and 12.

TEST	Oxide layer µm	Temp. °C	*n*	*k* 1/(sMPa^n)
puki-46	0.0	650	6.1	2.95E-15
puki-47	0.0	650	6.1	2.99E-15
puki-27	0.0	700	4.2	2.45E-11
puki-28	0.0	700	4.2	6.79E-11
puki-53	0.0	700	4.2	3.79E-11
puki-44	0.0	750	3.8	4.10E-10
puki-45	0.0	750	3.8	4.12E-10
puki-18	0.0	800	2.7	2.62E-07
puki-8	0.0	800	2.7	2.48E-07
puki-2	0.0	850	3.0	7.06E-07
puki-6	0.0	850	3.0	1.14E-06
puki-9	0.0	900	4.3	2.43E-06
puki-10	0.0	900	4.3	2.22E-06
puki-17	0.0	900	4.3	1.93E-06
puki-11	0.0	950	6.7	3.88E-08
puki-25	0.0	950	6.7	3.96E-08
puki-24	0.0	1000	10.4	3.30E-10
puki-12	0.0	1000	10.4	3.69E-10
puki-26	0.0	1000	10.4	4.06E-10
puki-13	0.0	1050	10.4	1.01E-09
puki-23	0.0	1050	10.4	1.48E-10
puki-14	0.0	1100	8.2	4.73E-08
puki-21	0.0	1100	8.2	3.94E-08
puki-22	0.0	1100	8.2	5.75E-08
puki-15	0.0	1150	12.0	6.65E-10
puki-20	0.0	1150	12.0	6.75E-10
puki-19	0.0	1200	7.3	7.52E-07
puki-16	0.0	1200	7.3	7.57E-07

Table 2. Parameters of the Norton eq. for oxide-free Zr1%Nb specimens

TEST	Oxide layer μm	Temp. °C	*n*	*k* 1/(sMPa^n)
puki-48	6.3	700	4.2	7.92E-12
puki-54	6.9	700	4.2	1.16E-11
puki-29	13.9	700	4.2	1.27E-11
puki-30	20.0	700	4.2	1.23E-11
puki-55	22.3	700	4.2	4.19E-11
puki-32	41.4	700	4.2	1.83E-10
puki-31	56.7	700	4.2	1.23E-10
puki-49	6.5	800	2.7	5.39E-08
puki-36	14.3	800	2.7	2.31E-08
puki-33	20.2	800	2.7	5.7E-08
puki-34	28.3	800	2.7	1.45E-07
puki-50	6.8	900	4.3	4.77E-08
puki-37	14.6	900	4.3	3.9E-08
puki-35	19.4	900	4.3	1.41E-07
puki-38	22.8	900	4.3	4.18E-08
puki-51	7.1	1000	10.4	1.61E-11
puki-40	15.1	1000	10.4	4.17E-11
puki-39	22.2	1000	10.4	1.45E-13
puki-52	7.5	1100	8.2	2.68E-08
puki-42	22.8	1100	8.2	5.67E-09
puki-43	24.2	1200	7.3	2.63E-07

Table 3. Parameters of the Norton eq. for pre-oxidized Zr1%Nb specimens

TEST	Oxide layer μm	Temp. °C	*n*	*k* 1/(sMPa^n)
puzry-26	0.0	700	6.2	3.08E-15
puzry-16	0.0	750	5.8	1.03E-13
puzry-30	0.0	800	4.9	1.7E-11
puzry-17	0.0	850	3.3	4.5E-08
puzry-18	0.0	900	3.8	5.39E-08
puzry-7	0.0	950	3.6	7.59E-07
puzry-8	0.0	1000	3.4	1.75E-05
puzry-9	0.0	1050	3.6	2.5E-05
puzry-10	0.0	1100	3.5	4.91E-05
puzry-11	0.0	1150	3.9	4.21E-05
puzry-12	0.0	1200	3.6	8.11E-05

Table 4. Parameters of the Norton eq. for oxide-free Zircaloy-4 specimens

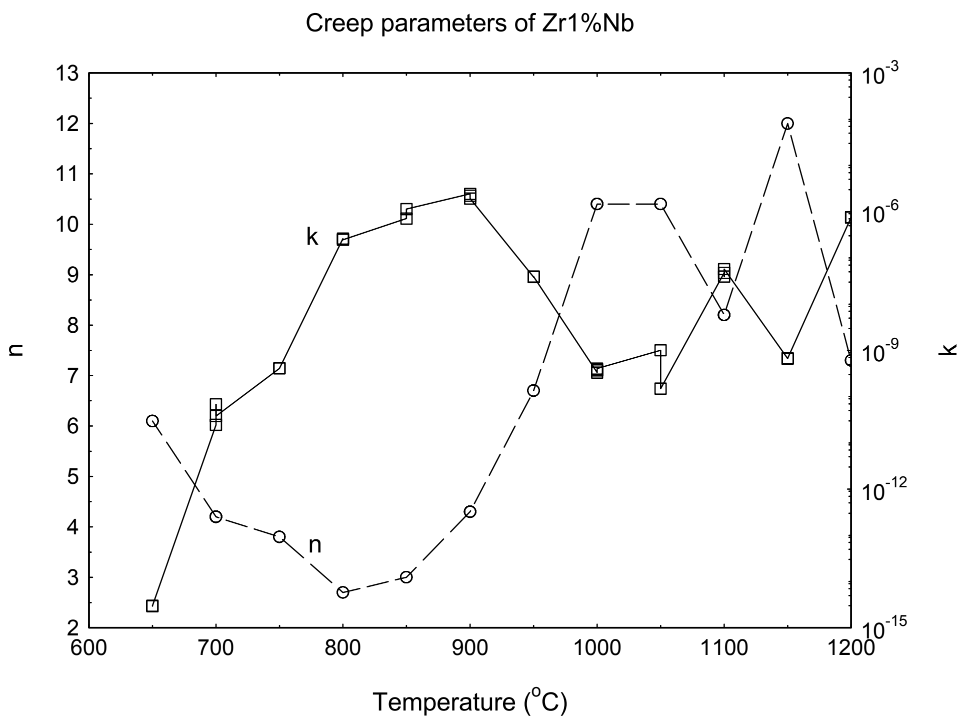

Figure 11. *n* and *k* parameters of the Norton equation for Zr1%Nb on the basis of tube ballooning tests

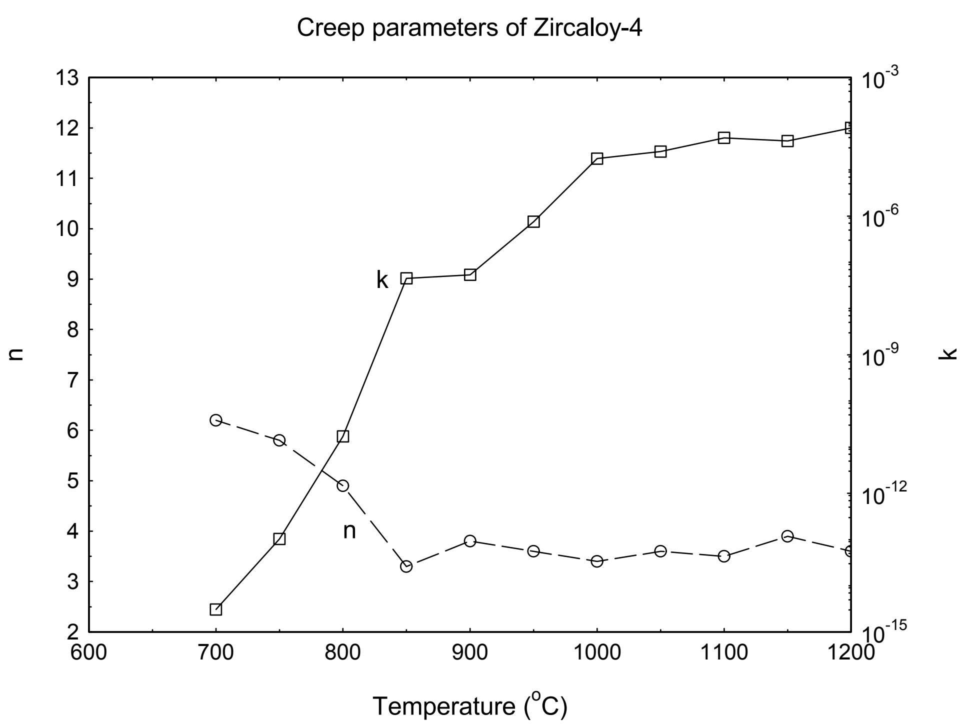

Figure 12. *n* and *k* parameters of the Norton equation for Zircaloy-4 on the basis of tube ballooning tests

3.2.2. Test series in hydrogen rich steam atmosphere

The ballooning experiments aimed to provide information about the effect of hydrogen rich steam oxidation and the effect of the hydrogen content on the cladding strength and deformation under simulated LOCA conditions. So far two test series were performed.

3.2.2.1. Description of the tests

The tests were carried out with 100 mm long tube specimens cut from original VVER claddings. The samples were closed with end-plugs. The pressurization was performed through a pipe attached to one end of the specimen. The tests were carried out under isothermal conditions in the temperature range of 900 – 1000°C. The inner pressure of the test tube was increased linearly until the burst of the sample. The pressure history was monitored on-line. After the burst tests, the residual deformation of the specimens was measured. Afterwards two ring pieces were cut from all tubes (not far from the burst) for determination of absorbed hydrogen.

<u>First test series</u>

The ballooning experiments with oxidized and as-received samples were performed in argon atmosphere.

The experimental data are summarised in the data file *'cohyra_balloon.prn'* and printed in Appendix 18. The measured temperature and pressure histories are stored in separated files for all experiments *'cohyra_balloon_history1.prn - cohyra_balloon_history8.prn'*.

<u>Second test series</u>

In order to investigate the effect of the hydrogen content on the mechanical strength and deformation, some as-received samples were treated in hydrogen-rich atmosphere during the ballooning tests. Different hydrogen partial pressures could be achieved by using different hydrogen-argon flow rates.

The experimental data are compiled in the summary file *'cohyra_balloon2.prn'* and printed in Appendix 19. The measured temperature and pressure histories are stored in separated files for all experiments *'cohyra_balloon2_history1.prn - cohyra_balloon2_history6.prn'*.

After the ballooning test some broken pieces of the cladding (at the burst) were used for determination of the hydrogen, as well. The measured data are in the summary file *'cohyra_balloon2.prn'*.

3.2.2.2. Results and conclusions

First test series

On the basis of the measured data the conclusions are the followings:

- The burst pressure of the pre-oxidized samples was higher than that of the as-received specimen.
- At low oxidation ratio the strength of the cladding increased and the cladding deformation decreased.
- The effect of hydrogen uptake is not obvious. The measurements of the hydrogen contents of the specimens carried out after the burst tests have indicated that most of the hydrogen absorbed in the pre-oxidized specimens was released during the high temperature burst tests.

Second test series

- The burst of the hydrided specimens occurred at higher pressure than the burst of the as-received sample.
- The measured hydrogen concentration around the burst was not different from the concentration at the burst.
- On the basis of the second test series we could not observe relationship between the hydrogen content and the cladding strength.
- The few performed tests did not make possible the comparison of the effect of different hydrogen content.

4. TENSILE TESTS

4.1. Test series in steam atmosphere

Beyond ballooning experiments tensile tests have been performed at the AEKI since 1989 in order to investigate the mechanical strength of VVER fuel cladding under reactor and temporary storage conditions. The tests were carried out with tube and sheet specimens in different projects partly supported by the National Committee for Technological Development [2, 6].

To investigate the effect of temperature and oxidation on the strength of Zr1%Nb alloy was the primary objective of the tensile tests. The temperature range of the tests was generally 20-350^{o}C but a limited number of experiments were performed at higher temperatures, to 600^{o}C, as well. The effect of oxidation on the mechanical strength was studied through the testing of pre-oxidized specimens. The maximum equivalent oxidation (ECR - Equivalent Cladding Reacted) of the specimens was 35%. In order to provide data for comparison, Zircaloy-4 specimens were tested, as well.

4.1.1. Description of the tests

The experiments were performed by a universal tensile-testing machine Instron 1195 according to the Hungarian Standard MSZ EN 10002-5. The crosshead speed was 1-2 mm/min. Digital data acquisition provided the recording of the force-displacement curves for the latter tests. Consequently, beyond the engineering stress-strain relations, the true stress-strain curves can be derived, as well. For early measurements only the data of the tensile strength, yield strength, strain and contraction are available.

There were specimens with two different geometries tested:

1. tube specimens (∅9.1 x 0.65) with the gauge length of 25 mm and
2. sheet specimens tooled at the workshop of the AEKI from original cladding tubes (Figure 13).

Both geometries supported the measurement of longitudinal strength parameters. (A new test series with ring specimens to investigate the claddings' strength in transversal direction is under preparation.) The applied E110 cladding tubes were received from two different deliveries in 1989 and in 1999.

Specimens with and without annealing as well as with and without pre-oxidation, were compared. The annealing of the specimens was performed at 580 ^{o}C or 700 ^{o}C for several hours.

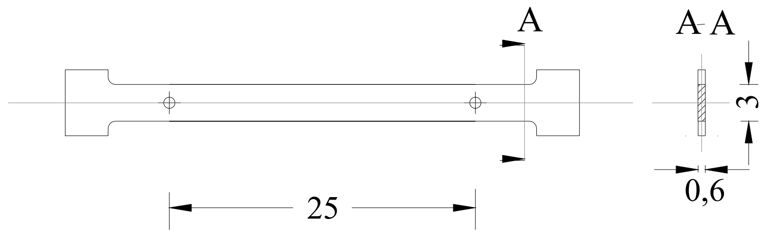

Figure 13. Drawing of the sheet specimen for tensile test

Pre-oxidation of the specimens was performed in steam atmosphere at 900 ^{o}C for different time intervals between 100 and 1600 s. Both the temperature and the steam flow rate were constant during the oxidation. Since the ends of the tube specimens were plugged only the outer surfaces were oxidized. The equivalent oxidation was calculated on the basis of the measured mass gain of the specimens. The oxide layer thickness on the specimens was also evaluated as follows:

Indicating the unknown ZrO_2 thickness with *x* we can write the following simple relation for the ZrO_2 mass in unit length:

$$\left[d_o^{\,2} - \left(d_o - 2x\right)^2\right]\frac{\pi}{4}\rho_{ZrO_2} = \Delta m \frac{M_{ZrO_2}}{M_{O_2}} \qquad (8)$$

Where:

Δm mass gain due to the oxidation for unit length

$$\Delta m = \frac{ECR}{100}\Delta m_{tot} \qquad (9)$$

Δm_{tot} theoretical maximum of the mass gain for unit length

$$\Delta m_{tot} = \frac{M_{O_2}}{M_{Zr}}\frac{\pi}{4}\pi(d_o^{\,2} - d_i^{\,2})\rho_{Zr} \qquad (10)$$

ECR equivalent oxidation in %
M_{O_2} molecular weight of oxygen (32)
M_{Zr} molecular weight of zirconium (91.2)
M_{ZrO_2} molecular weight of zirconium-dioxide (123.2)
d_o cladding outer diameter (measured after the oxidation)
d_i cladding inner diameter
ρ_{Zr} density of zirconium (6490 kg/m^3)
ρ_{ZrO_2} density of zirconium-dioxide (5820 kg/m^3)

Substituting equations (9) and (10) into (8) the following relationship can be derived between the equivalent oxidation (*ECR)* and the ZrO_2 layer thickness:

$$x = \frac{d_o}{2}\left(1 - \sqrt{1 - \frac{ECR}{100}\frac{\left(d_o^{\,2} - d_i^{\,2}\right)}{d_o^{\,2}}\frac{\rho_{Zr}}{\rho_{ZrO_2}}\frac{M_{ZrO_2}}{M_{Zr}}}\right) \quad (11)$$

$$x = \frac{d_o}{2}\left(1 - \sqrt{1 - \frac{ECR}{100}\frac{\left(d_o^{\,2} - d_i^{\,2}\right)}{d_o^{\,2}}1.5064}\right) \quad (12)$$

4.1.2. Results and conclusions

Experimental data have been summarised separately for Zr1%Nb and Zircaloy-4 sheet and tube specimens. The summary files are printed in Appendix 5.

The measured VVER cladding strength parameters corresponded to the data in international publications. The annealing did not influence the strength and the strain of the specimens considerably. Differences in tensile strength and elongation of the samples from the two different deliveries were in the range of the measurements' uncertainty.

On the other hand the pre-oxidation of the specimens in steam atmosphere resulted in relevant influences. Tensile test and ballooning experiments indicated analogous effects of the oxidation on cladding strength and deformation. Below the ECR of about 5% the tensile strength increases with the oxidation up to a definite maximum and decreases with further oxidation. This phenomenon is clearly indicated in Figure 14 representing the test data at three different temperatures as 20 ^oC, 150 ^oC and 300 ^oC. The measured strains of the specimens sharply decrease with the oxidation already at a low level of ECR (Figure 15). Tensile testing of deeply oxidized Zr1%Nb came up against technical difficulties due to the unstable fixing of the embrittled specimens.

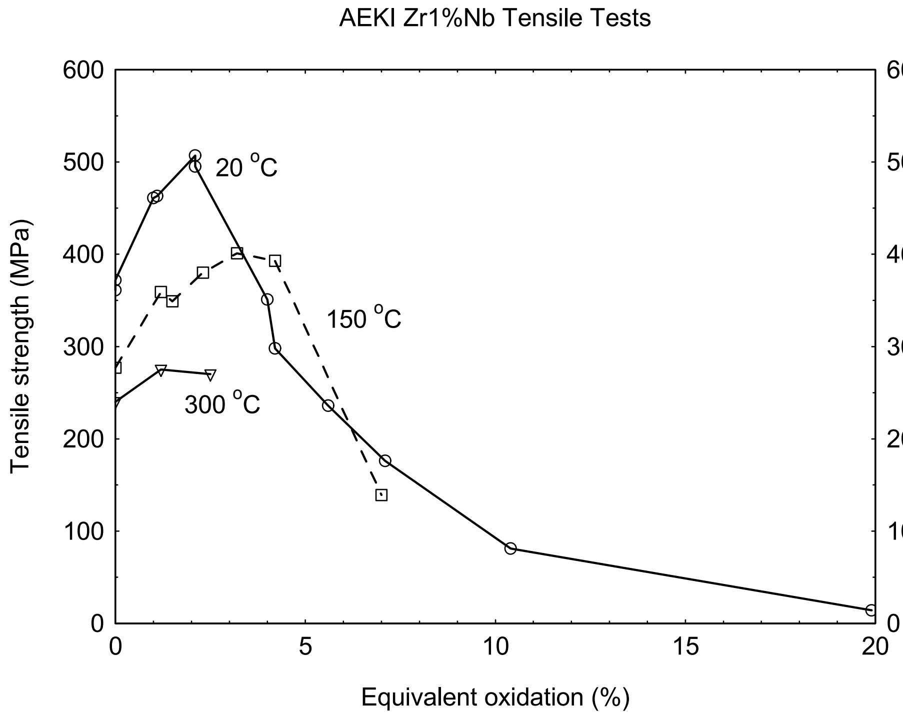

Figure 14. Tensile strength of Zr1%Nb tube as a function of the ECR and the temperature. AEKI tensile test data

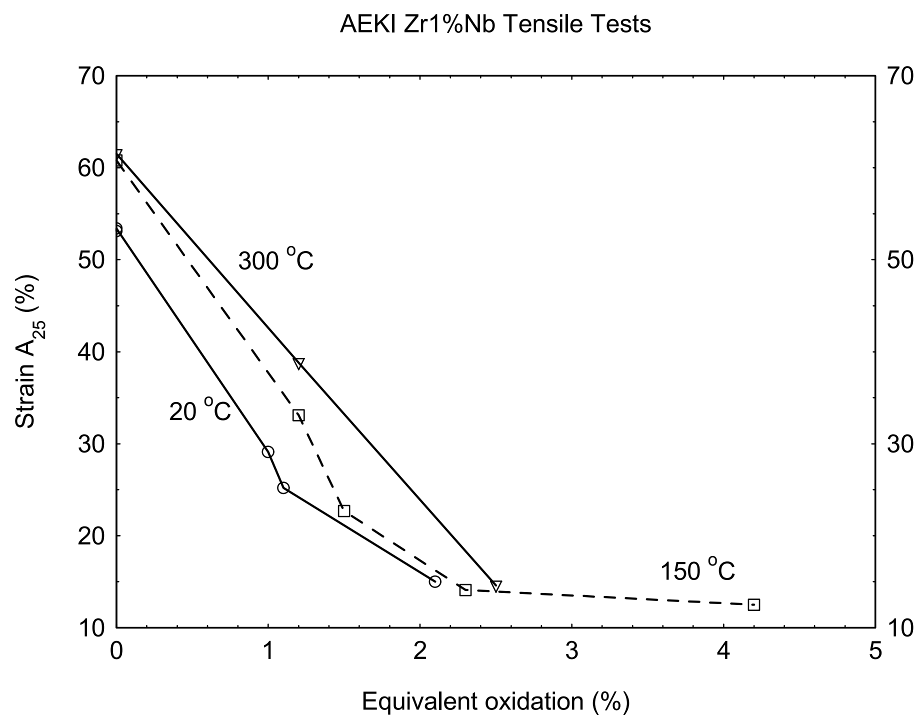

Figure 15. Strain of Zr1%Nb tube as a function of the ECR and the temperature. AEKI tensile test data

4.2. Test series in hydrogen rich steam atmosphere

The main objective of the tensile tests was to investigate the effect of hydrogen rich steam oxidation and the effect of the hydrogen content on the strength of E110 alloy.

4.2.1. Description of the tests

The tensile tests of cladding rings with 2 mm length were carried out at room temperature using INSTRON 1195 universal testing machine. The velocity of the crosshead moving was 0.5 mm/min. Digital data acquisition provided the recording of the load – displacement curves. The extent of the equivalent oxidation was lower than 6 % in the performed experiments.

The experimental data are compiled in the summary files *'cohyra_tensile.prn* and *cohyra_tensile_curves.pdf'*, and printed in Appendix 17.

4.2.2. Results and conclusions

Figure 16 represents the measured tensile strength of the E110 specimens versus the ECR. The effect of the oxidation was consistent with the results of earlier tensile tests with cladding specimens pre-oxidized in pure steam at 900^{o}C [18]. Below the equivalent oxidation of about 3 % the tensile strength increases with the oxidation up to a definite maximum and decreases with further oxidation. However, the tensile strength is slightly lower in steam-hydrogen mixture than in pure steam. It means that the fuel cladding is less loadable probably due to the higher hydrogen content of the cladding oxidized in hydrogen-rich steam.

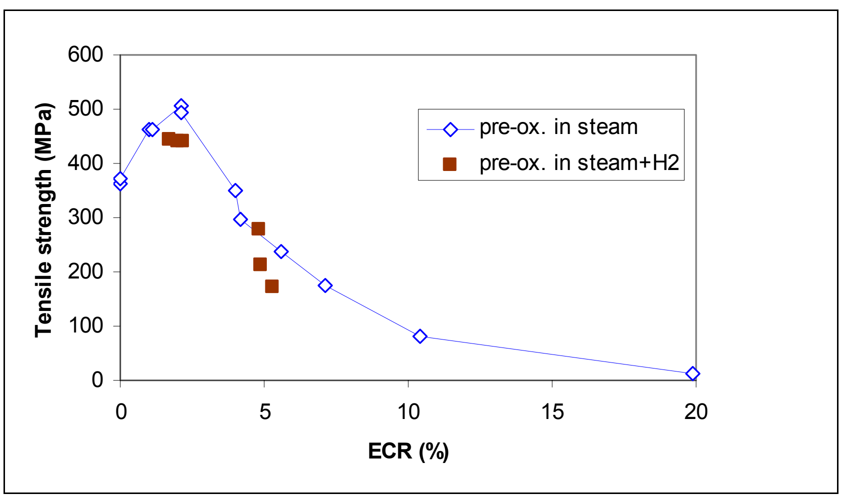

Figure 16. Tensile strength of E110 as a function of the oxidation

Figure 17 illustrates the tensile strength as a function of the hydrogen content of the specimens.

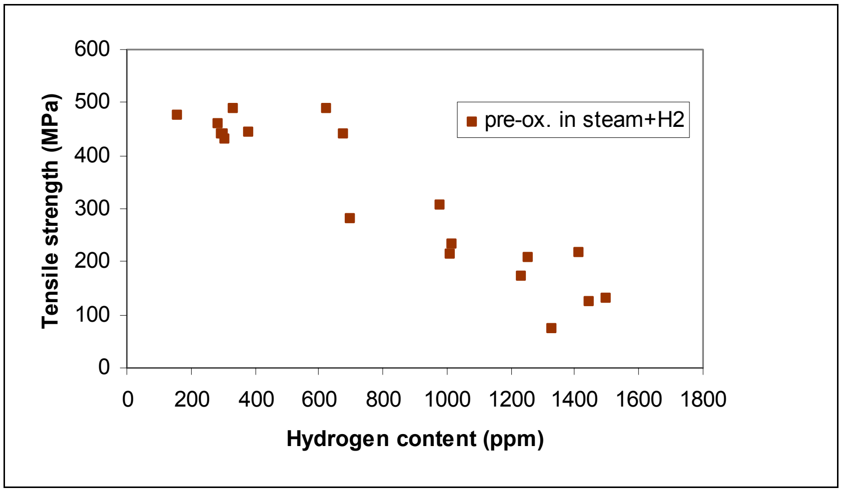

Figure 17. Tensile strength of E110 as a function of the hydrogen content.

On the basis of the COHYRA experiments the mechanical deterioration of the fuel cladding was observed above 600 wppm hydrogen content. The hydrogen content was not measured after the earlier tensile tests.

5. OXIDATION EXPERIMENTS

5.1. Test series in steam atmosphere

Data of seven different series of oxidation experiments were involved in the database. All the seven experiments aimed at the investigation of Zr1%Nb claddings' high temperature oxidation in steam atmosphere. The kinetics of the oxidation was studied at constant steam flow in the temperature range of 500-1200 ^oC. Some of the experiments were initiated to provide pre-oxidized samples for mechanical tests. Beyond this report, ref. [7] also summarizes information about the cladding corrosion tests performed at the AEKI.

5.1.1. Experiments 'PUKOX'

This series of experiments was performed in 1995 in order to provide pre-oxidized specimens for the ballooning tests 'PUKI' (described in chapter 3.2) [4]. The 50 mm long Zr1%Nb tube specimens were oxidized at 900 ^oC in constant steam flow. The time of oxidation varied between 50 - 3600 s resulting in the equivalent oxidation (ECR) of 0.6 - 6%. Only the outer surface of the specimens was oxidized, since both ends of the tubes were plugged. The weight of every specimen was measured before as well as after the oxidation. The equivalent oxidation and the ZrO_2 thickness were calculated on the basis of the measured mass gain. The achieved 0.6 – 6% of ECR corresponded to the ZrO_2 thickness of 6 – 60 μm. The oxidation rate constant was also tabulated for each specimen.

The measured data are tabulated in the data file *'pukox.prn'* and printed in Appendix 6.

5.1.2. Experiments 'EU-PECO'

This EU supported project initiated in 1995 aimed at the study of Zr1%Nb oxidation and hydriding phenomena in the temperature range of 900-1200 ^oC. The rate of mass gain and the formation of zirconium oxide layers were determined in high temperature steam oxidation tests performed with original VVER cladding tube specimens (∅9.14 x 0.70, length=40 mm).

The cladding specimens were tested under isothermal conditions in constant steam flow. The rate of oxidation was characterized by the mass gain measured by analytical balance. Metallographic tests were used to determine the thickness of the reaction layers. Hydrogen contents of the specimens were measured after the oxidation tests by means of hot extraction method.

The experimental facility consisted of a tube furnace, a steam generator, a super-heater, a quartz tube and a condenser (Figure 18.). The steam flow rate was about 7.5 mg/s, the super-heating temperature was 350 ^oC. The temperature of the furnace was controlled between 900 and 1200 ^oC with the accuracy of $\pm 1^oC$. The exposure time intervals varied between 5-166 minutes at 900 ^oC and 1-8 minutes at 1200 ^oC.

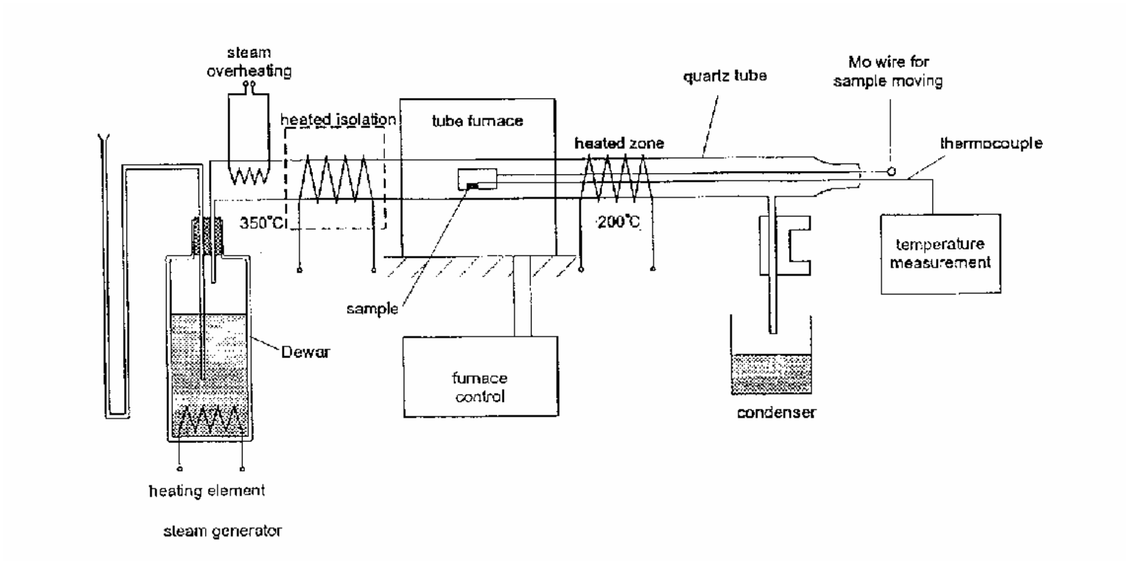

Figure 18. Schematic view of the test facility for cladding oxidation tests

The extent of oxidation did not exceed 20% ECR in the performed experiments. The kinetics of the oxidation was evaluated through the mass gain and the zirconium oxide layer growth. The measured data proved the square root relationship between the oxidation rate and the time indicating diffusion-controlled process. The rate constants calculated at different temperatures for the mass gain and the ZrO_2 layer growth are presented in Figures 19 and 20, respectively.

Multi-layer structure of the ZrO_2 was observed if the oxidation had been performed below 1100 ^oC. (See more in Chapter 5.1.4). Compact oxide layer formed at higher temperatures (1100-1200 ^oC).

Hot extraction methods indicated 10 - 40% uptake of the formed hydrogen. It was concluded that the kinetics of the hydrogen uptake strongly depends on the oxide layer structure. During steam exposure under 1050 ^oC the hydrogen uptake was nearly proportional to the mass gain. But, the compact oxide layer at higher temperatures impeded the hydrogen uptake.

Comparison of the experimental records with literature data indicated similar mass gain rates but different oxide layer morphologies for Zr1%Nb and Zircaloy-4 alloys. The hydrogen uptake of Zr1%Nb is more intensive than that of the Zircaloy.

Detailed description of the experiments and the comparison with literature data can be seen in reference [8]. The experimental data are tabulated in Appendix 7.

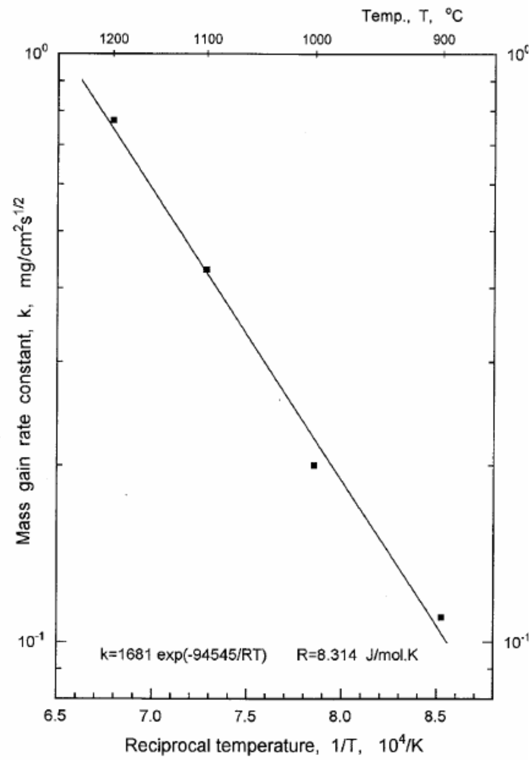

Figure 19. Temperature dependence of the mass gain on the basis of Zr1%Nb oxidation tests in steam between 900 - 1200 °C.

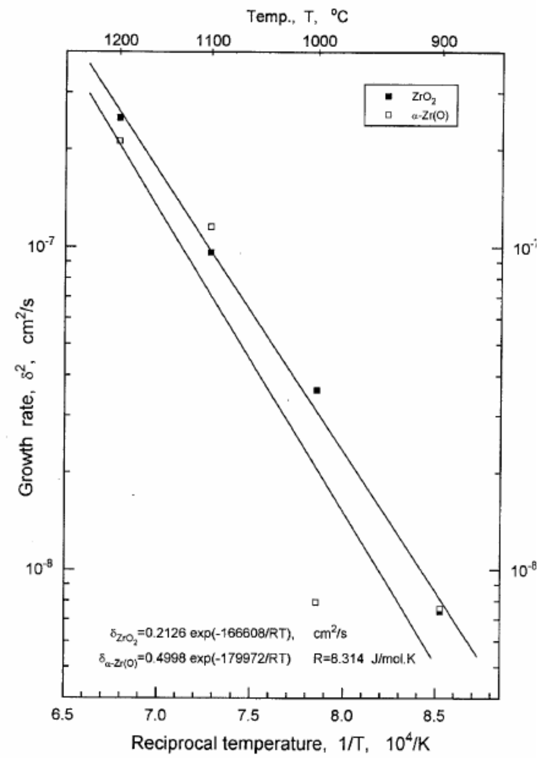

Figure 20. Temperature dependence of oxide layers' formation on the basis of Zr1%Nb oxidation tests in steam between 900 - 1200 °C.

5.1.3. Experiments 'IAEA-CRP'

The oxidation experiments were performed in the IAEA co-ordinated research programme in 1997 in order to investigate the oxygen uptake, ZrO_2 and α-Zr(O) layers' formation and hydrogen absorption of Zr1%Nb alloy in steam atmosphere in the temperature range of 500-900 °C [9].

The specimens were 5 mm long slices of VVER fuel cladding tubes (∅9.1 x 0.7). The total surface (inner and outer) area of the specimen was 3 cm^2. The experimental facility was similar to that of the former oxidation tests. The set-up involved a tube furnace with temperature control system and a steam generator with superheater to provide constant steam flow. The specimens and a thermocouple were located in a quartz tube passing through the furnace. Six specimens were oxidized simultaneously. The temperature control system provided isothermal conditions with the accuracy of ±1°C. The oxidation time varied from 30 s to 180 h, depending on the temperature of the test.

Mass gain due to the oxidation was derived by means of microbalance measurements before and after the test. The hydrogen content of the specimens was determined by post-test hot extraction method; i.e. the specimens were heated and flushed with argon gas and the released hydrogen was detected by means of gas chromatography. ZrO_2 and α-Zr(O) layers' thicknesses were measured as well (Appendix 8).

The oxidation rate constants were derived on the basis of the measured data. Figures 21 and 22 present the temperature dependencies of the rate constants for the mass gain, and the zirconium oxide layer formation, respectively. The relations fitted to the measured data are summarised below:

Mass gain rate ($mg \cdot cm^{-2} \cdot s^{-1/2}$):

$$k_{\Delta m} = 284.1 \cdot \exp(-79274 / RT) \tag{13}$$

Where:

R	-	8.314 *J/(mol.K)*
T	-	temperature in *K* [773; 1173]

ZrO_2 formation rate ($cm \cdot s^{-1/2}$):

$$k_{ZrO_2} = 2.88 \cdot \exp(-86468 / RT) \tag{14}$$

α-Zr(O) formation rate ($cm \cdot s^{-1/2}$)

$$k_{\alpha Zr(O)} = 18.0 \cdot \exp(-129419 / RT) \tag{15}$$

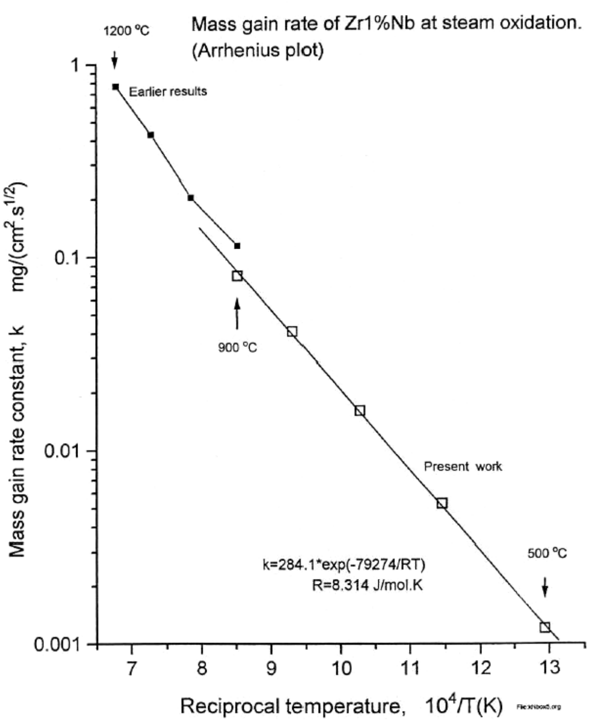

Figure 21. Temperature dependence of the mass gain on the basis of oxidation tests in steam

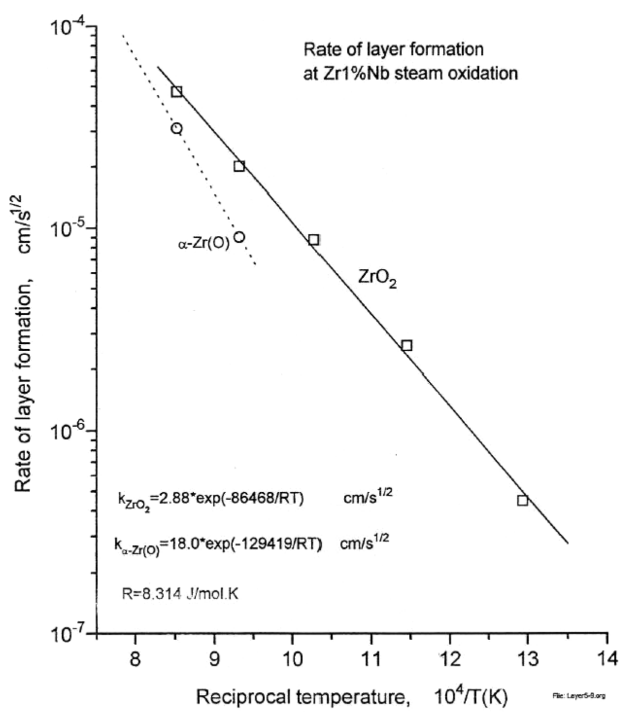

Figure 22. Temperature dependence of oxide layers' formation on the basis of oxidation tests in steam

5.1.4. Experiments 'OAH-ABA'

An experimental project supported by the Hungarian Atomic Energy Authority (HAEA) was initiated in 2000 in order to compare the oxidation and hydrogen uptake kinetics of Zr1%Nb and Zircaloy-4 cladding alloys [10, 11, 12].

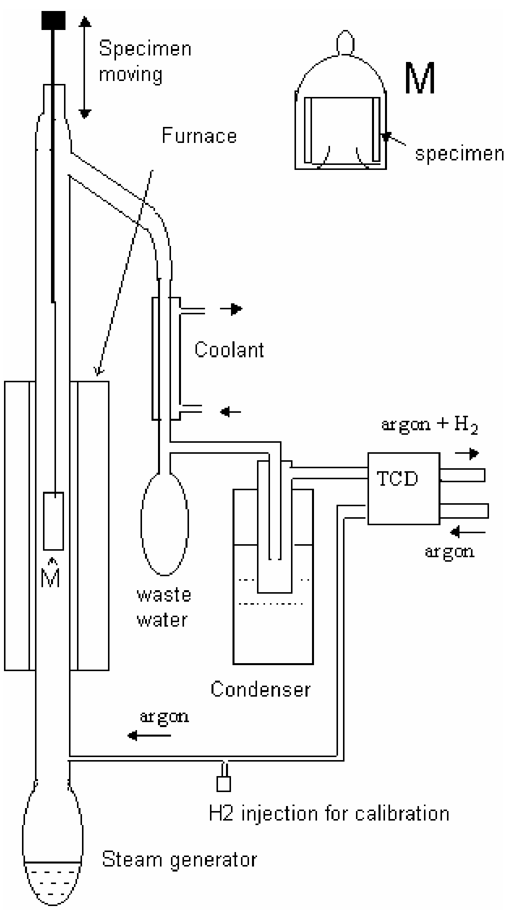

Figure 23. Test facility for steam oxidation of cladding specimens

The experimental set-up for the oxidation tests contained a steam generator, a tube furnace with precise temperature control system, a quartz tube as the reaction volume and a condenser (Figure 23). The H_2 formation was monitored on-line by gas thermal conductivity measurement: argon as carrier gas was fed to the steam flow in the concentration of 12 v%. (Experiments indicated that this amount of Ar gas does not influence the kinetics of the oxidation.) After condensing the steam at the outlet of the test tube the Ar-H gas mixture was monitored by a thermal conductivity detector (TCD). The signal of the detector was proportional to the H_2 concentration in the gas mixture.

Ring specimens of original cladding tubes (Zr1%Nb: ∅9.1 x 0.7, Zircaloy: ∅10.74 x 0.73) with the identical length of 8 mm were oxidized in steam under isothermal conditions at 900, 1000, 1100, and 1200 ^{o}C. The steam flow rate was 8.5-11 cm/s. Due to different oxidation temperatures and time intervals the ECR varied between 1 and 40%. The mass gain of the samples was measured by analytical balance with the accuracy of ± 1 mg.

Post-test investigations involved mechanical compression tests on tensile machine to analyse the embrittlement of the oxidized samples and also the hot extraction of absorbed hydrogen.

The performed experiments proved that the mass gain due to oxidation is linearly proportional to the square root of the exposure time. The mass gain for unit surface area can be described as follows:

$$\frac{\Delta m}{F} = A \cdot \exp\left(\frac{-Q}{RT}\right) \cdot t^{1/2} \qquad (16)$$

Where:

Δm mass gain (mg)
F surface area (cm^2)
A pre-exponential factor

Q	activation energy (J)
R	gas constant = 8.314 J/(mol·K)
T	temperature (K)
t	time of steam exposure (s)

$k = A \cdot \exp(\frac{-Q}{RT})$ is called to the reaction rate constant. On the basis of the mass gain data measured for Zr1%Nb and Zircaloy-4 the following relations were derived for the oxidation rate constants versus temperature (Figure 24):

$$k_{Zr1\%Nb} = 288.6 \cdot \exp\left(\frac{-77576}{R \cdot T}\right) \quad (17)$$

$$k_{Zircaloy} = 3273 \cdot \exp\left(\frac{-103667}{R \cdot T}\right) \quad (18)$$

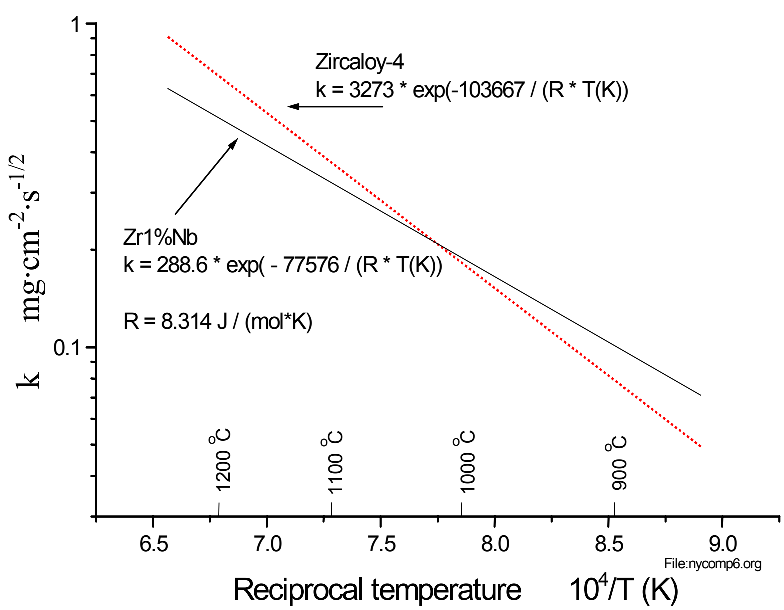

Figure 24. Oxidation rate constants for Zr1%Nb and Zircaloy-4 as a function of the temperature on the basis of experimental mass gain data

As it was observed on Zr1%Nb specimens during the oxidation at 900-1000 °C, the ZrO_2 layer periodically breaks away at the thickness of 8-14 μm. After the break-away phenomenon the oxidation and also the H_2 absorption accelerate. Consequently equation 17 is valid till the first break away of the ZrO_2 layer (at the thickness of about 10 μm). On the other hand, compact oxide layer formed if the oxidation temperature exceeded 1000 °C. At 1100 and 1200 °C there was no spalling of ZrO_2 observed and the on-line H_2 detection proved the validity of the square root relationship between the reaction rate and the time during the total oxidation period. Hot extraction method confirmed that the H_2 absorption was also limited by the compact ZrO_2 layer (Figure 25).

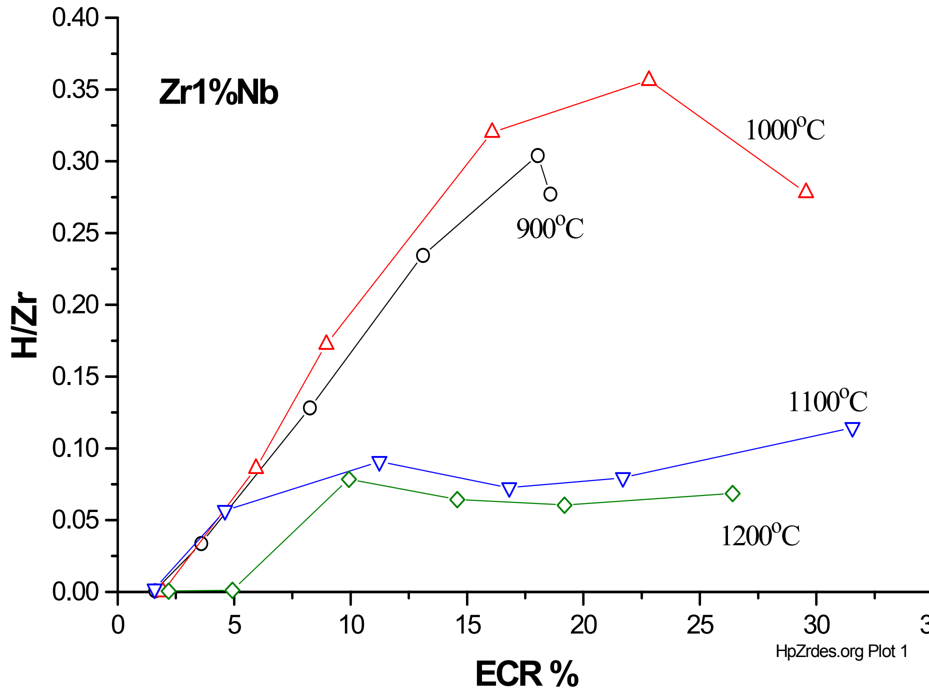

Figure 25. H/Zr ratio measured by hot extraction method in Zr1%Nb specimens oxidized to the ECR of 35% at different temperatures.

Oxidation of Zircaloy-4 specimens indicated more compact oxide layer formation and very limited H_2 absorption. Oxide spalling and measurable H_2 up-take occurred only at 1000 ^{o}C at a considerably thick ZrO_2 layer (> 60 μm) formed during a 40-minute steam exposure.

Ring compression tests pointed out that due to intensive H_2 absorption the Zr1%Nb cladding embrittles more widely during steam oxidation than the Zircaloy-4 tube.

Experimental data of Zr1%Nb and Zircaloy-4 specimens have been tabulated in files *'OAHzrnb.prn'* and *'OAHzry.prn'* (Appendix 9), respectively. More information concerning experimental results can be found in ref. [11].

5.1.5. Experiments 'HTARTOX'

Oxidation experiments performed with as-received and hydrided Zr1%Nb and Zircaloy-4 ring specimens in order to study the effect of the cladding's hydrogen content on the oxidation rate and the emission of hydrogen during the late phase of the steam oxidation [12, 13]. The experimental facility for steam oxidation is presented in chapter 5.4. The kinetics of the oxidation and the hydrogen emission were analysed on the basis of TCD signals proportional to the H_2 content of the exhaust gas mixture. Mass gain of the specimens was measured by analytical balance, too.

Data evaluation indicated, that the oxidation rate of hydrided specimens was lower than that of the as-received samples. On the other hand, the hydriding of the specimens did not influence considerably the hydrogen emission during the late phase of the oxidation.

The database contains the geometry, the mass gain data and the resulted oxidation rate of only the as-received specimens (file *'htartox.prn'*, Appendix 10).

5.1.6. Experiments 'OMFB-94'

One of the first oxidation tests performed in 1994 at the AEKI in the framework of a comprehensive project to study fuel rod performance. The project was supported by the National Committee for Technological Development (OMFB).

Zr1%Nb tube specimens were oxidized in steam at 1010 °C in order to check the square root relationship between the oxidation rate and the time for the VVER cladding alloy and to compare the reaction rate with published data. The time of oxidation varied from 500 s to 4000 s. Measured mass gain data and the derived oxidation rate constants are tabulated in file 'omfb-94.prn'.

The experiments nicely reproduced the reaction rate constants measured by other institutions (e.g. FZK, Karlsruhe – Figure 26) at the same temperature.

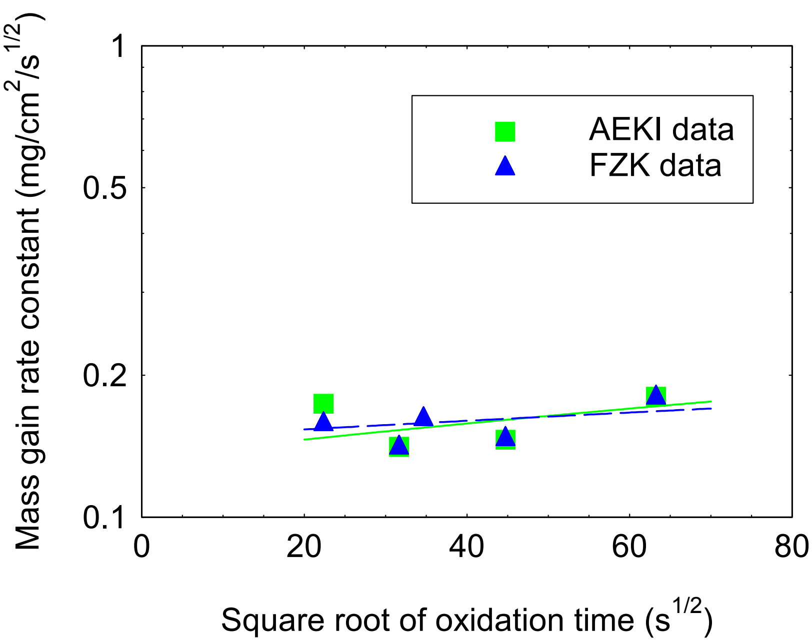

Figure 26. Comparison of mass gain rate constants derived from AEKI and FZK oxidation tests performed with Zr1%Nb alloy at 1010 °C.

5.2. Test series in hydrogen rich steam atmosphere

Data of four different series of oxidation experiments were involved in the database. The experiments were performed in order to provide pre-oxidized samples for ring compression, tensile and ballooning tests and to study the effect of the presence of hydrogen in steam atmosphere on the oxidation kinetics.

5.2.1. Description of the tests

Un-irradiated, original VVER cladding specimens (outer diameter: 9.14 mm) were oxidized in a controlled, mixed steam-hydrogen atmosphere under isothermal conditions between 900 and 1100 °C. Two test series (first and fourth series) were carried out for ring compression tests. In the first test series the hydrogen content in the steam was fixed between 0 and 36 vol. %. During the fourth series the experiments were performed in extended range (the H-content was 5 and 65% in the steam). The second and third oxidation series were performed in 20 – 36 vol. % hydrogen-steam mixture for ring tensile and ballooning tests. After steam exposure for different time periods the samples were characterized by their oxygen content. The oxygen content was defined as oxidation ratio. The extent of the oxidation was measured through the weight gain of the specimens. Prior to testing, the specimens were degreased in acetone.

A high temperature tube furnace was used for the oxidation of the samples. The experimental set-up consisted of a steam generator, a three-zone furnace and a condensing system (Figure 27). The outlet hydrogen flow rate was measured by calibrated Soap Bubble Gas Flow Meter, the steam flow was evaluated through the measured weight of the condensed water. When the temperature of the furnace and the steam + hydrogen flow became stabilized, the sample in a quartz boat was pushed to the centre of the furnace. At the end of oxidation the sample was withdrawn to the cold part of the quartz tube.

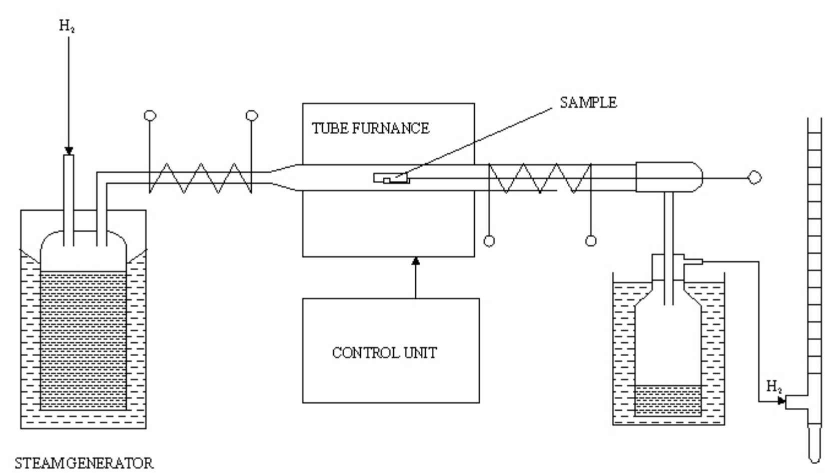

Figure 27. Scheme of the experimental set-up for oxidation tests

5.2.2. Pre-oxidation for ring compression tests

The oxidation was carried out at three different temperatures (900, 1000, 1100^{o}C) in a constant flow of steam-hydrogen mixture [14]. At each temperature several samples with 8 mm length were oxidized during different times in order to achieve different oxidation ratios. The extent of oxidation did not exceed 18 % ECR. In 2004 (1. test series) the hydrogen content of the steam was 0, 20, 28 or 36 vol. %. During the fourth series (2006) the H-content was 5 and 65 vol. % in the steam.

The experimental data are tabulated in the data files 'cohyra_ox1.prn' and 'cohyra_ox4.prn' printed in Appendix 13. The tabulated oxidation rate constants were derived from the measured weight gains and oxidation times assuming parabolic relation.

5.2.3. Pre-oxidation for ring tensile tests

The specimens with 2 mm length were oxidized in constant steam-hydrogen flow at the temperature of 900, 1000, or 1100 ^{o}C. The extent of oxidation did not exceed 6 % ECR in the performed experiments. The range of hydrogen content in the steam was 0 - 36 vol. %.

The measured data and the derived oxidation rate constants are tabulated in the data file 'cohyra_ox2.prn' and printed in Appendix 14.

5.2.4. Pre-oxidation for ballooning tests

The 100 mm long Zr1%Nb tube specimens were oxidized under isothermal conditions in constant steam-hydrogen flow. Only the outer surface of the specimens was oxidized, since both ends of the tubes were plugged. The maximum oxidation ratio was 5 %. The hydrogen content in the steam was 20 or 36 vol. %.

The information of these experiments are summarized in the data file 'cohyra_ox3.prn' and printed in Appendix 15.

5.2.5. Determination of hydrogen content

After a high temperature desorption (hot extraction) the amount of absorbed hydrogen was determined by gas chromatographic method using CHROMPACK MODEL 438A Gas Chromatograph with thermal conductivity detector (TCD). The broken pieces of the cladding rings after mechanical testing were used for high temperature desorption.

The measured data are tabulated in the data files 'cohyra_ox1.prn, cohyra_ox4.prn cohyra_ox2.prn, cohyra_ox3.prn, cohyra_compr.prn and cohyra_tensile.prn' and printed in Appendix 13-17.

5.2.6. Results and conclusions

The experiments confirmed that the mass gain due to the hydrogen-rich steam oxidation is linearly proportional to the square root of the exposure time. The mass gain for surface area can be described as follows:

$$\frac{\Delta m}{F} = k \cdot t^{1/2} = A \cdot \exp(\frac{-Q}{RT}) \cdot t^{1/2} \qquad (19)$$

Where:

Δm	mass gain (mg)
F	surface area (cm^2)
A	pre-exponential factor
Q	activation energy (J)
R	gas constant = 8.314 J/(mol·K)
T	temperature (K)
t	time of steam exposure (s)
k	reaction rate constant ($mg/cm^2/s^{1/2}$)

On the basis of the mass gain data measured for E110 in 20 vol. % hydrogen-steam atmosphere the following relation was derived for the oxidation rate constants versus temperature (Figure 28):

$$k = 117 \cdot \exp\left(\frac{-8680}{T}\right) \qquad (20)$$

The oxidation rates constants measured in pure steam and in different steam-H_2 mixture are represented in Figure 28 and Figure 29.

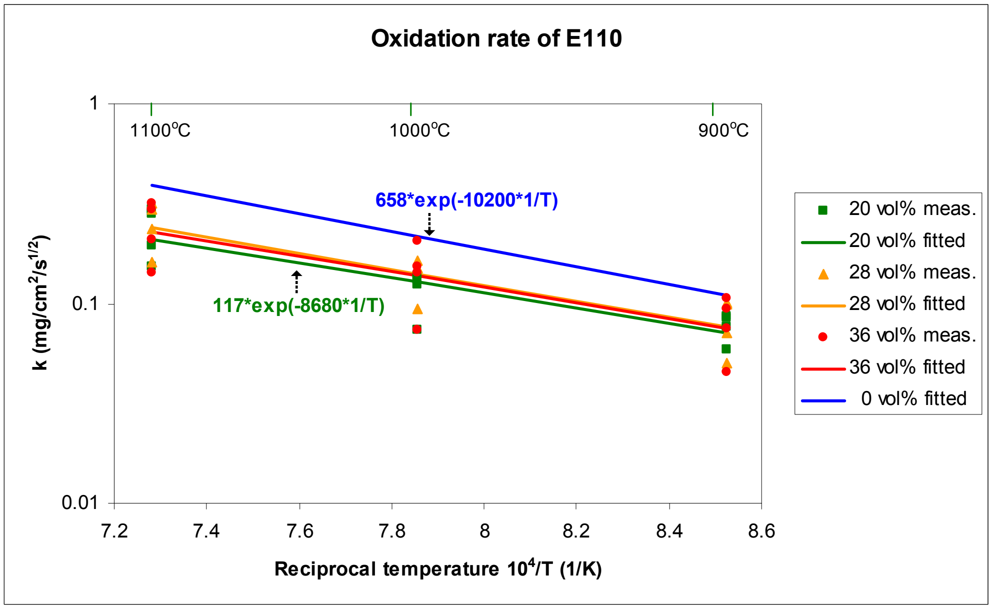

Figure 28. Oxidation rate constants for E110 as a function of reciprocal temperature in steam-hydrogen mixture (first test series)

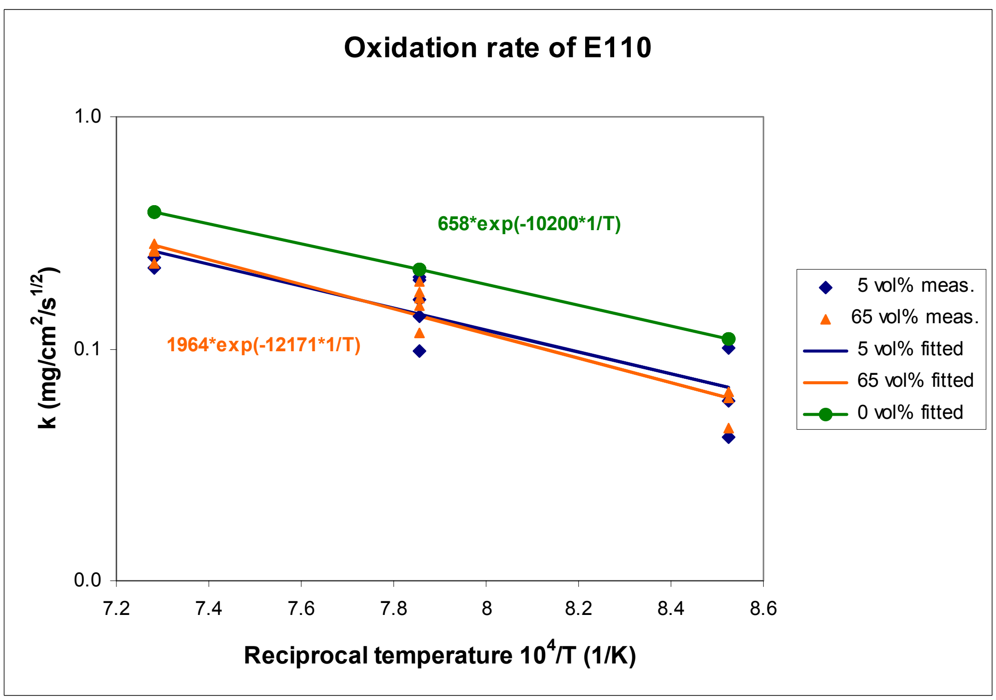

Figure 29. Oxidation rate constants for E110 as a function of reciprocal temperature in steam-hydrogen mixture (fourth test series)

The mass gain rate constants measured in 65 vol.% H-steam mixture have no significant difference as compared to the result in 5 vol.% H-steam mixture.

Comparing the oxidation rate constants measured in pure steam and in hydrogen-rich steam atmosphere, it can be concluded that the hydrogen content in the steam decelerates the cladding oxidation [15].

Comparing the hydrogen contents of the cladding specimens oxidized in pure steam and in steam-hydrogen mixture, enhanced hydrogen absorption was observed in hydrogen rich steam atmosphere (Figure 30 and Figure 31).

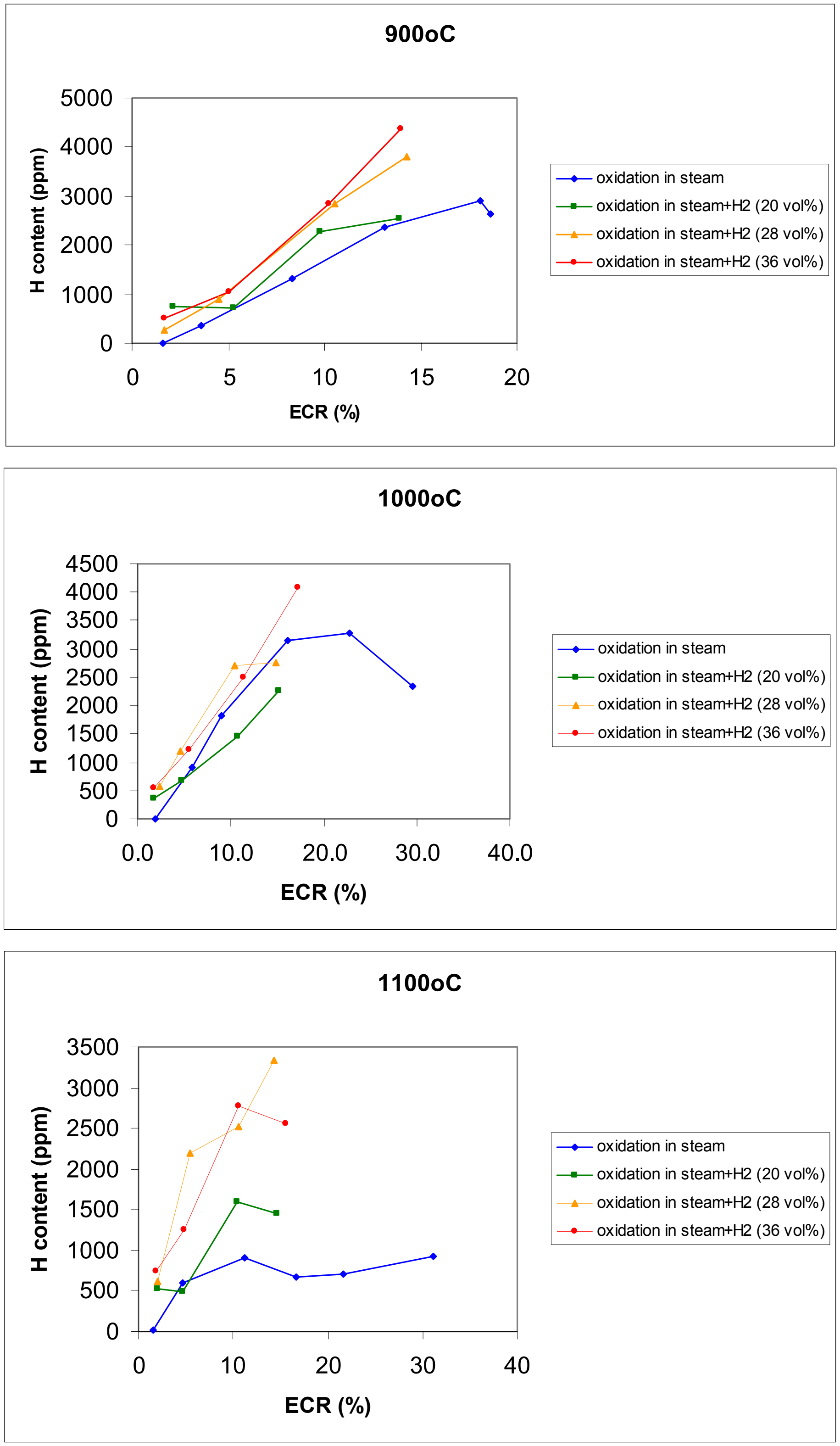

Figure 30. Hydrogen content of Zr1%Nb claddings oxidized in pure steam and in steam-hydrogen mixture at 900, 1000 and 1100 °C

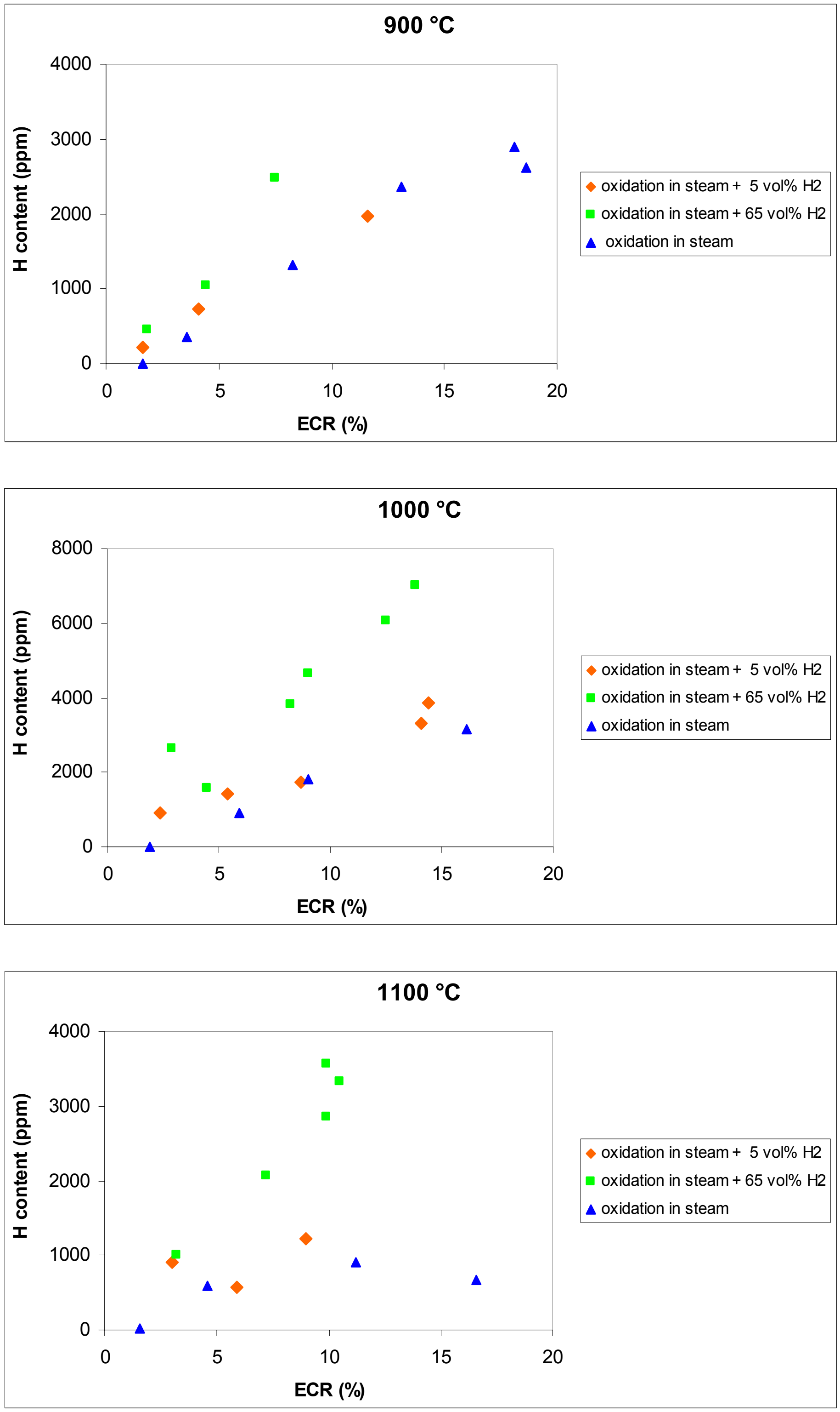

Figure 31. Hydrogen content of Zr1%Nb claddings oxidized in pure steam and in steam-hydrogen mixture at 900, 1000 and 1100 °C

6. RING COMPRESSION TESTS

6.1. Test series in steam atmosphere

For the samples with different oxidation conditions the same ring compression testing procedure was applied to characterize the embrittlement process of the two type alloys.

6.1.1. Description of the tests

The oxidized ring samples (E110 and Zircaloy-4) with 8 mm length were examined in radial compression tests using INSTRON 1195 universal testing machine. The velocity of the crosshead moving was 2 mm/min. The rings were loaded until the total plastic deformation or at least until the first indication of cracking. The load-displacement curves were recorded and the crushing force and deformation were determined.

The effect of ductile/brittle behaviour was expressed in the term of relative deformation.

6.1.2. Results and conclusions

Experimental data are summarised separately for Zr1%Nb and Zircaloy-4 ring specimens in the files 'comprzrn.prn and comprzry.prn'. The summary files are printed in Appendix 12.

The results of the radial compression tests well indicated the embrittlement of the cladding materials due to the oxidation process. Figure 32 shows typical compression diagrams for Zr1%Nb samples oxidized at 900°C at different extent of oxidation.

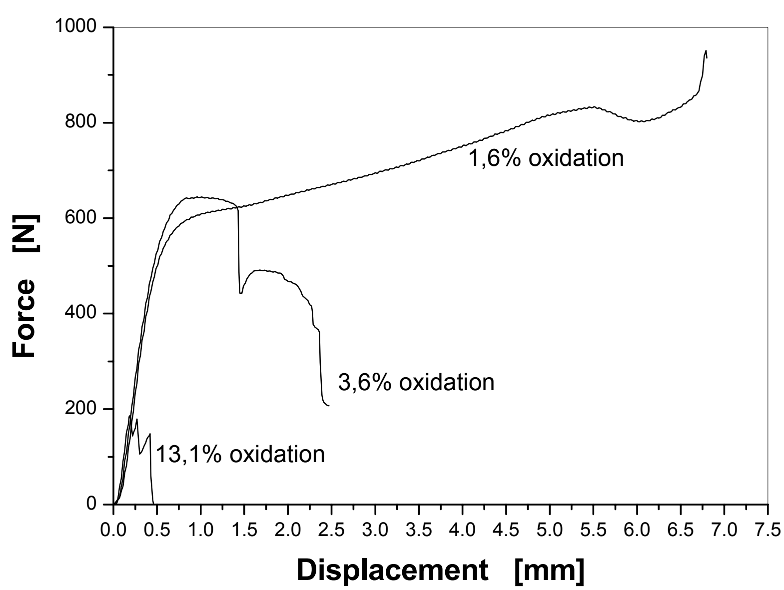

Figure 32. Force-displacement diagrams recorded during radial ring compression testing of Zr1%Nb samples oxidized in steam

The ring compression tests performed in AEKI showed different mechanical behaviour of the two alloys. At low (1 – 3 %) oxidation ratio the relative deformation for both types of samples was 40 – 60 % (Fig. 33). At ~5 % the difference became significant. Less than 10 % relative deformation was measured for Zr1%Nb and more than 10 % for Zircaloy-4. With increasing oxidation ratio the relative deformation decreased.

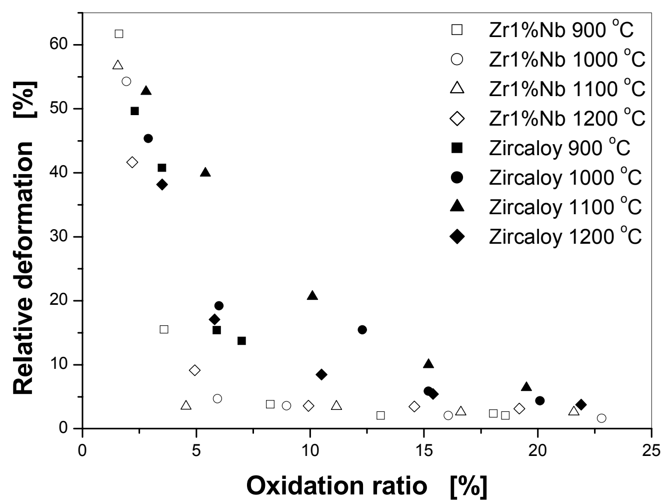

Figure 33. Relative deformation as a function of oxidation ratio for Zr1%Nb and Zircaloy-4 samples oxidized in steam

In Fig. 34 the experimental results are presented as relative deformation versus hydrogen content. It can be observed that the above 600 ppm hydrogen concentration both Zr1%Nb and Zircaloy-4 samples became brittle. The figure indicates that the Zircaloy-4 with close to zero hydrogen content can be very brittle as well, obviously due to the high extent of oxidation.

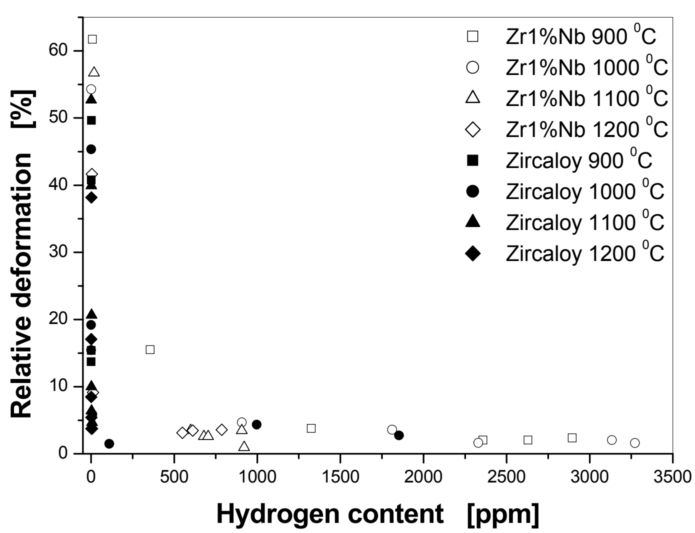

Figure 34. Relative deformation as a function of hydrogen content for Zr1%Nb and Zircaloy-4 samples oxidized in steam

6.2. Test series in hydrogen rich steam atmosphere

Investigation of the ductile-brittle transition of the cladding was the primary objective of the ring compression tests.

6.2.1. Description of the tests

The oxidized E110 ring samples with 8 mm length were examined in radial compression tests at room temperature using INSTRON 1195 universal testing machine. The velocity of the crosshead moving was 0.5 mm/min. The rings were loaded until the total plastic deformation or at least until the first indication of cracking. The load-displacement curves were recorded and the crushing force and deformation were determined. The cladding ductility was characterized with the specific energy at failure (i.e. the integral of the load-displacement curve for the unit length of the ring specimen):

$$E_s = \frac{1}{L}\int_0^{U_C} F(U)dU \tag{21}$$

Where:

- E_s specific energy (mJ/mm)
- L length of the specimen (mm)
- F force (N)
- U displacement (mm)
- U_C displacement at first cracking (mm)

The experimental data are summarised in the files 'cohyra_compr.prn, cohyra_compr2.prn' and printed in Appendix 16. The compression curves and the load-displacement data are collected in the files 'cohyra_compr_curves.pdf', 'cohyra_compr2_curves.pdf', '(cohyra_compr_data01–39).prn' and '(cohyra_compr2_data01 – 28).prn'

6.2.2. Results and conclusions

The hydrogen uptake strongly reduced the ductility of the cladding. According to our earlier studies with oxidized E110 rings [16, 17], 50 mJ/mm specific energy was found as a boundary of ductility. In view of this limit, the cladding oxidized in 20 – 36 vol% hydrogen-steam mixture, became brittle above ~500 ppm hydrogen content (Figure 35).

However, the embrittlement of the claddings oxidized in 5 vol% H-steam mixture have no significant difference compared to the result on 65 vol% H-steam mixture (Figure 36). (The specimens oxidized in 5 and 65 vol% hydrogen-steam mixture were probably cut from another E110 cladding than the specimens oxidized in 20 – 36 vol% hydrogen-steam mixture).

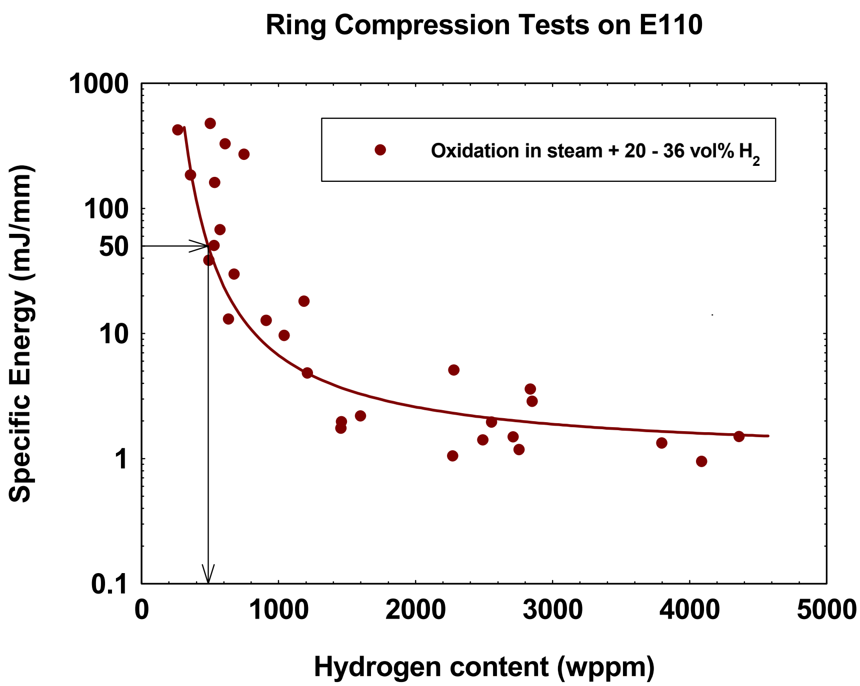

Figure 35. Specific energy at failure as a function of hydrogen content of the samples

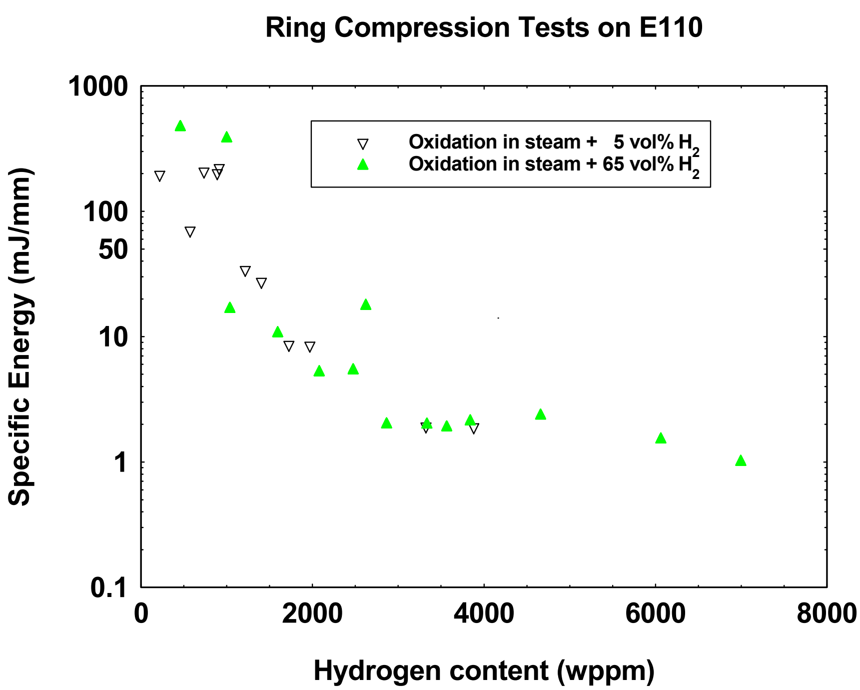

Figure 36. Specific energy at failure as a function of hydrogen content of the samples

The specific energies of specimens oxidized in pure steam and in different hydrogen-steam mixture (5, 65 and 20 – 36 vol% H_2) are compared in Figure 37. The figure clearly indicates that, due to a more intense hydrogen absorption the embrittlement of the cladding takes place at lower oxidation level (about 3 %) in hydrogen rich steam atmosphere than in pure steam or in steam with low hydrogen content (5 vol%).

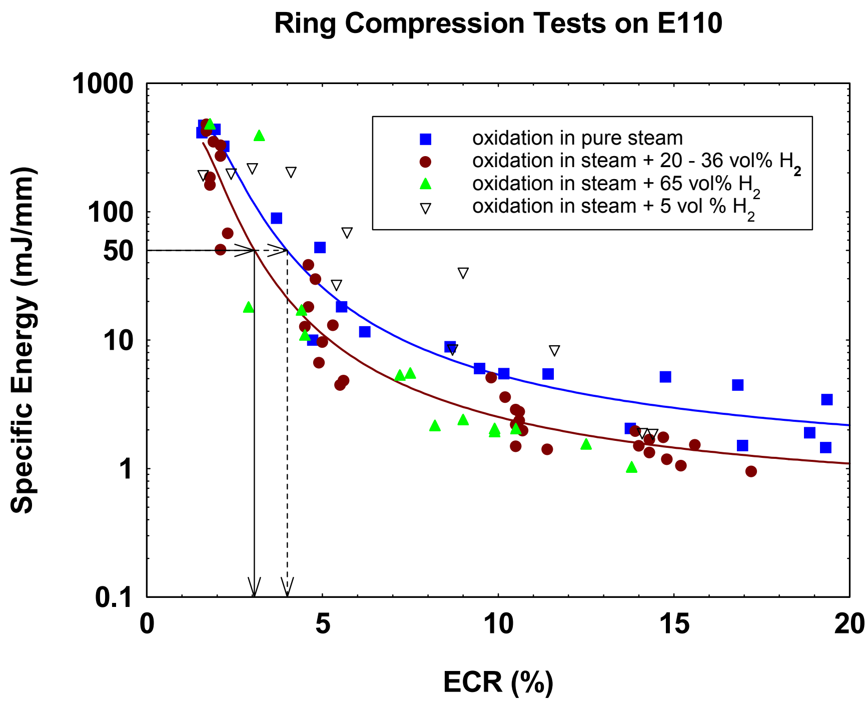

Figure 37. Specific energy at failure versus the measured oxidation ratio

Representing the time of oxidation as a function of the temperature and distinguishing brittle and ductile specimens on the basis of the specific energy of ring compression, a ductility limit (τ - oxidation time till cladding embrittlement) could be defined (Figure 38):

$$\tau_{E110} = 2 \cdot 10^{-4} \exp(17500 / T) \tag{22}$$

According to the results of the ring compression tests, the above correlation for the ductility limit of E110 is valid in hydrogen rich steam atmosphere, as well. Since the slow down of the oxidation compensates the mechanical deterioration of the cladding due to intense hydrogen uptake, the cladding embrittlement does not occur earlier in hydrogen-rich atmosphere than in pure steam.

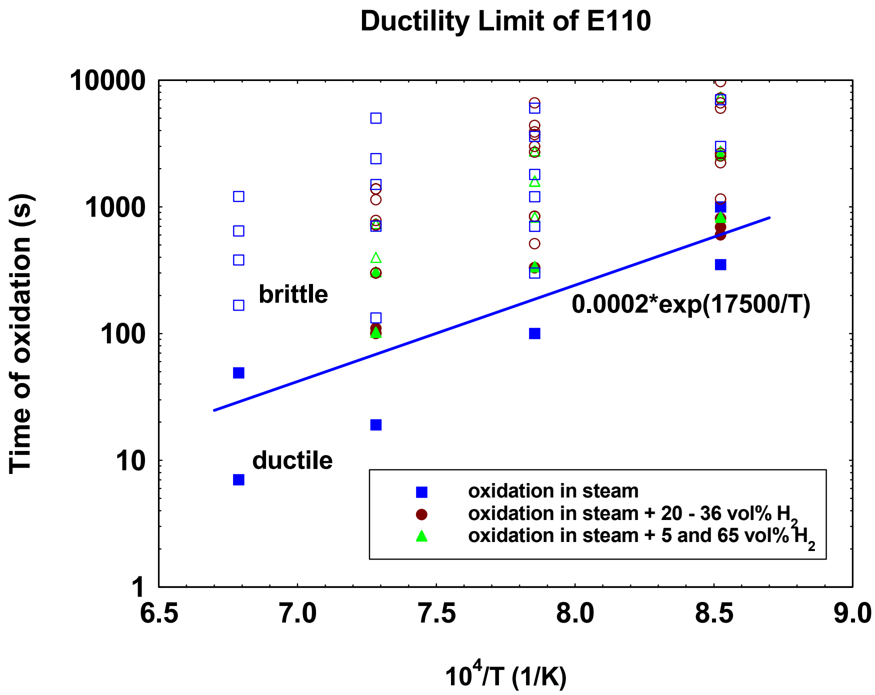

Figure 38. Time of oxidation versus the reciprocal of the oxidation temperature

7. POST-TEST INVESTIGATIONS

7.1. Test series in hydrogen rich steam atmosphere

7.1.1. Visual observations

The photographs of oxidized E110 samples after ring compression and tensile tests are collected in the files ‘cohyra_compr_photo.pdf, cohyra_tensile_photo.pdf’.

It has been observed that the oxidation in steam-hydrogen atmosphere produced cracked oxide layer at 900 and 1000 ^oC. The oxide scale flaked off from the cladding on most of the surface. The appearance of the oxide layer depended on the temperature and time of the hydrogen rich steam oxidation. At 1000 ^oC a cracked oxide layer with pinkish color was observed. The longer oxidation time resulted in a more cracked oxide layer. At higher temperature (1100 ^oC) the formation of a compact oxide layer was typical.

7.1.2. Metallographic analysis

Metallographic analysis of cross sections was performed with optical Reichert Me-F2 microscope. The investigation was carried out after the ring compression tests, thus some specimens can loose a part of their oxide layer.
The preparation of the specimens was the follows:

- Grinding
- Mechanical polishing
- Swab etching
- Washing in water
- Air drying

The cross sections of the oxidized E110 samples after ring compression test are collected in the file ‘cohyra_compr_metgraph.pdf’.

Metallographic investigation of selected burst specimens was carried out as well. The cross sections are stored in the file ‘cohyra_balloon_metgraph.pdf’

7.1.3. SEM analysis

The SEM analysis was performed on two types of samples:

1. Zr1%Nb tube samples prepared for ballooning test
2. Compressed ring samples with 8 mm length

From the first type of samples, sample pieces were cut from tubes, which were opened up at the ballooning tests. They were glued to SEM sample holders by means of special resin. Samples were studied directly, i.e. without any evaporated or sputtered carbon layer. Philips SEM 505 type of scanning electron microscope was operated at 5 KV (due to the sensitivity of the samples for the electron beam) by using a few $\times 10^{-10}$ A specimen current.

From the second type of samples, such pieces were selected, which had the oxide layers on both sides. These pieces were glued on the SEM holders in such way, that the cross section of them could be revealed. 20 kV accelerating voltage and a few times 10^{-10} A specimen current were applied.

7.1.3.1. Results of the ballooning samples

Figure 39 in the Appendix 20 shows digital secondary electron images (SEI) of the studied samples taken at 15 times of magnification. 4 mm x 4 mm sample areas are presented, revealing the opening up of the samples. It can be seen in the images that the opening up of the samples happened in various ways: sample Fuv_5 had the smallest opening size which did not decrease so much at the middle part.

Table 5. contains the data for lengths and widths of the openings up.

Mark of the sample	Opening length (mm)	Opening width (min, max; mm)
Fuv_1	3.93	0.26 – 0.49
Fuv_3	3.48	0.14 – 0.49
Fuv_5	1.67	0.28

Table 5. Opening sizes of the studied samples

Figures 40 and 41 (Appendix 20) show both ends of opening up for sample Fuv_3 and Fuv_5 at 100 times of magnification.

The digital secondary electron images of the studied samples are collected in the file ‘cohyra_balloon_sem.pdf’.

7.1.3.2. Results of the compressed ring samples

Figure 42 in the Appendix 20 shows digital SEI images of selected compressed ring samples oxidized at 900 ^{o}C temperature for different periods. At 9720 s oxidation time the thickness of the oxide was about 20 μm at some places, while at other areas about 50 μm thick oxide layers (four layers) could be found. At 11520 s several oxide layers (altogether with 60-70 μm thickness) can be revealed. These oxide layers could be removed easily. Beside the oxide layer(s) well crystallised alpha zirconium could be found, the thickness of it could be 40 – 60 μm. The structure of the next phase, the beta-zirconium consisted of relatively large base crystals and Widmanstätten structure was typical for the studied samples. All these features can be seen in Figure 43.

Figure 44 (Appendix 20) shows digital SEI images for samples oxidized at 1000 ^{o}C. The thickness of the oxide layer(s) increased by increasing of the oxidation time: at 330 s the thickness of the oxide was 15-20 μm. At 3900 s three oxide layers were found, having thicknesses between 10 and 15 μm. At 6600 s generally two oxide layers could be seen, each of them had thickness of 20-40 μm. The multiple oxide layers could be removed easily. The next layer, the alpha phase, stabilised by oxygen, had thicknesses from about 30 μm up to 80 μm. The beta phase consisted of larger crystals, inside of them lathes could be seen, which run parallel to each other. This is typical mainly for sample PUM-VH-12, which had the highest hydrogen content. Widmanstätten lines are also characteristic for the studied samples (see Figure 45). At the lowest hydrogen content (sample PUM-VH-1) the microstructure is typical for a ductile-rigid fracture.

Figure 46 shows digital SEI images for samples oxidized at 1100 ^{o}C. At 300 s the oxide layer (not always could be revealed) had thickness of 15-25 μm, while at 1140 s two or three oxide layers could be found altogether with about 50 μm thickness. Looking at the microstructure of the compressed ring samples, fracture surface similar to the original material could be seen at low amounts of added hydrogen. At higher hydrogen content fine-sized parallel plates could be found (see Figure 46).

The digital secondary electron images are stored in the file 'cohyra_compr_sem.pdf'.

8. DIRECTORY STRUCTURE OF THE DATABASE

The directory structure of the database followed the grouping presented in Chapter 2. The experimental data are stored in four main directories for the ballooning, the tensile, the compression and the oxidation tests. Separated directories contain the present and previous database reports and other English language publications.

All the experimental data are stored in formatted ascii files (*.prn) to support computerised processing independently from the applied operation system. The publications and figures are stored in pdf files. Photos are presented in jpeg, bmp or pdf formats.

Directories of the database and their contents

Directory \ Subdirectory	Content of the directory
OXIDATION	Oxidation Experiments
TENSILE	Tensile tests
TENSILE \ ZR1NB	with Zr1%Nb specimens
TENSILE \ ZRY-4	with Zircaloy-4 specimens
TENSILE\ COHYRADATA	Summarized experimental data and Load – displacement data
TENSILE\ COHYRAPICS	Photos of the specimens and tensile curves
BALLOON	Ballooning experiments
BALLOON \ BALL	Single rod tests BALL
BALLOON \ BALL \ CUTS	Photos of the cuts
BALLOON \ BALL \ EXP1	Data of the 1st test series
BALLOON \ BALL \ EXP2	Data of the 2nd test series
BALLOON \ 7ROD	7-rod bundle tests
BALLOON \ 7ROD \ CUTS	Photos of the cuts (compiled)
BALLOON \ 7ROD \ CUTS \ SPLIT	Bitmap of each cut
BALLOON \ 7ROD \ EXP	Experimental data, histories
BALLOON \ 7ROD \ PICS	Auxiliary photos
BALLOON \ 7ROD \ GRAPHS	Figures of the experimental data
BALLOON \ PUKI	Single rod tests PUKI (Zr1%Nb specimens)
BALLOON \ PUKI \ EXP	Experimental data, histories
BALLOON \ PUKI \ PICS	Photos of the burst specimens
BALLOON \ PUZRY	Single rod tests PUZRY (Zircaloy specimens)
BALLOON \ PUZRY \ EXP	Experimental data, histories
BALLOON \ PUZRY \ PICS	Photos of the burst specimens
BALLOON \ COHYRADATA	Summarized experimental data, temperature and pressure histories

BALLOON \ COHYRAPICS	Photos, cross sections and SEI of the burst specimens
COMPRESSION	Compression tests with
COMPRESSION \ ZR1NB	Zr1%Nb specimens
COMPRESSION \ ZRY-4	Zircaloy-4 specimens
COMPRESSION \ COHYRADATA	Summarized experimental data and Load – displacement data
COMPRESSION \ COHYRAPICS	Photos of the specimens, compression curves, cross sections and SEI of the rings
PUBLICAT	English language publications about the experiments
REPORT	Present database report Previous database report (2002) Previous database report (2006)

9. REFERENCES

[1] Cs. Győri, Z. Hózer: Extension of TRANSURANUS Code Applicability with Nb Containing Cladding Models: EXTRA Project, Description of Work; Annex 1 of contract FIKS-CT2001-00173

[2] Horváth L., Windberg P., Hózer Z.: *Felfúvódásos és Besugárzásos Mérések VVER Fűtőelem Burkolattal;* Research Report in Hungarian, OMFB-00033/98 (98-97-45-1636), Budapest, 1999 december.

[3] Z. Hózer, L. Maróti, L. Matus, P. Windberg: Experiments with VVER Fuels to Confirm Safety Criteria; ENS TopFuel 2001, P2-14, Stockholm, Sweden, May 2001. (File: topfuel-01.pdf)

[4] Frecska J., Matus L., Pummer I.,: *Fűtőelemviselkedés VVER Reaktortípusnál*; Research Report in Hungarian , OMFB-94-97-47-0817/2.5, 1996.

[5] Cs. Győri, Z. Hózer, L. Maróti, L. Matus: VVER Ballooning Experiments; EHPG Meeting Lillehammer, March 1998; HPR-349/40. (File: ehpg-98.pdf)

[6] Á. Griger, L. Maróti, L. Matus, P. Windberg: Ambient and High Temperature Mechanical Properties of ZrNb1 Cladding with Different Oxygen and Hydrogen Content; EHPG Meeting May 1999, Loen; HPR-351/35. (File: ehpg-99.pdf)

[7] L. Matus, L. Vasáros, Z. Hózer: Experimental Results on the Interaction Between Hydrogen and Zirconium Claddings; Report KFKI-2001-02/G, 2001. (File: kfki-01-02.pdf)

[8] J. Frecska, G. Konczos, L. Maróti, L. Matus: Oxidation and Hydriding of Zr1%Nb Alloys by Steam; Report KFKI-1995-17/G, 1995. (File: kfki-95-17.pdf)

[9] J. Frecska, L. Matus, L. Vasáros: Hydrogen Uptake of Zr1%Nb Cladding by Steam Oxidation During Loss of Coolant Accident; IAEA CRP 9284/R0, Final Report, September 1997. (File: iaea-9284.pdf)

[10] Matus L., Horváth M. Vasáros L.: *Zr1%Nb és Zircaloy-4 Összehasonlítása Vízgőzös Oxidációban*; Research report in Hungarian, OAH-ABA-41/00, 2000.

[11] Z. Hózer *et al.*: Ring Compression Tests with Oxidized and Hydrided Zr1%Nb and Zircaloy-4 Claddings; Report KFKI-2002-01/G, 2002.

[12] L. Matus, L. Vasáros, Z. Hózer: Some Experimental Results on Hydrogen – Cladding Material Interactions; EHPG Meeting Lillehammer, March 2001, HPR-356/27. (File: ehpg-01.pdf)

[13] L. Matus, L. Vasáros: Steam Oxidation of Zr Alloys with H Content, Release of Absorbed Hydrogen; 5th International QUENCH Workshop, FZK Karlsruhe, 1999. (File: quench-5-99.pdf)

[14] E. Perez-Feró, L. Vasáros, Cs. Győri, P. Windberg, Z. Hózer: Oxidation of E110 cladding in hydrogen rich steam atmosphere, 1st. interim report (Contract No. 370037-2004-10 F1ED KAR HU), June 2005.

[15] Cs. Győri, Z. Hózer, E. Perez-Feró, Paul Van Uffelen, Arndt Schubert and Jacques van de Laar: Applying the Transuranus code to VVER fuel under accident conditions. SMiRT 18, Beijing, China, August 7-12, 2005

[16] Z. Hózer, Cs. Győri: Derivation of LOCA Ductility Limit from AEKI Ring Compression Tests, SEGFSM Topical Meeting on LOCA Issues, ANL, May 2004

[17] Cs. Győri, P. Van Uffelen, A. Schubert and J. van de Laar, Z. Hózer: IMPLEMENTING EXPERIMENTAL DATA ON THE ACCIDENTAL BEHAVIOUR OF THE WWER CLADDING OBTAINED AT THE AEKI IN THE TRANSURANUS FUEL PERFORMANCE CODE , 6th Int. Conf. on WWER Fuel Performance, Modelling and Experimental Support, Albena, September 2005.

[18] Cs. Győri *et al.*: Experimental Database of Zr1%Nb Cladding Alloy for Model Development and Code Validation; EVOL-EXTRA-D-1 (FIKS-CT2001-00173), August 2002.

Appendix 1: Data of 7-rod bundle tests

```
# Summary sheet of VVER 7-rod bundle blockage tests (1999)
#
# Measured parameters
#
# P0     - initial pressure (bar)
# P1     - maximum pressure (bar)
# T1     - temperature at failure (C)
# Tmax   - maximum temperature (C)
# Oxid   - average oxide layer at the elevation of burst (um)
# Block  - flow area blockage rate (%)
# Atmo   - atmosphere of the test
#
#
# References:
#
# [1] Horvath L., Windberg P., Hozer Z.: Felfuvodasos es besugarzasos
#     meresek VVER futoelem burkolattal; OMFB-00033/98 (98-97-45-1636),
#     Budapest, 1999 december.
#
# [2] Z. Hozer, L. Maroti, L. Matus, P. Windberg: Experiments with
#     VVER fuels to confirm safety criteria; ENS TopFuel 2001, P2-14
#     Stockholm, Sweden, May 2001. (File: topfuel-01.pdf)
#
#
# Test     P0      P1     T1     Tmax    Oxid    Block   Atmo
#         [bar]   [bar]   [C]    [C]     [um]     [%]
#
   1      10.0    23.0    800    1000      0       72   # argon
   2       3.0     7.5   1100    1200      0       57   # argon
   3      20.0    35.0    900     900      0       59   # argon
   4      30.0    46.0    800     900      0        -   # argon
   5      30.0    53.0    800     900      0       76   # argon
   6      30.0    55.0    900     900      -       43   # steam
   7      20.0    36.0    800     900      -       55   # steam
   8      10.0    20.0    900     900    165       57   # steam
   9       3.0     7.0     -     1300     19       34   # steam
```

File: ‘balloon\7rod\exp\bundle.prn’

```
# AEKI 7-rod bundle tests
# Total rod cross section areas as a function of the axial position
#
#
# Bundle - number of test bundle
# Axpos  - axial position of cut measured from the location of the rods' failure (mm)
# Rod-i  - cross section area of the i-th rod (mm^2) (A1+A2)
# Summ   - total cross section area of the rods (mm^2)
# Block  - flow blockage rate (%)
#
#
# Bundle  Axpos     Rod-1   Rod-2   Rod-3   Rod-4   Rod-5   Rod-6   Rod-7   Summ  Block
#         [mm]     [mm^2]  [mm^2]  [mm^2]  [mm^2]  [mm^2]  [mm^2]  [mm^2]  [mm^2] [%]
# ===================================================================================
#
   1       20.0     78.8    76.0    86.7    90.6    96.4    76.8   109.9   615.2  35.8
   1       12.0     81.4    71.3   101.1   102.7   150.3   150.3   118.2   775.3  71.6
   1        8.0     85.9    72.3   100.4   116.6   144.8    73.2   123.8   717.0  58.5
   1        0.0     87.4    74.5    91.4   115.2   151.0    72.0   123.6   715.1  58.1
   1      -10.0     73.0    68.3    75.4    86.6   135.8    64.8    93.2   597.1  31.7
   1      -20.0     75.9    74.5    65.4    75.1    77.0    67.1    76.8   511.8  12.6
#
   2       20.0     66.9    63.5    63.1    62.9    65.6    66.4    68.4   456.8  0.3
   2        8.0     86.6    85.9    74.0    79.8    82.2   107.5    72.7   588.7  29.8
   2        0.0    101.5   100.8    90.8   100.7   104.0   109.6   101.2   708.6  56.7
   2       -8.0     74.9    76.9    76.7    86.3    76.4    87.3    83.9   562.4  24.0
   2      -20.0     87.5    91.9    77.5    84.8    97.8    89.1    88.1   616.7  36.1
#
   3       20.0     66.9    63.6    63.1    62.9    65.6    66.4    68.4   456.9  0.4
   3       12.0     70.6    68.1    65.7    84.5    69.8    70.7    76.5   505.9  11.3
   3       10.0     72.0    81.7    70.3    92.6    65.5    68.9    80.3   531.3  17.0
   3        2.0    104.9    98.2    84.7    87.8    85.4    74.0   105.4   640.4  41.4
   3        0.0    100.1   106.4    87.8    72.9    89.8    86.4   121.8   665.2  47.0
   3       -2.0    107.8   115.5    96.6    77.7    95.7    92.8   131.1   717.2  58.6
   3      -10.0     81.3    80.5    92.9    71.9    72.7    77.7   110.9   587.9  29.7
   3      -12.0     69.0    66.9    91.4    66.8    64.1    63.2    84.6   506.0  11.3
   3      -20.0     65.3    65.6    65.3    67.0    64.6    62.4    70.6   460.8  1.2
#
   5       20.0     71.6    86.6    78.5    77.8    73.9    71.8    85.9   546.1  20.3
   5       10.0     97.7   131.2    93.0    95.5   143.2   125.1   110.8   796.5  76.3
   5        0.0     66.4   125.5    82.9    96.6   140.7   123.4   104.8   740.3  63.8
   5      -10.0     74.4    80.1    77.8    87.1   143.8    94.0    85.6   642.8  41.9
   5      -12.0     73.2    77.3    75.1    81.0   128.8    78.7    76.9   591.0  30.4
   5      -20.0     71.7    74.1    73.8    77.0    80.1    75.1    77.0   528.8  16.4
#
   6       20.0     69.2    70.5    70.4    71.3    69.7    66.8    68.7   486.6  7.0
   6       10.0     73.5    79.6    85.3   104.8    71.4    71.3    86.2   572.1  26.1
   6        0.0     91.8    84.9    80.0   110.2    82.5    87.6   110.4   647.4  43.0
   6      -10.0     74.8    74.0    71.4    74.2    94.8    81.2    77.2   547.6  20.7
   6      -20.0     72.3    68.0    69.4    69.3    72.2    69.6    70.7   491.5  8.1
#
   7       20.0     69.7    70.9    73.0    71.4    67.8    69.0    70.4   492.2  8.3
   7       10.0     82.0    79.8    88.2    83.6    78.2    76.2    80.2   568.2  25.3
   7        0.0     95.3    99.0    95.0   106.9   105.0   104.5    96.8   702.5  55.3
   7      -10.0     73.1    75.0    71.5    78.3    87.5    77.6    71.3   534.3  17.7
   7      -20.0     69.9    70.7    71.5    70.6    72.8    71.5    71.3   498.3  9.6
#
   8       20.0     71.9    78.4    67.7    77.7    67.3    68.0    65.0   496.0  9.1
   8       10.0    100.8   100.6    74.6   109.6    80.2    90.7    85.6   642.1  41.8
   8        0.0    106.0   102.2    80.4   107.9    97.8   105.7   108.3   708.3  56.6
   8      -10.0     73.9    75.0   100.6    77.8    83.7    77.0   105.4   593.4  30.9
   8      -20.0     66.3    66.7    65.9    65.1    63.8    62.7    63.9   454.4  -0.2
#
   9       20.0     92.1    68.5    76.5    78.8    76.5    78.6    93.8   564.8  24.5
   9       10.0     84.2    81.5    90.4    87.5    77.6    82.8    76.5   580.5  28.0
   9        0.0     87.5    79.9    77.0    77.0    83.4    83.4    92.6   580.8  28.1
   9      -10.0     92.9    87.0    78.1    78.1    84.5    84.5    95.5   600.6  32.5
   9      -20.0     96.8    94.7    85.3    85.3    77.9    77.9    88.1   606.0  33.7
```

File: ‘balloon\7rod\exp\block.prn’

Appendix 2: Data of single rod ballooning tests PUKI

```
# Isothermal ballooning tests with Zr1%Nb tube specimens (1995)
#
#   T       - temperature [C]
#   p       - burst pressure [bar]
#   time    - time to burst [s]
#   dp/dt   - pressure rate [bar/s]
#   D0      - initial diameter [mm]
#   L0      - initial length [mm]
#   L1      - lenght after test [mm]
#   Ld      - deformed length [mm]
#   V0      - initial tube volume [ml]
#   V1      - tube volume after test [ml]
#   epstav  - average tangential deformation [%]
#   epstm   - maximum tangential deformation [%]
#   epsa    - axial deformation [%]
#   oxlayer - thickness of outer ZrO2 layer [um]
#
#  References:
#
#   [1]   Frecska J., Konczos G., Matus L., Vasaros L.: Kiserletek a VVER
#         futoelemek meghatarozo parametereinek meresere;
#         OMFB 94-97-47-0817/2.4, 1995.
#
#   [2]   Frecska J., Matus L., Pummer I.: Futoelemviselkedes VVER reaktor-
#         tipusnal; OMFB 94-97-47-0817/2.5, 1996.
#
#   [3]   Maroti L., Matus L.: Futoelemviselkedes VVER reaktortipusnal;
#         Zarojelentes OMFB 94-97-47-0817, 1996.
#
#   [4]   Cs. Gyori, Z. Hozer, L. Maroti, L. Matus: VVER ballooning experiments;
#         EHPG Meeting Lillehammer, March 1998; HPR-349/40. (File: ehpg-98.pdf)
#
#
```

# No.	T [C]	p [bar]	time [s]	dp/dt [bar/s]	D0 [mm]	L0 [mm]	L1 [mm]	Ld [mm]	V0 [ml]	V1 [ml]	epstav [%]	epstm [%]	epsa [%]	oxlayer [um]		treatment	File
1	844	25.90	357.0	0.0725	9.15	50.00	-	-	-	-	-	51.60	-	0.0	#	a.r.	puki-02
2	852	23.30	283.3	0.0822	8.95	50.35	50.08	42.00	3.166	4.50	22.68	40.34	-0.54	0.0	#	a.r.	puki-06
3	800	43.70	566.4	0.0772	8.93	50.32	48.20	41.00	3.150	6.00	45.27	57.41	-4.21	0.0	#	a.r.	puki-08
4	900	10.80	130.0	0.0831	8.93	50.55	50.20	43.00	3.164	4.50	22.32	37.06	-0.69	0.0	#	a.r.	puki-09
5	902	11.10	134.5	0.0825	8.98	50.05	49.52	44.50	3.168	5.50	35.19	56.32	-1.06	0.0	#	a.r.	puki-10
6	952	10.40	144.8	0.0718	8.98	50.25	50.00	44.50	3.181	4.80	25.49	39.73	-0.50	0.0	#	a.r.	puki-11
7	1000	8.88	122.4	0.0725	8.96	50.15	49.75	45.50	3.161	4.90	26.75	36.57	-0.80	0.0	#	a.r.	puki-12
8	1052	8.11	114.5	0.0708	8.96	50.55	50.15	45.50	3.186	4.80	25.02	37.42	-0.79	0.0	#	a.r.	puki-13
9	1100	7.70	100.7	0.0765	8.95	50.40	49.95	45.50	3.169	4.50	21.04	34.18	-0.89	0.0	#	a.r.	puki-14

10	1152	7.01	91.8	0.0764	8.96	50.18	49.80	45.00	3.162	4.40	19.85	28.03	-0.76	0.0	#	a.r.	puki-15
11	1201	6.47	82.5	0.0784	8.96	50.10	49.50	45.00	3.157	4.80	25.67	35.44	-1.20	0.0	#	a.r.	puki-16
12	901	7.23	870.9	0.0083	8.96	50.30	50.00	44.00	3.170	4.00	13.99	29.95	-0.60	0.0	#	a.r.	puki-17
13	801	23.70	2985.0	0.0079	8.94	50.10	48.45	44.00	3.143	7.00	54.83	78.29	-3.29	0.0	#	a.r.	puki-18
14	1196	4.84	700.7	0.0069	9.16	50.45	49.65	41.60	3.323	5.54	34.50	55.05	-1.59	0.0	#	a.r.	puki-19
15	1147	5.81	864.4	0.0067	9.13	50.55	50.25	43.60	3.308	5.36	31.12	46.36	-0.59	0.0	#	a.r.	puki-20
16	1101	6.05	869.1	0.0070	9.14	50.60	50.10	45.40	3.318	4.78	22.10	31.76	-0.99	0.0	#	a.r.	puki-21
17	1102	5.83	817.2	0.0071	9.16	50.02	49.45	45.70	3.295	5.11	26.61	43.97	-1.14	0.0	#	a.r.	puki-22
18	1050	7.83	1133.8	0.0069	9.13	50.10	49.77	47.00	3.278	4.38	16.54	39.57	-0.66	0.0	#	a.r.	puki-23
19	1003	7.30	1052.2	0.0069	9.14	50.20	49.75	47.00	3.292	6.04	37.53	68.70	-0.90	0.0	#	a.r.	puki-24
20	951	7.67	1101.3	0.0070	9.15	50.30	49.65	46.10	3.306	5.27	28.39	49.81	-1.29	0.0	#	a.r.	puki-25
21	999	7.17	1032.6	0.0069	9.14	50.15	49.75	45.90	3.289	5.80	35.44	63.92	-0.80	0.0	#	a.r.	puki-26
22	699	85.30	2844.0	0.0300	9.13	52.30	48.23	42.30	3.422	5.96	38.45	69.58	-7.78	0.0	#	a.r.	puki-27
23	700	70.21	2345.0	0.0299	9.00	50.38	44.70	40.12	3.203	7.30	61.43	86.12	-11.27	0.0	#	a.r.	puki-28
24	699	108.40	3644.0	0.0297	9.18	49.95	49.32	44.30	3.304	4.93	24.69	34.06	-1.26	13.9	#	pukox-11	puki-29
25	698	105.90	3515.0	0.0301	9.18	50.90	50.43	46.50	3.367	4.55	17.66	27.49	-0.92	20.0	#	pukox-20	puki-30
26	698	69.40	2228.0	0.0311	9.29	50.25	50.13	46.10	3.404	4.07	10.14	30.02	-0.24	56.7	#	pukox-29	puki-31
27	698	59.20	1884.0	0.0314	9.21	47.50	47.30	42.90	3.163	3.67	8.51	17.64	-0.42	41.4	#	pukox-06	puki-32
28	802	57.75	1832.0	0.0315	9.18	50.10	50.05	46.20	3.314	4.52	18.09	47.10	-0.10	20.2	#	pukox-09	puki-33
29	802	38.73	1212.0	0.0320	9.16	50.40	50.35	45.90	3.320	3.70	6.10	22.46	-0.10	28.3	#	pukox-07	puki-34
30	902	17.45	532.6	0.0328	9.19	50.35	50.20	45.10	3.338	4.05	11.27	31.06	-0.30	19.4	#	pukox-15	puki-35
31	799	55.78	2943.2	0.0190	9.17	50.60	50.55	46.50	3.340	4.12	11.99	23.50	-0.10	14.3	#	pukox-13	puki-36
32	899	17.34	961.6	0.0180	9.19	50.20	50.14	45.50	3.328	4.05	11.32	13.03	-0.12	14.6	#	pukox-17	puki-37
33	900	22.41	258.1	0.0868	9.25	50.25	50.20	46.20	3.375	4.00	9.61	11.07	-0.10	22.8	#	pukox-22	puki-38
34	1003	14.92	940.5	0.0159	9.23	50.95	50.90	48.00	3.407	3.65	3.71	4.01	-0.10	22.2	#	pukox-30	puki-39
35	1001	10.44	617.3	0.0169	9.18	50.85	50.80	46.00	3.364	4.03	10.40	21.52	-0.10	15.1	#	pukox-14	puki-40
36	1100	8.77	490.2	0.0179	9.23	50.80	50.75	46.30	3.397	3.76	5.69	13.80	-0.10	22.8	#	pukox-19	puki-42
37	1200	7.04	391.3	0.0180	9.20	50.20	50.10	47.30	3.335	4.13	11.93	32.00	-0.20	24.2	#	pukox-08	puki-43
38	751	55.60	3688.7	0.0151	9.16	52.30	50.02	39.58	3.445	5.92	39.64	74.77	-4.36	0.0	#	a.r.	puki-44
39	752	89.38	597.9	0.1495	9.15	52.24	46.11	35.88	3.433	7.97	71.03	80.23	-11.73	0.0	#	a.r.	puki-45
40	651	134.40	919.3	0.1462	9.13	52.53	48.46	40.06	3.437	6.10	42.02	53.54	-7.75	0.0	#	a.r.	puki-46
41	650	95.42	7318.0	0.0130	9.15	52.07	49.80	42.29	3.422	5.45	31.46	48.91	-4.36	0.0	#	a.r.	puki-47
42	700	93.60	7361.4	0.0127	9.15	50.72	49.81	45.01	3.333	4.33	15.62	20.96	-1.79	6.3	#	pukox-41	puki-48
43	800	52.39	2283.8	0.0229	9.12	51.83	51.49	45.29	3.384	4.72	20.49	40.95	-0.66	6.5	#	pukox-35	puki-49
44	899	17.23	738.6	0.0233	9.16	50.86	50.79	45.33	3.350	3.73	6.23	11.75	-0.14	6.8	#	pukox-40	puki-50
45	1000	11.96	513.3	0.0233	9.15	50.75	50.36	46.11	3.335	4.69	20.29	30.43	-0.77	7.1	#	pukox-37	puki-51
46	1101	8.22	351.3	0.0234	9.15	49.71	49.29	45.08	3.267	4.42	17.82	31.92	-0.84	7.5	#	pukox-34	puki-52
47	702	108.10	651.4	0.1660	9.14	52.14	49.03	42.65	3.419	6.11	40.03	46.48	-5.96	0.0	#	a.r.	puki-53
48	699	140.00	885.0	0.1582	9.15	50.46	49.78	45.70	3.316	4.46	17.51	19.80	-1.35	6.9	#	pukox-39	puki-54
49	699	113.26	690.3	0.1641	9.15	50.53	50.44	44.89	3.321	3.91	9.54	23.69	-0.18	22.3	#	pukox-42	puki-55
50	698	78.42	3309.0	0.0237	9.15	50.45	46.35	44.00	3.316	6.58	45.91	92.09	-8.13	0.0	#	iodin	pukjod-1
51	799	34.03	1906.0	0.0179	9.16	50.55	49.00	44.00	3.330	6.22	41.33	74.23	-3.07	0.0	#	iodin	pukjod-2
52	898	12.46	690.4	0.0180	9.16	50.50	50.20	46.00	3.326	4.74	21.10	47.28	-0.59	0.0	#	iodin	pukjod-3
53	1000	9.12	509.2	0.0179	9.15	50.30	49.90	46.50	3.306	4.95	24.02	46.18	-0.80	0.0	#	iodin	pukjod-4
54	649	95.31	7447.0	0.0128	9.15	50.20	46.70	41.44	3.299	6.83	51.56	62.70	-6.97	0.0	#	iodin	pukjod-5

File: 'balloon\puki\exp\pukizrnb.prn'

Appendix 3: Data of single rod ballooning tests PUZRY

```
# Isothermal ballooning tests with Zircaloy-4 tube specimens (1995)
#
#
#   T       - temperature [C]
#   p       - burst pressure [bar]
#   time    - time to burst [s]
#   dp/dt   - pressure rate [bar/s]
#   D0      - initial diameter [mm]
#   L0      - initial length [mm]
#   L1      - lenght after test [mm]
#   Ld      - deformed length [mm]
#   V0      - initial tube volume [ml]
#   V1      - tube volume after test [ml]
#   epstav  - average tangential deformation [%]
#   epstm   - maximum tangential deformation [%]
#   epsa    - axial deformation [%]
#
#
#  References:
#
#   [1]   Frecska J., Konczos G., Matus L., Vasaros L.: Kiserletek a VVER
#         futoelemek meghatarozo parametereinek meresere;
#         OMFB 94-97-47-0817/2.4, 1995.
#
#   [2]   Frecska J., Matus L., Pummer I.: Futoelemviselkedes VVER reaktor-
#         tipusnal; OMFB 94-97-47-0817/2.5, 1996.
#
#   [3]   Maroti L., Matus L.: Futoelemviselkedes VVER reaktortipusnal;
#         Zarojelentes OMFB 94-97-47-0817, 1996.
#
#   [4]   Cs. Gyori, Z. Hozer, L. Maroti, L. Matus: VVER ballooning experiments;
#         EHPG Meeting Lillehammer, March 1998; HPR-349/40. (File: ehpg-98.pdf)
#
#
#
```

# No.	T [C]	p [bar]	time [s]	dp/dt [bar/s]	D0 [mm]	L0 [mm]	L1 [mm]	Ld [mm]	V0 [ml]	V1 [ml]	epstav [%]	epstm [%]	epsa [%]		File
1	1201.3	3.41	531.9	0.0064	10.73	50.00	49.15	43.61	4.519	8.21	39.128	60.01	-1.70	#	puzry-01
2	1154.4	3.70	566.0	0.0065	10.75	50.00	49.19	43.73	4.536	8.39	40.377	60.48	-1.62	#	puzry-02
3	1102.1	3.83	607.8	0.0063	10.75	50.00	49.20	44.07	4.536	8.89	44.531	66.88	-1.60	#	puzry-03
4	1053.2	4.38	705.3	0.0062	10.76	50.00	49.35	44.85	4.544	8.67	41.858	64.51	-1.30	#	puzry-04
5	997.9	5.02	810.7	0.0062	10.76	50.00	49.42	46.26	4.544	7.78	33.062	52.15	-1.16	#	puzry-05
6	950.5	8.73	1805.4	0.0048	10.75	50.00	49.10	44.77	4.536	9.05	45.271	87.06	-1.80	#	puzry-06
7	952.9	15.80	208.2	0.0759	10.75	50.00	49.20	44.22	4.536	8.60	41.912	86.48	-1.60	#	puzry-07
8	1001.0	8.90	116.7	0.0763	10.75	50.00	49.27	44.58	4.536	9.52	49.452	80.37	-1.46	#	puzry-08
9	1051.6	7.45	104.7	0.0712	10.75	50.00	49.22	44.21	4.536	9.23	47.344	73.86	-1.56	#	puzry-09

10	1102.6	6.53	92.0	0.0710	10.76	50.00	49.06	43.81	4.544	9.15	46.865	72.76	-1.88	#	puzry-10
11	1149.8	6.03	84.1	0.0717	10.75	50.00	49.20	43.85	4.536	8.61	42.276	61.30	-1.60	#	puzry-11
12	1197.7	5.78	80.0	0.0723	10.75	50.00	49.00	43.35	4.536	8.98	45.942	71.62	-2.00	#	puzry-12
13	698.8	88.83	2828.0	0.0314	10.76	50.00	46.06	45.43	4.544	8.61	40.854	81.48	-7.88	#	puzry-13
14	702.2	106.16	892.4	0.1190	10.75	50.00	44.25	42.60	4.536	10.13	56.447	83.62	-11.50	#	puzry-14
15	802.1	63.18	538.4	0.1173	10.76	50.00	44.21	41.20	4.544	10.45	60.536	109.53	-11.58	#	puzry-15
16	750.3	83.06	678.5	0.1224	10.75	50.00	45.95	43.20	4.536	8.69	43.527	82.59	-8.10	#	puzry-16
17	850.1	39.79	342.3	0.1162	10.76	50.00	48.20	45.90	4.544	9.35	46.697	92.61	-3.60	#	puzry-17
18	900.2	26.89	233.7	0.1151	10.76	50.00	49.46	47.20	4.544	8.63	39.729	74.29	-1.08	#	puzry-18
19	900.6	19.51	801.3	0.0243	10.76	50.00	49.37	47.10	4.544	9.90	50.037	91.79	-1.26	#	puzry-19
20	849.7	27.22	1211.1	0.0225	10.75	50.00	49.54	46.90	4.536	10.20	52.686	99.42	-0.92	#	puzry-20
21	800.8	45.30	2693.3	0.0168	10.76	50.00	46.18	44.70	4.544	9.27	47.079	88.55	-7.64	#	puzry-21
22	749.9	60.80	4105.1	0.0148	10.76	50.00	45.33	43.10	4.544	9.72	52.358	99.90	-9.34	#	puzry-22
23	748.6	72.58	1011.8	0.0717	10.75	50.00	44.44	42.40	4.536	10.14	56.748	103.87	-11.12	#	puzry-23
24	698.8	80.75	4522.2	0.0179	10.75	50.00	44.35	41.70	4.536	10.31	58.946	107.71	-11.30	#	puzry-24
25	698.3	79.78	4623.5	0.0173	10.76	50.00	45.67	43.10	4.544	9.39	49.567	84.84	-8.66	#	puzry-25
26	698.4	106.05	888.8	0.1193	10.76	50.00	42.59	41.20	4.544	11.40	68.252	100.97	-14.82	#	puzry-26
27	801.4	48.18	1946.0	0.0248	10.74	50.00	45.47	42.50	4.527	9.77	53.698	94.15	-9.06	#	puzry-27
28	800.0	52.94	1244.7	0.0425	10.76	50.00	45.31	42.80	4.544	9.79	53.249	92.20	-9.38	#	puzry-28
29	799.9	57.95	804.5	0.0720	10.76	50.00	44.21	41.80	4.544	10.58	60.896	107.86	-11.58	#	puzry-29
30	800.4	72.51	275.7	0.2630	10.76	50.00	45.03	42.60	4.544	11.11	64.189	104.28	-9.94	#	puzry-30
31	800.4	67.88	346.2	0.1961	10.75	50.00	44.40	42.40	4.536	10.18	57.079	90.39	-11.20	#	puzry-31

File: ‘balloon\puzry\exp\pukizry.prn’

Appendix 4: Data of single rod ballooning tests BALL

```
# Ballooning tests at temperature increase with pre-pressurized Zr1%Nb tube specimens (2000)
#
#
#   dT/dt      - temperature increase rate [K/s]
#   p0         - initial pressure [bar] (nominal at cold state)
#   T1         - temperature at burst [C]
#   p1         - pressure at burst [bar] (over pressure)
#   D0         - initial diameter (nominal) [mm]
#   v0         - initial wall thickness (nominal) [mm]
#   L0         - initial length [mm]
#   A1         - cross section area of the cut (at elevation of the maximum deformation) [mm^2]
#   C1         - circumference of the cut (at the elevation of the maximum deformation) [mm^2]
#   D1         - maximum diameter assuming idealised deformation [mm]: D1=(C1/4+SQRT((C1/4)**2-A1))/3.14159
#   epsm       - maximum tangential deformation [%]
#   Atmo       - atmosphere of the test
#
#
#  References:
#
#
```

# No. of sample	dT/dt [K/s]	p0 [bar]	T1 [C]	p1 [bar]	D0 [mm]	v0 [mm]	L0 [mm]	A1 [mm^2]	C1 [mm]	D1 [mm]	epsm [%]		Atmo
1	6.4	10.	640.	15.90	9.15	0.70	150.0	33.2	108.3	17.04	86.2	#	steam
2	8.2	10.	900.	14.00	9.15	0.70	150.0	25.6	96.7	15.22	66.3	#	steam
3	8.9	40.	845.	60.80	9.15	0.70	150.0	25.8	72.7	11.34	23.9	#	Ar
4	8.5	40.	863.	48.70	9.15	0.70	150.0	27.5	73.6	11.47	25.4	#	Ar
5	6.7	20.	876.	32.00	9.15	0.70	150.0	29.1	74.5	11.60	26.8	#	Ar
6	11.4	20.	898.	32.90	9.15	0.70	150.0	20.2	71.6	11.21	22.5	#	Ar
7	12.8	20.	889.	30.10	9.15	0.70	150.0	27.1	73.1	11.39	24.5	#	steam
8	6.5	10.	840.	17.70	9.15	0.70	150.0	25.3	86.9	13.64	49.1	#	Ar
9	13.0	10.	942.	14.10	9.15	0.70	150.0	28.6	92.5	14.52	58.7	#	Ar
10	9.9	10.	921.	15.40	9.15	0.70	150.0	21.3	112.5	17.78	94.4	#	Ar
11	12.3	40.	830.	68.10	9.15	0.70	150.0	27.3	80.7	12.62	37.8	#	steam
12	13.5	40.	868.	56.10	9.15	0.70	150.0	19.7	66.1	10.33	12.9	#	Ar

File: ‘balloon\ball\exp1\ball-e1.prn’

```
# Isothermal ballooning tests at linear pressure increase with Zr1%Nb tube specimens (2000)
#
#
#   dp/dt      - pressure increase rate [K/s]
#   T          - temperature [C] (nominal)
#   p1         - pressure at burst [bar] (over pressure)
#   D0         - initial diameter (nominal) [mm]
#   v0         - initial wall thickness (nominal) [mm]
#   L0         - initial length [mm]
#   A1         - cross section area of the cut (at elevation of the maximum deformation) [mm^2]
#   C1         - circumference of the cut (at the elevation of the maximum deformation) [mm^2]
#   D1         - maximum diameter assuming idealised deformation [mm]: D1=(C1/4+SQRT((C1/4)**2-A1))/3.14159
#   epsm       - maximum tangential deformation [%]
#   Atmo       - atmosphere of the test
#
#
#  References:
#
#
#  No. of    dp/dt      T       p1     D0     v0     L0       A1      C1      D1      epsm     Atmo
#  sample   [bar/s]    [C]     [bar]  [mm]   [mm]   [mm]    [mm^2]   [mm]    [mm]     [%]
#
   13        0.6      800.   83.30   9.15   0.70   150.0    27.8    92.2   14.48    58.2   #  Ar
   14        2.7      800.   72.40   9.15   0.70   150.0    18.2    68.8   10.78    17.8   #  Ar
   15        2.8      800.   36.60   9.15   0.70   150.0    21.9    86.6   13.62    48.9   #  Ar
   16        6.3      800.   95.20   9.15   0.70   150.0    25.4    79.2   12.40    35.5   #  Ar
   17        0.6      900.   16.60   9.15   0.70   150.0    25.1    78.3   12.25    33.9   #  Ar
   18        2.7      900.   20.30   9.15   0.70   150.0    19.3    67.4   10.54    15.2   #  Ar
   19        4.5      900.   20.90   9.15   0.70   150.0    20.4    73.5   11.52    25.9   #  Ar
   20        6.5     1000.   18.30   9.15   0.70   150.0    23.7    96.6   15.22    66.3   #  Ar
   21        0.6     1000.   14.50   9.15   0.70   150.0    18.4    85.0   13.39    46.3   #  Ar
   22        2.9     1000.   16.50   9.15   0.70   150.0    18.3    82.1   12.92    41.2   #  Ar
   23        0.6     1100.   14.20   9.15   0.70   150.0    18.5    81.9   12.89    40.9   #  Ar
   25        6.6     1200.   11.60   9.15   0.70   150.0    18.1    82.9   13.05    42.7   #  Ar
```

File: ‘balloon\ball\exp2\ball-e2.prn’

Appendix 5: Data of tensile tests

```
#  AEKI tensile tests summary file: Zr1Nb (alloy E110) sheet specimens
#
#
#    b          [mm]    width of sheet specimen
#    a          [mm]    thickness of sheet specimen
#    So         [mm2]   original cross-sectional area
#    Su         [mm2]   cross-sectional area at rupture
#    Fmax       [N]     maximum load
#    Fe         [N]     load at yield
#    Fu         [N]     load at rupture
#    Re         [MPa]   yield strength (Fe/So)
#    Rm         [MPa]   tensile strength (Fmax/So)
#    Ru         [Mpa]   true stress at burst (Fu/Su)
#    Lo         [mm]    initial gauge length
#    Lu         [mm]    gauge length after rupture
#    A20, A25   [%]     strain at rupture (100*(Lu-Lo)/Lo)
#    Z          [%]     contraction (100*(So-Su)/So)
#    ECR        [%]     equivalent oxidation on the basis of the measured mass gain
#    T          [C]     temperature of tensile test
#
#  Sketch of the specimen
#                                         A                    A-A
#      _______                            |   _______
#     |       \_______________________________/       |          _
#     |                                               |         | |
#     |            o                     o            |         | |b
#     |        _______________________________        |         |_|
#     |_______/    |                     |    \_______|          a
#                  |          Lo         | |
#                  |<------------------->| A
#
#
# References:
#
#  [1] Maroti L.: Sulyos baleseti folyamatok laboratoriumi vizsgalata;
#                 OMFB 3356/910927, Budapest 1991.
#
#
# Test series in 1989 [1]
#
#  No.     T     ECR     a      b      So     Su    Fmax    Rm     Fe     Re     Fu     Ru     Lo     Lu     A20     Z       Label
#         [C]    [%]   [mm]   [mm]   [mm2]  [mm2]   [N]   [MPa]   [N]   [MPa]   [N]   [MPa]  [mm]   [mm]   [%]    [%]
#
   1      20     0.0    0.6   2.95   1.77   0.69    735   415.0   440   249.0    -      -    24.66  31.1   26.0   61.0  #   No. 1
   2      20     0.0    0.6   3.00   1.80   0.77    750   417.0   470   261.0    -      -    24.65  30.3   23.0   57.2  #   No. 2
   3      20     0.0    0.6   3.00   1.80   0.92    729   405.0   344   191.0    -      -    20.0   24.4   22.0   49.0  #   No. 3
   4      20     0.0    0.6   3.00   1.80   0.94    733   407.0   432   240.0    -      -    20.0   25.4   27.0   48.0  #   No. 4
```

```
   5     20   0.0   0.6    3.00   1.80   0.97    783  435.0    409  227.0    -       -    20.0    24.6   23.0    46.0  #   No. 5
   6     20   0.0   0.6    3.00   1.80   0.83    761  423.0    419  233.0    -       -    20.0    24.8   24.0    54.0  #   No. 6
   7     20  17.0   0.6    3.00   1.80   1.48    704  391.0    441  245.0    -       -    20.0    21.6    8.1    17.6  #   No. 7
   8     20  19.0   0.6    3.00   1.80   1.19    684  380.0    400  222.0    -       -    20.0    21.6    8.2    34.0  #   No. 8
   9     20  35.0   0.6    3.00   1.80   1.10    529  294.0    387  215.0    -       -    20.0    21.1    5.5    39.0  #   No. 9
  10     19   0.0   0.6    3.06   1.84   0.60    645  351.3    520  283.2   817   816.7    -       -       -     68.0  #   No.10
  11     19   0.0   0.6    3.08   1.85   0.77    615  332.8    490  265.2   490   265.2  19.77   23.70   20.0    58.0  #   No.11
  12    310   0.0   0.6    3.07   1.84   0.44    370  200.9    320  173.7   320   173.7  19.33   24.33   26.0    76.0  #   No.12
  13    300   0.0   0.6    3.06   1.84   0.39    375  204.2    330  179.7   330   179.7  19.25   23.81   24.0    79.0  #   No.13
  14    450   0.0   0.6    3.12   1.87   0.35    258  137.8    210  112.2   210   112.2  19.48   24.45   26.0    82.0  #   No.14
  15    600   0.0   0.6    3.01   1.81   0.02    100   55.4     90   49.8    90    49.8  19.50   32.28   66.0    99.0  #   No.15
  16    600   0.0   0.6    3.00   1.80   0.08     75   41.7     60   33.3    60    33.3  19.60   36.23   85.0    96.0  #   No.16
  17    450   0.0   0.6    2.96   1.78   0.21    270  152.0    250  140.8   250   140.8  19.63   26.38   34.0    88.0  #   No.17
  18     20   0.8   0.6    3.00   1.80    -       -   347.0     -   264.0    -       -      -       -    28.6    56.5  #   No.20
  19     20   0.7   0.6    3.00   1.80    -       -   346.0     -   295.0    -       -      -       -    19.0    59.4  #   No.21
  20     20   0.7   0.6    3.00   1.80    -       -   328.0     -   243.0    -       -      -       -    24.7    60.0  #   No.22
  21     20   1.4   0.6    3.00   1.80    -       -   363.0     -   247.0    -       -      -       -    21.6    61.1  #   No.23
  22     20   1.7   0.6    3.00   1.80    -       -   344.0     -   239.0    -       -      -       -    14.6    57.6  #   No.24
  23     20   2.1   0.6    3.00   1.80    -       -   452.0     -   292.0    -       -      -       -    13.8    41.6  #   No.25
  24     20   1.3   0.6    3.00   1.80    -       -   383.0     -   262.0    -       -      -       -    20.6    53.8  #   No.26
  25     20   1.6   0.6    3.00   1.80    -       -   374.0     -   302.0    -       -      -       -    20.2    47.8  #   No.28
  26     20   2.1   0.6    3.00   1.80    -       -   376.0     -   254.0    -       -      -       -    19.3    46.9  #   No.29
  27     20   3.9   0.6    3.00   1.80    -       -   384.0     -   332.0    -       -      -       -    11.0    33.1  #   No.30
  28     20   0.9   0.6    3.00   1.80    -       -   368.0     -   286.0    -       -      -       -    22.9    57.1  #   No.31
  29     20   1.0   0.6    3.00   1.80    -       -   348.0     -   259.0    -       -      -       -    17.4    53.8  #   No.32
  30     20   0.9   0.6    3.00   1.80    -       -   369.0     -     -      -       -      -       -    31.2    63.3  #   No.41
  31     20   1.4   0.6    3.00   1.80    -       -   369.0     -   336.0    -       -      -       -    23.3    54.4  #   No.42
  32     20   2.1   0.6    3.00   1.80    -       -   435.0     -   391.0    -       -      -       -    22.0    50.6  #   No.43
  33     20   2.4   0.6    3.00   1.80    -       -   394.0     -   346.0    -       -      -       -    17.1    41.8  #   No.44
#
# Test series in 2000
#
#  No.    T    ECR    a       b      So     Su     Fmax   Rm      Fe    Re      Fu    Ru     Lo      Lu     A25     Z          Label
#        [C]   [%]   [mm]    [mm]   [mm2]  [mm2]   [N]   [MPa]   [N]   [MPa]   [N]   [MPa]  [mm]    [mm]    [%]    [%]
#
  34     20   0.0   0.67   4.82   3.23   0.78   1203  372.5    834  258.3   944  1210.4  25.0    32.4   29.0    75.8  # R-ZN-S-HK-1
  35     20   0.0   0.67   4.86   3.26   0.80   1286  394.9    888  272.7  1017  1271.5  25.0    32.8   31.0    75.5  # R-ZN-S-HK-2
  36     20   0.0   0.70   4.90   3.43   1.61   1468  428.0   1080  314.9  1103   685.3  25.0    33.5   34.0    53.1  # U-ZN-S-HK-1
  37     20   0.0   0.69   4.88   3.37   1.56   1392  413.4   1011  300.2  1068   684.5  25.0    32.3   29.0    53.7  # U-ZN-S-HK-2
  38    150   0.0   0.69   4.81   3.32    -     1075  323.9    869  261.8   778     -    25.0    32.7   30.0     -    # R-ZN-S-HK-1
  39    150   0.0   0.68   4.95   3.37    -     1051  312.2    845  251.0   747     -    25.0    34.8   39.0     -    # R-ZN-S-HK-2
  40    150   0.0   0.71   4.92   3.49    -     1001  349.5    975  279.1   890     -    25.0    32.8   31.0     -    # U-ZN-S-HK-1
  41    150   0.0   0.70   4.83   3.38    -     1145  338.7    910  269.2   876     -    25.0    32.7   30.0     -    # U-ZN-S-HK-2
  42    300   0.0   0.70   4.88   3.42    -      784  229.5    654  191.5   550     -    25.0    31.7   26.0     -    # R-ZN-S-HK-1
  43    300   0.0   0.71   5.03   3.57    -      837  234.4    668  187.0   596     -    25.0    32.6   30.0     -    # R-ZN-S-HK-2
  44    300   0.0   0.71   4.85   3.44    -      888  257.9    732  212.6   604     -    25.0    32.4   29.0     -    # U-ZN-S-HK-1
  45    300   0.0   0.72   4.95   3.56    -      890  249.7    725  203.4    -      -    25.0    32.5   30.0     -    # U-ZN-S-HK-2
```

File: ‘tensile\zr1nb\sheetzrn.prn’

```
#  AEKI tensile tests summary file: Zircaloy-4 sheet specimens
#
#    b         [mm]    width of sheet specimen
#    a         [mm]    thickness of sheet specimen
#    So        [mm2]   original cross-sectional area
#    Su        [mm2]   cross-sectional area at rupture
#    Fmax      [N]     maximum load
#    Fe        [N]     load at yield
#    Fu        [N]     load at rupture
#    Re        [MPa]   yield strength (Fe/So)
#    Rm        [MPa]   tensile strength (Fmax/So)
#    Ru        [Mpa]   true stress at burst (Fu/Su)
#    Lo        [mm]    initial gauge length
#    Lu        [mm]    gauge length after rupture
#    A25       [%]     strain at rupture (100*(Lu-Lo)/Lo)
#    Z         [%]     contraction (100*(So-Su)/So)
#    ECR       [%]     equivalent oxidation on the basis of the measured mass gain
#    T         [C]     temperature of tensile test
#
#
#
#  Sketch of the specimen
#                                       A                    A-A
#     _______                           |    _______
#    |       \_______________________________/       |         _
#    |                                                |        | |
#    |           o                    o               |        | |b
#    |        ________________________________        |        |_|
#    |_______/    |                   |    \_______|          a
#                 |         Lo        | |
#                 |<------------------>| A
#
#
#
# Test series in 2000
#
#  No.    T     ECR     a       b       So      Su      Fmax     Rm      Fe      Re      Fu      Ru     Lo      Lu     A25     Z          Label
#        [C]    [%]    [mm]    [mm]    [mm2]   [mm2]    [N]     [MPa]   [N]     [MPa]   [N]     [MPa]  [mm]    [mm]    [%]    [%]
#
```

No.	T	ECR	a	b	So	Su	Fmax	Rm	Fe	Re	Fu	Ru	Lo	Lu	A25	Z		Label
1	20	0.0	0.71	5.09	3.61	1.03	2009	555.9	1517	419.8	1646	1597.8	25.0	31.2	24.0	71.5	#	ZRY-S-HK-1
2	20	0.0	0.70	4.85	3.40	1.14	1910	562.7	1441	424.4	1532	1343.8	25.0	31.2	24.0	66.5	#	ZRY-S-HK-2
3	150	0.0	0.71	4.96	3.52	-	1556	441.8	1169	332.0	1224	-	25.0	31.8	27.0	-	#	ZRY-S-HK-1
4	150	0.0	0.68	4.91	3.34	-	1513	453.2	1139	341.1	1408	-	25.0	31.4	25.0	-	#	ZRY-S-HK-2
5	300	0.0	0.74	5.10	3.77	-	1175	311.3	940	249.1	-	-	25.0	32.7	30.0	-	#	ZRY-S-HK-1
6	300	0.0	0.72	4.95	3.56	-	1162	326.0	870	244.1	888	-	25.0	32.5	30.0	-	#	ZRY-S-HK-2

File: ‘tensile\zry-4\sheetzry.prn’

```
#  AEKI tensile tests summary file: Zr1Nb (alloy E110) tube specimens
#
#
#    Do        [mm]    outer diameter
#    v         [mm]    wall thickness
#    So        [mm2]   original cross-sectional area
#    Fmax      [N]     maximum load
#    Fe        [N]     load at yield
#    Rm        [MPa]   tensile strength
#    Re        [MPa]   yield strength
#    Lo        [mm]    initial gauge length (25 mm)
#    Lu        [mm]    gague length after rupture
#    A25       [%]     strain at rupture
#    Oxid      [um]    oxid layer thickness calculated from ECR
#    ECR       [%]     equivalent oxidation on the basis of the measured mass gain
#    T         [C]     temperature of tensile test
#
# References:
#
#  [1]  Horvath, Windberg, Hozer: Felfuvodasos es besugarzasos meresek
#       VVER futoelem burkolattal; OMFB-00033/98 (98-97-45-1636)
#
#  [2]  Griger, Maroti, Matus, Windberg: Ambient and high temperature
#       mechanical properties of ZrNb1 cladding with different oxygen
#       hydrogen content; EHPG Meeting May 1999, Loen; HPR-351/35.
#       (File: ehpg-99.pdf)
#
#
#  Test series in 1998 [1,2]
#
# No.      T     Oxid    ECR     Do      v      So     Fmax     Rm      Fe      Re      Lo    Lu     A25         Label
#         [C]    [um]    [%]    [mm]    [mm]   [mm2]    [N]    [MPa]    [N]    [MPa]   [mm]  [mm]    [%]
#
   1      20      0.0    0.0    9.13    0.70   18.54   6700   361.0     -       -      25    38.3   53.1  #    No.39
   2      20      0.0    0.0    9.14    0.69   18.32   6810   372.0     -       -      25    38.4   53.4  #    No.40
   3      20      9.5    1.0    9.15    0.74   19.55   9020   461.0     -       -      25    32.3   29.1  #    No.18
   4      20     11.0    1.1    9.17    0.75   19.84   9190   463.0     -       -      25    31.3   25.2  #    No.32
   5      20     21.0    2.1    9.17    0.74   19.60   9940   507.0     -       -      25    28.8   15.0  #    No.28
   6      20     21.0    2.1    9.20    0.74   19.67   9740   495.0     -       -      25     -      -    #    No.21
   7      20     40.0    4.0    9.24    0.78   20.73   7280   351.0     -       -      25     -      -    #    No.30
   8      20     42.0    4.2    9.23    0.78   20.71   6180   298.0     -       -      25     -      -    #    No.25
   9      20     54.0    5.6    9.27    0.80   21.29   5030   236.0     -       -      25     -      -    #    No.38
  10      20     69.0    7.1    9.33    0.82   21.92   3860   176.0     -       -      25     -      -    #    No.35
  11      20    104.0   10.4    9.38    0.84   22.54   1820    81.0     -       -      25     -      -    #    No.22
  12      20    198.0   19.9    9.48    0.89   24.02   340     14.0     -       -      25     -      -    #    No.04
  13     150      0.0    0.0    9.15    0.71   18.83   5220   277.0     -       -      25    40.2   60.8  #    No.41
  14     150     12.0    1.2    9.16    0.73   19.33   6940   359.0     -       -      25    33.3   33.1  #    No.16
  15     150     15.0    1.5    9.17    0.73   19.36   6760   349.0     -       -      25    30.7   22.7  #    No.09
```

```
  16     150    23.0     2.3    9.21    0.76   20.18    7660   380.0     -       -       25    28.5    14.1  #    No.20
  17     150    31.0     3.2    9.22    0.78   20.68    8300   401.0     -       -       25     -        -   #    No.12
  18     150    42.0     4.2    9.23    0.79   20.95    8230   393.0     -       -       25    28.1    12.5  #    No.34
  19     150    72.0     7.0    9.3     0.81    21.6    3010   139.0     -       -       25     -        -   #    No.37
  20     300     0.0     0.0    9.14    0.72   19.05    4570   240.0     -       -       25    40.4    61.5  #    No.43
  21     300    12.0     1.2    9.15    0.74   19.55    5370   275.0     -       -       25    34.7    38.8  #    No.33
  22     300    25.0     2.5    9.21    0.76   20.18    5450   270.0     -       -       25    28.7    14.6  #    No.17
#
#
#  Test series in 2000
#
# No.      T     Oxid     ECR     Do      v      So      Fmax     Rm      Fe      Re       Lo     Lu     A25       Label
#         [C]    [um]     [%]    [mm]    [mm]   [mm2]     [N]    [MPa]    [N]    [MPa]    [mm]   [mm]    [%]
#
  23      20     0.0     0.0    9.15    0.69    18.3    6765   368.9    4558   248.5     25    38.3    53.2  #  R-ZN-T-AR-1
  24      20     0.0     0.0    9.15    0.69    18.3    6698   365.2    4369   238.2     25    36.7    46.8  #  R-ZN-T-AR-2
  25      20     0.0     0.0    9.15    0.70    18.6    7113   382.8    4824   259.6     25    32.4    29.6  #  R-ZN-T-HK-1
  26      20     0.0     0.0    9.14    0.71    18.8    6724   357.6    5179   275.4     25    32.8    31.2  #  R-ZN-T-HK-2
  27      20     0.0     0.0    9.14    0.71    18.8    7376   392.3    4752   252.7     25    37.0    48.0  #  U-ZN-T-AR-1
  28      20     0.0     0.0    9.14    0.71    18.8    7572   402.7    4762   253.3     25    36.7    46.8  #  U-ZN-T-AR-2
  29      20     0.0     0.0    9.14    0.73    19.3    7673   397.8    5558   288.2     25    33.5    34.0  #  U-ZN-T-HK-1
  30      20     0.0     0.0    9.14    0.72    19.0    7627   400.5    5352   281.0     25    32.3    29.2  #  U-ZN-T-HK-2
  31     150     0.0     0.0    9.15    0.70    18.6    5678   305.6    3639   195.8     25    37.2    48.8  #  R-ZN-T-150-1
  32     150     0.0     0.0    9.15    0.71    18.8    5507   292.5    4126   219.2     25    38.0    52.0  #  R-ZN-T-150-2
  33     150     0.0     0.0    9.14    0.71    18.8    5716   304.0    3794   201.8     25    37.2    48.8  #  U-ZN-T-150-1
  34     150     0.0     0.0    9.14    0.71    18.8    5693   302.8    3881   206.4     25    36.8    47.2  #  U-ZN-T-150-2
  35     300     0.0     0.0    9.14    0.70    18.6    4512   243.1    2983   160.7     25    37.2    48.8  #  R-ZN-T-300-1
  36     300     0.0     0.0    9.02    0.61    16.1    3600   223.4    2432   150.9     25    37.6    50.4  #  R-ZN-T-300-2
  37     300     0.0     0.0    9.14    0.71    18.8    4934   262.4    3304   175.7     25    36.4    45.6  #  U-ZN-T-300-1
  38     300     0.0     0.0    9.14    0.71    18.8    4780   254.2    3074   163.5     25    37.0    48.0  #  U-ZN-T-300-2
```

File: ‘tensile\zr1nb\tubezrn.prn’

```
#  AEKI tensile tests summary file: Zircaloy-4 tube specimens
#
#
#    Do         [mm]    outer diameter
#    v          [mm]    wall thickness
#    So         [mm2]   original cross-sectional area
#    Fmax       [N]     maximum load
#    Fe         [N]     load at yield
#    Rm         [MPa]   tensile strength
#    Re         [MPa]   yield strength
#    Lo         [mm]    initial gauge length (25 mm)
#    Lu         [mm]    gauge length after rupture
#    A25        [%]     strain at rupture
#
#
# No.    T       Do       v      So     Fmax     Rm      Fe       Re      Lo      Lu      A25        Label
#       [C]     [mm]     [mm]   [mm2]    [N]    [MPa]    [N]     [MPa]   [mm]    [mm]    [%]
#
   1    20     10.77    0.73    23.0   16320   708.8   13022   565.6     25     30.7    22.8  #  ZRY-T-AR-1
   2    20     10.77    0.73    23.0   16303   708.0   12914   560.9     25     30.8    23.2  #  ZRY-T-AR-2
   3    20     10.77    0.74    23.3   12459   534.3    9256   397.0     25     31.2    24.8  #  ZRY-T-HK-1
   4    20     10.77    0.74    23.3   12499   536.0    9441   404.9     25     31.2    24.8  #  ZRY-T-HK-2
   5   150     10.77    0.74    23.3   14451   619.7   11653   499.8     25     31.3    25.2  #  ZRY-T-150-1
   6   150     10.76    0.73    23.0   14866   646.3   12089   525.6     25     30.6    22.4  #  ZRY-T-150-2
   7   300     10.78    0.74    23.3   11019   472.1    8967   384.2     25     30.8    23.2  #  ZRY-T-300-1
   8   300     10.76    0.74    23.3   10798   463.5    8887   381.5     25     31.0    24.0  #  ZRY-T-300-2
```

File: ‘tensile\zry-4\tubezry.prn’

Appendix 6: Data of oxidation tests PUKOX

```
# One side oxidation in steam
# date: March 1996
# Project: OMFB 94-97-47-0817 (task 2.4)
# Zr1%Nb tube samples
#
# T   [C]         oxidation temperature
# t   [s]         oxidation time
# m0    [g]             initial mass
# m1    [g]             mass after oxidation
# dm    [mg]            mass gain
# ECR   [%]             equivalent cladding reacted (dm/m0/3.508)
# D     [mm]            outer diameter of the sample
# L     [mm]            length of the sample
# F     [cm^2]          surface area
# x     [um]            calculated ZrO2 layer thickness
# k     [mg/cm^2/s^0.5] rate constant
#
# Reference:
#
# [1] J. Frecska, L. Matus, I. Pummer, L. Vasaros: Futoelemviselkedes VVER
#     reaktortipusnal; OMFB 94-97-47-0817 / 2.5, AEKI, Budapest 1996.
#
#
#  T      t      m0        m1       dm      ECR      D      L        F       x       k      sample
#
  900    400   8.39070   8.43962   48.92    1.66    9.13   70.0    20.07    17.1   0.122  # pukox-1
  900    400   8.60770   8.64080   33.10    1.10    9.13   71.58   20.52    11.6   0.081  # pukox-2
  900    400   8.53580   8.56812   32.32    1.08    9.13   70.98   20.35    11.3   0.079  # pukox-3
  900    400   8.08350   8.13603   52.53    1.85    9.13   67.22   19.27    18.4   0.136  # pukox-4
  900    400   8.55020   8.59430   44.10    1.47    9.13   71.10   20.38    15.4   0.108  # pukox-5
  900    400   8.16370   8.28207  118.37    4.13    9.13   67.89   19.46    41.4   0.304  # pukox-6
  900    400   7.98640   8.06745   81.05    2.89    9.13   66.41   19.04    28.3   0.213  # pukox-7
  900    400   8.55280   8.62218   69.38    2.31    9.13   71.12   20.39    24.2   0.170  # pukox-8
  900    400   8.57900   8.63682   57.82    1.92    9.13   71.34   20.45    20.2   0.141  # pukox-9
  900    400   8.45455   8.51287   58.32    1.97    9.13   70.31   20.16    20.4   0.145  # pukox-10
  900    400   8.36375   8.40365   39.90    1.36    9.13   69.88   20.03    13.9   0.100  # pukox-11
  900    400   8.54945   8.58475   35.30    1.18    9.13   69.87   20.03    12.3   0.088  # pukox-12
```

900	400	8.56880	8.60960	40.80	1.36	9.14	69.96	20.08	14.3	0.102	# pukox-13
900	400	8.58425	8.62752	43.27	1.44	9.13	70.07	20.09	15.1	0.108	# pukox-14
900	400	8.45230	8.50790	55.60	1.88	9.13	70.02	20.07	19.4	0.138	# pukox-15
900	400	8.54925	8.60540	56.15	1.87	9.14	70.06	20.11	19.6	0.140	# pukox-16
900	400	8.45465	8.49650	41.85	1.41	9.14	70.05	20.10	14.6	0.104	# pukox-17
900	800	8.44665	8.52097	74.32	2.51	9.14	70.01	20.09	26.0	0.131	# pukox-18
900	800	8.18320	8.24850	65.30	2.27	9.12	70.11	20.08	22.8	0.115	# pukox-19
900	800	8.38460	8.44185	57.25	1.95	9.12	70.07	20.07	20.0	0.101	# pukox-20
900	800	8.10850	8.17992	71.42	2.51	9.14	67.35	19.33	25.0	0.131	# pukox-21
900	1600	8.45900	8.52410	65.10	2.19	9.14	70.26	20.16	22.8	0.081	# pukox-22
900	1600	8.43950	8.52430	84.80	2.86	9.14	70.10	20.12	29.6	0.105	# pukox-23
900	3600	8.16475	8.33860	173.85	6.07	9.14	67.82	19.46	60.8	0.149	# pukox-24
900	2700	8.55678	8.67281	116.03	3.87	9.14	71.07	20.40	40.6	0.109	# pukox-25
900	2700	8.53035	8.63455	104.20	3.48	9.14	70.85	20.33	36.4	0.099	# pukox-26
900	2700	8.52930	8.65526	125.96	4.21	9.14	70.84	20.33	44.0	0.119	# pukox-27
900	2700	8.45131	8.63780	186.49	6.29	9.14	70.20	20.15	65.2	0.178	# pukox-28
900	1800	8.42320	8.58547	162.27	5.49	9.14	69.96	20.08	56.7	0.190	# pukox-29
900	1800	8.44443	8.50795	63.52	2.14	9.14	70.14	20.13	22.2	0.074	# pukox-30
900	200	8.42790	8.45795	30.05	1.02	9.15	70.0	20.11	10.5	0.106	# pukox-31
900	200	8.47422	8.50630	32.08	1.08	9.15	70.06	20.13	11.2	0.113	# pukox-32
900	100	8.15526	8.17805	22.79	0.80	9.14	70.04	20.10	8.0	0.113	# pukox-33
900	75	8.48485	8.50633	21.48	0.72	9.15	70.02	20.12	7.5	0.123	# pukox-34
900	50	7.93585	7.95458	18.73	0.67	9.12	70.06	20.06	6.5	0.132	# pukox-35
900	50	8.18182	8.19855	16.73	0.58	9.14	70.07	20.11	5.8	0.118	# pukox-36
900	50	8.47975	8.50000	20.25	0.68	9.15	70.03	20.12	7.1	0.142	# pukox-37
900	50	8.10985	8.12715	17.30	0.61	9.13	70.02	20.07	6.0	0.122	# pukox-38
900	60	8.32770	8.34748	19.78	0.68	9.15	70.07	20.13	6.9	0.127	# pukox-39
900	60	8.56655	8.58597	19.42	0.65	9.16	69.71	20.05	6.8	0.125	# pukox-40
900	60	8.40010	8.41810	18.00	0.61	9.15	70.03	20.12	6.3	0.115	# pukox-41
900	600	8.17185	8.23750	65.65	2.29	9.15	69.97	20.10	22.9	0.133	# pukox-42
900	1200	8.59810	8.73995	141.85	4.70	9.15	70.09	20.14	49.6	0.203	# pukox-43
900	1200	8.59178	8.70910	117.32	3.89	9.15	70.04	20.12	41.0	0.168	# pukox-44

File: ‘oxidation\pukox.prn

Appendix 7: Data of oxidation tests EU-PECO

```
# Double side oxidation in steam
# date: June 1995
# Project: EU PECO (Contract FI3SCT920001)
# Zr1%Nb tube samples
# Geometry: outer diameter = 9.14mm, wall thickness = 0.7mm , length = 40mm

# Surface area= 2158.3mm^2
#
# T   [C]               oxidation temperature
# t   [s]               oxidation time
# dm  [mg/cm^2]         mass gain
# k   [mg/cm^2*s^0.5]   rate constant
# x   [um]              ZrO2 layer thickness
#
#
# Reference:
#
# [1] J. Frecska, G. Konczos, L. Maroti, L. Matus: Oxidation and hydriding
#     of Zr1%Nb alloys by steam at 900-1200 C; KFKI-1995-17/G report.
#    (File:  kfki-95-17.pdf)
#
#
# No.    T     t       dm         k         x      sample
#
   1    900   100     1.18     0.118     4.5     95-20
   2    900   300     2.16     0.125    14.0     95-19
   3    900   1000    3.36     0.106    37.0     95-5
   4    900   2000    4.78     0.107    44.0     95-4
   5    900   4000    6.01     0.095    48.0     95-2
   6    900   10000   13.14    0.131    81.0     95-3
#
   7   1000   500     5.15     0.230    44.0     95-9
   8   1000   1025    6.36     0.199    77.0     95-6
   9   1000   2000    8.43     0.188    82.0     95-7
  10   1000   4000    12.48    0.197   103.0     95-8
#
  11   1100   125     4.38     0.392    45.0     95-14
  12   1100   250     7.10     0.449    53.0     95-13
  13   1100   500     9.86     0.441    84.0     95-12
  14   1100   1000    14.1     0.446    89.0     95-11
  15   1100   2000    18.85    0.422   117.0     95-10
#
  16   1200   62.5     5.78    0.731    48.0     95-15
  17   1200   125      8.88    0.795    54.0     95-16
  18   1200   250     12.44    0.787    84.0     95-17
  19   1200   500     17.25    0.771    95.0     95-18
```

File: ‘oxidation\eu-peco.prn’

Appendix 8: Data of oxidation tests IAEA-CRP

```
# Double side oxidation in steam
# date: 1997
# Project: IAEA CRP (Contract 9284/R0)
# Zr1%Nb tube samples
# Geometry: outer diameter = 9.14mm, wall thickness = 0.7mm length =5mm
# Surface area= 3.01cm^2
#
# T   [C]          oxidation temperature
# t   [s]          oxidation time
# dma [mg]         absolute mass gain
# dm  [mg/cm^2]    mass gain / surface area
# k   [mg/cm^2*s^0.5] rate constant
#
#
# Reference:
#
# [1] J. Frecska, L. Matus, L. Vasaros: Hydrogen uptake of Zr1%Nb cladding
#     by steam oxidation during loss of coolant accident; IAEA CRP 9284/R0,
#     Final report, September 1997. (File: iaea-9284.pdf)
#
#
#
# No.    T      t       dma      dm        k        Sample
#
   1    500   163000   1.38    0.461    0.00114  #  500A2
   2    500   653000   3.05    0.986    0.00122  #  500B1
   3    500   653000   2.91    0.980    0.00121  #  500B3
#
   4    600     2400   0.83    0.276    0.00563  #  600A1
   5    600     2400   1.31    0.435    0.00888  #  600A2
   6    600    10800   1.51    0.502    0.00483  #  600B1
   7    600   138600   5.95    1.980    0.00532  #  600C2
#
   8    700      171   0.74    0.245    0.01875  #  700A1
   9    700      171   0.79    0.261    0.01994  #  700A2
  10    700     1200   1.91    0.635    0.01834  #  700B3
  11    700     4800   3.19    1.060    0.01530  #  700C1
  12    700     4800   3.19    1.058    0.01528  #  700C3
#
  13    800       69   1.17    0.390    0.04691  #  800A1
  14    800       69   1.14    0.380    0.04575  #  800A2
  15    800      277   2.40    0.796    0.04785  #  800B1
  16    800      277   2.29    0.762    0.04579  #  800B2
  17    800     1107   3.86    1.281    0.03850  #  800C1
  18    800     1107   3.82    1.270    0.03817  #  800C2
#
  19    900       30   1.74    0.579    0.10572  #  900A1
  20    900       30   1.67    0.556    0.10148  #  900A2
  21    900      120   3.00    0.998    0.09107  #  900B1
  22    900      120   3.06    1.017    0.09286  #  900B2
  23    900      480   1.51    0.503    0.02296  #  900C1
  24    900      480   1.35    0.448    0.02046  #  900C2
```

File: ‘oxidation\iaea-crp.prn’

Appendix 9: Data of oxidation tests OAH-ABA

```
# Double side oxidation in steam
# date: June 2000
# Project: OAH-ABA-41/00
# Zr1%Nb tube samples
# Geometry: outer diameter = 9.14mm, wall thickness = 0.7mm
#
# L   [mm]          length of a sample
# T   [C]           oxidation temperature
# t   [s]           oxidation time
# dma [mg]          absolute mass gain
# dm  [mg/cm^2]     mass gain / surface area
# k   [mg/cm^2*s^0.5] rate constant ( Dm/SQRT(t) )
#
# References:
#
# [1] L. Matus, L. Vasaros: Hydrogen release kinetics during steam
#     oxidation of Zr1%Nb and zircaloy-4; 6th International QUENCH
#     Workshop, Forschugzentrum Karlsruhe, October 10-12, 2000.
#     (File: quench-6-00.pdf)
#
# [2] Matus L., Horvath M. Vasaros L.: Zr1%Nb es Zircaloy-4
#     osszehasonlitasa vizgozos oxidacioban; OAH-ABA-41/00, 2000.
#
# [3] Hozer Z. et al.: Ring compression tests with oxidised and
#     hydrided Zr1%Nb and Zircaloy-4 claddings; KFKI-2002-01/G.
#     (File: kfki-02-01.pdf)
#
#
# No.     T     t      dma     dm       k      L       sample
#
   1     900   360    5.58    1.208   0.064   8.00   #  N-14
   2     900   1000   12.53   2.767   0.087   7.83   #  N-13
   3     900   3000   29.30   6.455   0.118   7.85   #  N-11
   4     900   7000   47.18   10.297  0.123   7.93   #  N-12
   5     900  11000   64.36   14.178  0.135   7.85   #  N-10
   6     900  14000   66.28   14.550  0.123   7.88   #  N-9
#
   7    1000   100    6.66    1.454   0.145   7.93   #  N-7
   8    1000   700    21.1    4.637   0.175   7.87   #  N-2
   9    1000   1200   32.53   7.100   0.205   7.93   #  N-6
  10    1000   1800   57.83   12.710  0.300   7.87   #  N-5
  11    1000   3600   82.05   17.764  0.296   8.00   #  N-3
  12    1000   6000   103.85  22.613  0.292   7.95   #  N-1
#
  13    1100   19     5.25    1.166   0.268   7.78   #  N-19
  14    1100   133    16      3.533   0.306   7.83   #  N-18
  15    1100   704    39.3    8.548   0.322   7.96   #  N-17
  16    1100   1500   57.59   12.555  0.324   7.94   #  N-16
  17    1100   2400   74.1    16.305  0.333   7.86   #  N-15
  18    1100   5000   107.17  23.554  0.333   7.87   #  N-8
#
  19    1200    7     7.43    1.641   0.620   7.83   #  N-25
  20    1200    49    16.98   3.693   0.528   7.96   #  N-24
  21    1200   167    34.55   7.620   0.590   7.84   #  N-23
  22    1200   380    50.15   11.035  0.566   7.86   #  N-22
  23    1200   646    66.00   14.455  0.569   7.90   #  N-21
  24    1200   1205   90.85   19.783  0.570   7.95   #  N-20
```

File: ‘oxidation\oahzrnb.prn’

```
# Double side oxidation in steam
# date: June 2000
# Project: OAH-ABA-41/00
# Zircaloy-4 tube samples
# Geometry: outer diameter = 10.74mm, wall thickness = 0.73mm
#
# L     [mm]             lengh of a sample
# T     [C]              oxidation temperature
# t     [s]              oxidation time
# dma   [mg]             absolute mass gain
# dm    [mg/cm^2]        mass gain / surface area
# k     [mg/cm^2*s^0.5] rate constant ( Dm/SQRT(t) )
#
# References:
#
# [1] L. Matus, L. Vasaros: Hydrogen release kinetics during steam
#     oxidation of Zr1%Nb and zircaloy-4; 6th International QUENCH
#     Workshop, Forschugzentrum Karlsruhe, October 10-12, 2000.
#     (File: quench-6-00.pdf)
#
# [2] Matus L., Horvath M. Vasaros L.: Zr1%Nb es Zircaloy-4
#     osszehasonlitasa vizgozos oxidacioban; OAH-ABA-41/00, 2000.
#
# [3] Hozer Z. et al.: Ring compression tests with oxidised and
#     hydrided Zr1%Nb and Zircaloy-4 claddings; KFKI-2002-01/G.
#     (File: kfki-02-01.pdf)
#
#
# No.     T     t      dma     dm       k      L       sample
#
   1     900    300      9.4    1.72   0.100   7.93   #  Y-11
   2     900   1000     14.4    2.64   0.084   7.92   #  Y-10
   3     900   5000    25.06    4.50   0.064   8.12   #  Y-8
   4     900  11000    28.85    5.32   0.051   7.88   #  Y-9
#
   5    1000     87       12    2.19   0.235   7.97   #  Y-6
   6    1000    464    24.85    4.56   0.212   7.92   #  Y-5
   7    1000   2600    50.15    9.25   0.181   7.88   #  Y-1
   8    1000   3300    63.97   11.52   0.201   8.09   #  Y-7
   9    1000   4090     83.8   15.42   0.241   7.90   #  Y-4
  10    1000   7270   181.25   33.40   0.392   7.89   #  Y-3
  11    1000  11360   314.75   58.61   0.550   7.80   #  Y-2
#
  12    1100     27    11.70    2.14   0.412   7.95   #  Y-17
  13    1100    102    22.55    4.14   0.410   7.93   #  Y-16
  14    1100    398    41.33    7.64   0.383   7.86   #  Y-15
  15    1100    900    65.10   11.54   0.385   8.23   #  Y-14
  16    1100   1500    83.95   14.78   0.382   8.29   #  Y-13
  17    1100   3000   110.64   20.25   0.370   7.95   #  Y-12
#
  18    1200     10    14.57    2.63   0.832   8.07   #  Y-23
  19    1200     40    23.85    4.35   0.688   7.98   #  Y-22
  20    1200    163    43.39    7.93   0.621   7.96   #  Y-21
  21    1200    367    63.85   11.63   0.607   7.99   #  Y-20
  22    1200    790    91.41   16.54   0.588   8.05   #  Y-18
  23    1200   1100   105.67   19.29   0.582   7.97   #  Y-19
```

File: ‘oxidation\oahzry.prn’

Appendix 10: Data of oxidation tests HTARTOX

```
# Double side oxidation in steam
# date: December 1998
# Zr1%Nb tube samples
# Geometry: ring samples of different sizes without hydrogen content
#
# T   [C]         oxidation temperature
# t   [s]         oxidation time
# m1  [g]         mass of sample before oxidation
# m2  [g]         mass of sample after oxidation
# L1  [mm]        length of sample before oxidation
# L2  [mm]        length of sample after oxidation
# dL  [%]         relative change of length
# D1  [mm]        diameter of a sample before oxidation
# D2  [mm]        diameter of a sample after oxidation
# dD  [%]         relative change of diameter of a sample
# f   [cm^2]      surface area of a sample before oxidation
# dm  [mg/cm^2]   mass gain
# k   [mg/cm^2*s^0.5] rate constant
#
# Reference:
#
# [1] L. Vasaros, L.Matus: Steam oxidation of Zr-alloys with H content,
#     release of absorbed hidrogen; 5th International QUENCH Workshop,
#     Forschungscentrum Karlsruhe, October 19-21 1999. (File: quench-5-99.pdf)
#
#
# No.    T      t      m1        m2        dm      L1      L2      dL      D1      D2      dD       f        k
#
```

No.	T	t	m1	m2	dm	L1	L2	dL	D1	D2	dD	f	k
1	800	3600	0.4854	0.49045	5.05	4.45	4.49	0.90	9.05	9.16	1.22	2.69	0.031
2	900	880	0.49965	0.5051	5.45	4.48	4.50	0.45	9.07	9.11	0.44	2.72	0.068
3	1000	220	0.49706	0.50372	6.66	4.44	4.48	0.90	9.08	9.13	0.55	2.70	0.166
4	1100	60	0.49027	0.49583	5.56	4.44	4.45	0.23	9.07	9.09	0.22	2.70	0.266
5	1100	900	0.52011	0.54677	26.66	4.76	4.82	1.26	9.03	9.07	0.44	2.84	0.313
6	1100	900	0.51605	0.5434	27.35	4.64	4.73	1.94	9.01	9.1	1.00	2.77	0.330
7	1100	900	0.4776	0.50323	25.63	4.3	-	-	9.02	-	-	2.59	0.329
8	1100	900	0.49615	0.5226	26.45	4.45	-	-	9.02	-	-	2.67	0.330

File: ‘oxidation\htartox.prn’

Appendix 11: Data of oxidation tests OMFB-94

```
# Double side oxidation in steam
# date:  1994
# Project: OMFB 94-97-47-0817 (task 2.2)
# Zr1%Nb tube samples
# Geometry: outer diameter = 9.16mm, wall thickness = 0.72mm
#
# L   [cm]              length of a sample
# F   [cm^2]            surface area
# T   [C]               oxidation temperature
# t   [s]               oxidation time
# dm  [mg/cm^2]         mass gain
# k  [mg/cm^2*s^0.5]    rate constant
#
#
#       T       t      L      F      dm       k
#
      1010  500    3.75   20.27   71.7     0.158
      1010  1000   3.67   19.84   88.7     0.141
      1010  1200   3.88   20.96   117.9    0.162
      1010  2000   3.73   20.16   132.2    0.147
      1010  4000   3.86   20.85   296.3    0.225
      1010  4000   3.715  20.08   229      0.180
```

File: ‘oxidation\omfb-94.prn’

Appendix 12: Data of ring compression tests

```
#             AEKI compression tests summary file
#             date: 2000
#             Zr1%Nb ring samples
#
#             ECR [%]           equivalent oxidation on the basis of the measured mass gain
#             Hc [wppm]         hydrogen content of the sample after the oxidation
#             Ha [%]            absorbed hydrogen
#             D0 [mm]           diameter before oxidation
#             D [mm]            diameter after oxidation
#             F [N]             force
#             dl [mm]           deformation
#             dl/D [%]          relative deformation
#             E [mJ]            energy
#
```

# No	ECR	Hc	Ha	D0	D	F	dl	dl/D	E		Sample
1	1.62	7.9	1.13	9.15	9.19	822.4	5.67	61.7	3762.1	#	N-14
2	3.69	355.9	22.72	9.15	9.23	616	1.43	15.49	711.2	#	N-13
3	8.63	1325.1	36.18	9.15	9.27	421.9	0.35	3.78	70.9	#	N-11
4	13.76	2359	40	9.16	9.38	186.6	0.19	2.03	16.4	#	N-12
5	18.86	2896.2	36	9.15	9.38	116.8	0.22	2.35	15.2	#	N-10
6	19.32	2629.7	31.74	9.15	9.39	147.7	0.19	2.02	11.7	#	N-9
7	1.94	1.3	0.16	9.15	9.18	840.7	4.98	54.25	3505.8	#	N-7
8	6.20	907.8	34.42	9.15	9.25	482.5	0.43	4.65	92.9	#	N-2
9	9.47	1811.9	44.56	9.15	9.28	376.8	0.33	3.56	48.1	#	N-6
10	16.95	3135.1	43.37	9.16	9.38	164.4	0.19	2.03	12.1	#	N-5
11	23.72	3273.8	31.92	9.16	9.43	125.5	0.15	1.59	7.3	#	N-3
12	30.23	2330.1	17.95	9.17	9.38	105.8	0.15	1.6	6.1	#	N-1
13	1.57	17.6	2.68	9.16	9.17	872.3	5.2	56.71	3294.2	#	N-19
14	4.72	598.2	29.91	9.16	9.19	478.4	0.32	3.48	80	#	N-18
15	11.42	906.8	18.46	9.16	9.25	320.3	0.32	3.46	43.5	#	N-17
16	16.82	678.8	9.43	9.16	9.29	264	0.24	2.58	35.8	#	N-16
17	21.78	704	7.6	9.17	9.32	197.4	0.24	2.58	21.7	#	N-15
18	31.47	920.3	6.87	9.15	9.35	70.5	0.09	0.96	3.36	#	N-8
19	2.19	4.4	0.47	9.16	9.17	761.5	3.82	41.66	2582.9	#	N-25
20	4.93	11	0.52	9.16	9.19	765.1	0.84	9.14	420.1	#	N-24
21	10.16	785.6	18.19	9.16	9.22	330.1	0.33	3.58	43.8	#	N-23
22	14.76	611.2	9.75	9.16	9.24	298.6	0.32	3.46	41.4	#	N-22
23	19.35	549.5	6.66	9.16	9.25	217.9	0.29	3.14	27.5	#	N-21
24	26.58	580.3	5.11	9.16	9.32	121.5	0.22	2.36	11.7	#	N-20

```
#               AEKI compression tests summary file
#               date: 2000
#               Zircaloy ring samples
#
##              ECR [%]           equivalent oxidation on the basis of the measured mass gain
#               Hc [wppm]         hydrogen content of the sample after the oxidation
#               Ha [%]            absorbed hydrogen
#               D0 [mm]           diameter before oxidation
#               D [mm]            diameter after oxidation
#               F [N]             force
#               dl [mm]           deformation
#               dl/D [%]          relative deformation
#               E [mJ]            energy
#
```

#	No	ECR	Hc	Ha	D0	D	F	dl	dl/D	E		Sample
	1	2.28	2.6	0.22	10.74	10.84	789.5	5.38	49.63	3301.1	#	Y-11
	2	3.49	2.3	0.13	10.74	10.89	677.5	4.44	40.77	2549.3	#	Y-10
	3	5.93	1.6	0.05	10.74	10.93	674.7	1.68	15.37	836.9	#	Y-8
	4	7	0.4	0.01	10.74	10.94	615.9	1.5	13.71	669.7	#	Y-9
	5	2.89	1.2	0.08	10.74	10.83	661.3	4.91	45.34	2665.8	#	Y-6
	6	6.02	0.9	0.03	10.74	10.9	619	2.09	19.17	1013.9	#	Y-5
	7	12.26	0.6	0.01	10.75	10.95	462.6	1.69	15.43	302.2	#	Y-1
	8	15.18	8	0.1	10.74	10.97	431.7	0.64	5.83	179.7	#	Y-7
	9	20.37	997.2	9.52	10.74	11.09	288.6	0.48	4.33	73.7	#	Y-4
	10	44.03	1853.8	8.18	10.74	11.44	118.6	0.31	2.72	17.5	#	Y-3
	11	77.29	110.2	0.28	10.75	12.23	26.1	0.18	1.48	2.9	#	Y-2
	12	2.83	0.6	0.04	10.74	10.82	758.3	5.7	52.68	3452.1	#	Y-17
	13	5.45	1.4	0.05	10.74	10.85	690.1	4.33	39.91	2744.5	#	Y-16
	14	10.11	2.6	0.05	10.74	10.89	659.2	2.25	20.66	1179.3	#	Y-15
	15	15.21	1.6	0.02	10.74	10.9	553.6	1.09	10	382.5	#	Y-14
	16	19.49	2.1	0.02	10.74	10.93	424.5	0.7	6.4	183.8	#	Y-13
	17	26.77	5.5	0.04	10.74	10.97	256.8	0.51	4.65	72.2	#	Y-12
	18	3.48	1.6	0.085	10.74	10.82	706.5	4.13	38.17	2473.1	#	Y-23
	19	5.76	0.7	0.025	10.74	10.84	676.7	1.85	17.07	1044.3	#	Y-22
	20	10.48	0.9	0.016	10.74	10.87	625.4	0.92	8.46	313.4	#	Y-21
	21	15.36	1.4	0.017	10.74	10.88	407.9	0.59	5.42	119.1	#	Y-20
	22	21.85	4.9	0.043	10.74	10.92	279.8	0.41	3.75	72.1	#	Y-18
	23	25.73	1.1	0.008	10.74	10.93	206.4	0.41	3.75	43.7	#	Y-19

Appendix 13: Data of oxidation tests COHYRA

Double side oxidation in hydrogen rich steam atmosphere
date: 2004-2005
Project: Zr Cladding Oxidation in Hydrogen Rich Atmosphere (COHYRA)
Zr1%Nb tube samples
Wall thickness = 0.65 mm
#
T [C] oxidation temperature
t [s] oxidation time
Hs [vol. %] hydrogen content in the steam
dma [g] absolute mass gain
D [mm] outer diameter of the sample
L [mm] length of the sample
F [cm^2] surface area
k [mg/cm^2/s^0.5] rate constant
ECR [%] equivalent cladding reacted
Hc [wppm] hydrogen content of the sample after the oxidation
#
Reference
[11] E. Perez-Feró, L. Vasáros, Cs. Győri, P. Windberg, Z. Hózer: Oxidation of E110 cladding in

hydrogen rich steam atmosphere, AEKI, Budapest, June 2005
#
#

#	No	T	t	Hs	dma	D	L	F	k	ECR	Hc		Sample
#													
	1	1000	330	20	0.0062	9.1	8.08	4.63	0.0736	1.8	357.9	#	PUM-VH-1
	2	1000	840	20	0.0167	9.1	8.04	4.61	0.1249	4.8	675.4	#	PUM-VH-2
	3	1000	3720	20	0.037	9.12	8.08	4.65	0.1306	10.7	1459.6	#	PUM-VH-3
	4	1000	6600	20	0.0521	9.16	8.01	4.63	0.1385	15.2	2270.2	#	PUM-VH-4
	5	1000	330	28	0.0079	9.16	8.03	4.64	0.0937	2.3	572.9	#	PUM-VH-5
	6	1000	510	28	0.0157	9.16	8.04	4.65	0.1496	4.6	1185.4	#	PUM-VH-6
	7	1000	2700	28	0.0362	9.16	8.02	4.64	0.1503	10.5	2712.1	#	PUM-VH-7
	8	1000	4380	28	0.0508	9.16	8.04	4.65	0.1652	14.8	2755.2	#	PUM-VH-8
	9	1000	330	36	0.0063	9.15	8.08	4.66	0.0744	1.8	533.8	#	PUM-VH-9
	10	1000	840	36	0.0191	9.16	8.03	4.64	0.142	5.6	1211.2	#	PUM-VH-10

	11	1000	3000	36	0.0391	9.16	8.02	4.64	0.154	11.4	2490.3	#	PUM-VH-11
	12	1000	3900	36	0.0588	9.16	7.97	4.61	0.2043	17.2	4086.9	#	PUM-VH-12
#													
	13	900	810	36	0.006	9.16	8.07	4.66	0.0452	1.7	501.7	#	PUM-VH-13
	14	900	2520	36	0.0176	9.16	8.15	4.71	0.0745	5	1040.9	#	PUM-VH-14
	15	900	6600	36	0.0358	9.16	8.1	4.68	0.0942	10.2	2838.3	#	PUM-VH-15
	16	900	9720	36	0.0481	9.15	8.02	4.63	0.1054	14	4360.9	#	PUM-VH-16
	17	900	600	28	0.0057	9.15	8.02	4.63	0.0503	1.7	264.9	#	PUM-VH-17
	18	900	2220	28	0.0155	9.15	8.02	4.63	0.071	4.5	909.7	#	PUM-VH-18
	19	900	6000	28	0.0359	9.15	8.02	4.63	0.1001	10.5	2851.3	#	PUM-VH-19
	20	900	11520	28	0.0499	9.15	8.1	4.67	0.0995	14.3	3797.2	#	PUM-VH-20
	21	900	690	20	0.0072	9.15	8.12	4.68	0.0585	2.1	747.6	#	PUM-VH-21
	22	900	2640	20	0.0184	9.16	8.18	4.72	0.0759	5.3	707.9	#	PUM-VH-22
	23	900	7200	20	0.0342	9.16	8.06	4.66	0.0865	9.8	2279.9	#	PUM-VH-23
	24	900	14880	20	0.0485	9.15	8.11	4.68	0.085	13.9	2554.4	#	PUM-VH-24
#													
	25	1100	110	20	0.0075	9.14	8.07	4.65	0.1537	2.1	529.6	#	PUM-VH-25
	26	1100	300	20	0.0159	9.15	8.1	4.67	0.1964	4.6	492.2	#	PUM-VH-26
	27	1100	780	20	0.0368	9.15	8.08	4.66	0.2826	10.5	1598.4	#	PUM-VH-27
	28	1100	1380	20	0.0512	9.15	8.07	4.66	0.296	14.7	1454.3	#	PUM-VH-28
	29	1100	100	28	0.0075	9.14	8.08	4.66	0.1611	2.1	610.9	#	PUM-VH-29
	30	1100	300	28	0.019	9.15	8.08	4.66	0.2353	5.5	2188.7	#	PUM-VH-30
	31	1100	720	28	0.0369	9.15	8.02	4.63	0.297	10.6	2526.6	#	PUM-VH-31
	32	1100	1140	28	0.0499	9.16	8.1	4.68	0.3159	14.3	3330.4	#	PUM-VH-32
	33	1100	100	36	0.0066	9.15	8.06	4.65	0.1419	1.9	744.7	#	PUM-VH-33
	34	1100	300	36	0.0169	9.16	8.05	4.65	0.2098	4.9	1259.2	#	PUM-VH-34
	35	1100	720	36	0.0369	9.16	8.07	4.66	0.2949	10.6	2776.2	#	PUM-VH-35
	36	1100	1380	36	0.0545	9.15	8.05	4.65	0.3158	15.6	2548.5	#	PUM-VH-36
	39	1000	480	0	0.0155	-	-	-	-	4.5	-	#	Proba 1000_H2/5

```
#     Double side oxidation in hydrogen rich steam atmosphere
#     date: 2006
#     Project: Zr Cladding Oxidation in Hydrogen Rich Atmosphere (COHYRA)
#     Zr1%Nb tube samples
#     Wall thickness = 0.65 mm
#
#     T [C]                   oxidation temperature
#     t [s]                   oxidation time
#     Hs [vol. %]             hydrogen content in the steam
#     dma [g]                 absolute mass gain
#     D [mm]                  outer diameter of the sample
#     L [mm]                  length of the sample
#     F [cm^2]                surface area
#     k [mg/cm^2/s^0.5]       rate constant
#     ECR [%]                 equivalent cladding reacted
#
#
```

# No	T	t	Hs	dma	D	L	F	k	ECR		Sample
1	1000	480	0	0.0098	9.14	8	4.61	0.0969	2.8	#	TEO-1
2	1000	760	0	0.0146	9.14	8	4.61	0.1148	4.2	#	TEO-2
3	1000	2520	0	0.0478	9.14	8	4.61	0.2064	14.1	#	TEO-5
4	1000	810	5	0.0182	9.14	8	4.61	0.1386	5.4	#	VH-04
5	1000	330	5	0.0082	9.14	8	4.61	0.0978	2.4	#	VH-05
6	1000	2700	5	0.0477	9.14	8	4.61	0.199	14.1	#	VH-06
7	1000	1560	5	0.0296	9.14	8	4.61	0.1624	8.7	#	VH-07
8	1000	2700	5	0.0488	9.14	8	4.61	0.2035	14.4	#	VH-11
9	1000	2700	65	0.047	9.14	8	4.61	0.196	13.8	#	VH-12
10	1000	1560	65	0.0278	9.14	8	4.61	0.1525	8.2	#	VH-13
11	1000	810	65	0.0153	9.14	8	4.61	0.1165	4.5	#	VH-14
12	1000	1560	65	0.0302	9.14	8	4.61	0.1657	9	#	VH-18
13	1000	330	65	0.0098	9.14	8	4.61	0.1169	2.9	#	VH-19
14	1000	2700	65	0.042	9.14	8	4.61	0.1752	12.5	#	VH-20
15	900	2520	5	0.0138	9.14	8	4.61	0.0596	4.1	#	VH-01
16	900	7200	5	0.0393	9.14	8	4.61	0.1004	11.6	#	VH-02
17	900	810	5	0.0055	9.14	8	4.61	0.0419	1.6	#	VH-03
18	900	7200	65	0.0254	9.14	8	4.61	0.0649	7.5	#	VH-15
19	900	810	65	0.006	9.14	8	4.61	0.0457	1.8	#	VH-16

20	900	2700	65	0.0147	9.14	8	4.61	0.0613	4.4	#	VH-17
21	1100	300	5	0.0198	9.14	8	4.61	0.2478	5.9	#	VH-08
22	1100	100	5	0.0103	9.14	8	4.61	0.2232	3	#	VH-09
23	1100	720	5	0.0307	9.14	8	4.61	0.248	9	#	VH-10
24	1100	100	65	0.0107	9.14	8	4.61	0.2319	3.2	#	VH-21
25	1100	390	65	0.0241	9.14	8	4.61	0.2645	7.2	#	VH-22
26	1100	720	65	0.0352	9.14	8	4.61	0.2843	10.5	#	VH-23
27	1100	720	65	0.0333	9.14	8	4.61	0.269	9.9	#	VH-24
28	1100	720	65	0.0331	9.14	8	4.61	0.2673	9.9	#	VH-25

Appendix 14: Data of oxidation tests COHYRA

Double side oxidation in hydrogen rich steam atmosphere
date: 2004-2005
Project: Zr Cladding Oxidation in Hydrogen Rich Atmosphere (COHYRA)
Zr1%Nb tube samples
Wall thickness = 0.65 mm
#
T [C] oxidation temperature
t [s] oxidation time
Hs [vol. %] hydrogen content in the steam
dma [g] absolute mass gain
D [mm] outer diameter of the sample
L [mm] length of the sample
F [cm^2] surface area
k [mg/cm^2/s^0.5] rate constant
ECR [%] equivalent cladding reacted
Hc [wppm] hydrogen content of the sample after the oxidation
#
#

#	No	T	t	Hs	dma	D	L	F	k	ECR	Hc		Sample
#													
	1	1000	160	20	0.0016	9.13	2.14	1.49	0.0851	1.8	624.3	#	PUM2-VH-1
	2	1000	390	20	0.0047	9.13	2.14	1.49	0.1601	5.2	1253.4	#	PUM2-VH-2
	3	1000	150	28	0.0015	9.14	2.13	1.48	0.0826	1.7	331.8	#	PUM2-VH-3
	4	1000	360	28	0.0046	9.14	2.14	1.49	0.1629	5.1	1412.3	#	PUM2-VH-4
	5	1000	160	36	0.0016	9.16	2.13	1.49	0.0851	1.8	283.4	#	PUM2-VH-5
	6	1000	360	36	0.0044	9.14	2.15	1.49	0.1553	4.9	1443.7	#	PUM2-VH-6
#													
	7	900	390	36	0.0018	9.12	2.13	1.48	0.0616	2	675.8	#	PUM2-VH-7
	8	900	1980	36	0.0048	9.13	2.14	1.49	0.0726	5.3	1235.6	#	PUM2-VH-8
	9	900	360	28	0.0015	9.14	2.14	1.49	0.0531	1.7	382.6	#	PUM2-VH-9
	10	900	1740	28	0.0044	9.13	2.15	1.49	0.0707	4.9	1009.3	#	PUM2-VH-10
	11	900	510	20	0.002	9.12	2.13	1.48	0.0599	2.2	302.4	#	PUM2-VH-11
	12	900	1920	20	0.0043	9.13	2.15	1.49	0.0658	4.8	696.4	#	PUM2-VH-12

#

13	1100	50	20	0.0018	9.14	2.15	1.49	0.1704	2	159.4	#	PUM2-VH-13
14	1100	180	20	0.0043	9.12	2.13	1.48	0.2166	4.8	979.4	#	PUM2-VH-14
15	1100	55	28	0.0016	9.13	2.14	1.49	0.1451	1.8	306.3	#	PUM2-VH-15
16	1100	200	28	0.005	9.14	2.17	1.5	0.235	5.5	1018.9	#	PUM2-VH-16
17	1100	55	36	0.0018	9.13	2.15	1.49	0.1627	2	298.5	#	PUM2-VH-17
18	1100	190	36	0.0051	9.13	2.14	1.49	0.2489	5.7	1329.1	#	PUM2-VH-18
19	1100	180	36	0.0049	9.16	2.15	1.5	0.244	5.4	1497.4	#	PUM2-VH-19

Appendix 15: Data of oxidation tests COHYRA

One side oxidation in hydrogen rich steam atmosphere
date: 2004-2005
Project: Zr Cladding Oxidation in Hydrogen Rich Atmosphere (COHYRA)
Zr1%Nb tube samples
Geometry: outer diameter = 9.14mm, wall thickness = 0.65mm, length =100mm
Surface area= 28.71cm^2
#
T [C] oxidation temperature
t [s] oxidation time
Hs [vol. %] hydrogen content in the steam
dma [g] absolute mass gain
k [mg/cm^2/s^0.5] rate constant
ECR [%] equivalent cladding reacted
Hc [wppm] hydrogen content of the sample after the oxidation
#
#

#	No	T	t	Hs	dma	k	ECR	Hc		Sample
#										
	1	900	1800	36	0.0648	0.0532	0.7	647	#	P1
	2	900	960	20	0.0663	0.0745	0.7	645.7	#	P2
	3	1000	540	36	0.1226	0.1838	1.2	477.9	#	P3
	4	1000	900	20	0.4995	0.5799	4.8	551.2	#	P4
	5	1100	180	36	0.1544	0.4008	1.5	627.9	#	P5
	6	1100	300	20	0.1245	0.2504	1.2	430.3	#	P6b
	7	1000	900	0	0.0452	0.0525	0.5	_	#	P7

Appendix 16: Data of compression tests COHYRA

AEKI compression tests summary file
date: 2004-2005
Project: Zr Cladding Oxidation in Hydrogen Rich Atmosphere (COHYRA)
Zr1%Nb ring samples
#
ECR [%] equivalent oxidation on the basis of the measured mass gain
Hc [wppm] hydrogen content of the sample after the oxidation
a [mm] width
b [mm] wall thickness
D [mm] outer diameter
F [N] force
dl [mm] deformation
dl/D [%] relative deformation
E [mJ] energy
rducp [%] residual ductility
rducm [mm] residual ductility
Espec [mJ/mm] specific energy at failure

#
#
No ECR Hc a b D F dl dl/D E rducp rducm Espec Sample
#

No	ECR	Hc	a	b	D	F	dl	dl/D	E	rducp	rducm	Espec		Sample
1	1.8	357.9	8.1	0.73	9.15	702.6	2.54	27.76	1497.56	22.62	2.07	184.88	#	PUM-VH-1
2	4.8	675.4	8.11	0.72	9.19	709.4	0.593	6.45	242.18	1.52	0.14	29.86	#	PUM-VH-2
3	10.7	1459.6	8.15	0.75	9.25	193.5	0.177	1.91	16.02	0.17	0.016	1.97	#	PUM-VH-3
4	15.2	2270.2	8.14	0.75	9.26	144.5	0.12	1.3	8.58	0	0	1.05	#	PUM-VH-4
5	2.3	572.9	8.05	0.72	9.16	639.3	1.103	12.04	544.94	7.75	0.71	67.69	#	PUM-VH-5
6	4.6	1185.4	8.11	0.71	9.18	589.8	0.457	4.98	146.95	0.76	0.07	18.12	#	PUM-VH-6
7	10.5	2712.1	8.13	0.75	9.29	188.2	0.137	1.47	12.09	0	0	1.49	#	PUM-VH-7
8	14.8	2755.2	8.17	0.74	9.28	96.5	0.217	2.34	9.65	0	0	1.18	#	PUM-VH-8
9	1.8	533.8	8.09	0.71	9.15	675.1	2.27	24.81	1300.92	19.89	1.82	160.81	#	PUM-VH-9
10	5.6	1211.2	8.04	0.74	9.2	341.9	0.233	2.53	38.76	0	0	4.82	#	PUM-VH-10

11	11.4	2490.3	8.12	0.73	9.23	186	0.17	1.84	11.47	0	0	1.41	#	PUM-VH-11
12	17.2	4086.9	8.14	0.72	9.35	149.9	0.11	1.18	7.7	0	0	0.95	#	PUM-VH-12
13	1.7	501.7	8.04	0.7	9.16	952.8	5.493	59.97	3843.24	51.97	4.76	478.01	#	PUM-VH-13
14	5	1040.9	8.25	0.73	9.29	451.1	0.377	4.06	79.43	0.3	0.028	9.63	#	PUM-VH-14
15	10.2	2838.3	8.23	0.75	9.36	285.2	0.247	2.64	29.58	0	0	3.59	#	PUM-VH-15
16	14	4360.9	8.21	0.74	9.44	175	0.173	1.83	12.34	0	0	1.5	#	PUM-VH-16
17	1.7	264.9	8.06	0.71	9.2	901	5.13	55.76	3411.71	48.04	4.42	423.29	#	PUM-VH-17
18	4.5	909.7	8.09	0.75	9.31	468.8	0.423	4.54	102.93	0.61	0.057	12.72	#	PUM-VH-18
19	10.5	2851.3	8.19	0.76	9.42	256.4	0.207	2.2	23.51	0	0	2.87	#	PUM-VH-19
20	14.3	3797.2	8.29	0.76	9.5	164.3	0.16	1.68	11.01	0	0	1.33	#	PUM-VH-20
21	2.1	747.6	8.16	0.72	9.24	762.8	3.543	38.34	2209.59	32.25	2.98	270.78	#	PUM-VH-21
22	5.3	707.9	8.32	0.73	9.33	496.2	0.417	4.47	108.44	0.43	0.04	13.03	#	PUM-VH-22
23	9.8	2279.9	8.25	0.74	9.38	325.8	0.257	2.74	42.11	0	0	5.1	#	PUM-VH-23
24	13.9	2554.4	8.3	0.74	9.39	196.8	0.177	1.88	16.27	0.11	0.01	1.96	#	PUM-VH-24
25	2.1	529.6	8.08	0.7	9.14	701	0.883	9.66	408.01	4.27	0.39	50.5	#	PUM-VH-25
26	4.6	492.2	8.13	0.74	9.16	725.6	0.743	8.11	312.72	2.51	0.23	38.47	#	PUM-VH-26
27	10.5	1598.4	8.17	0.74	9.28	225.3	0.177	1.91	17.88	0	0	2.19	#	PUM-VH-27
28	14.7	1454.3	8.16	0.74	9.26	195.4	0.167	1.8	14.26	0	0	1.75	#	PUM-VH-28
29	2.1	610.9	8.08	0.7	9.14	788	3.917	42.86	2648.53	35.01	3.2	327.79	#	PUM-VH-29
30	5.5	2188.7	8.06	0.74	9.21	326	0.26	2.82	36.14	0	0	4.48	#	PUM-VH-30
31	10.6	2526.6	8.15	0.75	9.21	281.5	0.233	2.53	22.54	0	0	2.77	#	PUM-VH-31
32	14.3	3330.4	8.17	0.74	9.19	204	0.173	1.88	13.73	0	0	1.68	#	PUM-VH-32
33	1.9	744.7	8.05	0.7	9.15	821.3	4.13	45.14	2807.16	38.25	3.5	348.72	#	PUM-VH-33
34	4.9	1259.2	8.06	0.75	9.22	402.2	0.343	3.72	53.67	0	0	6.66	#	PUM-VH-34
35	10.6	2776.2	8.15	0.74	9.2	249	0.213	2.32	19.25	0	0	2.36	#	PUM-VH-35
36	15.6	2548.5	8.12	0.76	9.23	193.4	0.173	1.87	12.45	0	0	1.53	#	PUM-VH-36
39	4.5	-	8.07	0.79	9.20	673.7	-	-	-	-	-	-	#	Proba 1000_H2/5

```
#              AEKI compression tests summary file
#              date: 2007
#              Project: Zr Cladding Oxidation in Hydrogen Rich Atmosphere (COHYRA)
#              Zr1%Nb ring samples
#
#              ECR [%]          equivalent oxidation on the basis of the measured mass gain
#              Hc [wppm]        hydrogen content of the sample after the oxidation
#              a [mm]           width
#              b [mm]           wall thickness
#              D [mm]           outer diameter
#              F [N]            force
#              dl [mm]          deformation
#              dl/D [%]         relative deformation
#              E [mJ]           energy
#              rducp [%]        residual ductility
#              rducm [mm]       residual ductility
#              Espec [mJ/mm]    specific energy at failure
#
```

No	ECR	Hc	a	b	D	F	dl	dl/D	E	Espec	rducm	rducp		Sample
1	2.8	578	8.03	0.73	9.23	665.9	1.847	20.0	217.5	27.08	1.34	14.5	#	TEO-1
2	4.2	1384	8.02	0.74	9.23	726.9	0.807	8.7	319.7	39.86	0.22	2.3	#	TEO-2
3	14.1	2713	8.18	0.80	9.32	198.6	0.270	2.9	17.9	2.19	0.01	0.1	#	TEO-5
4	4.1	734	8.17	0.74	9.25	594.7	2.880	31.1	1684.1	206.14	-	-	#	VH-01
5	11.6	1970	8.18	0.80	9.38	366.7	0.453	4.8	68.8	8.42	0.01	0.1	#	VH-02
6	1.6	218	8.09	0.71	9.21	682.6	2.837	30.8	1574.8	194.66	2.21	24.0	#	VH-03
7	5.4	1405	8.08	0.72	9.23	626.6	0.717	7.8	220.0	27.23	0.11	1.2	#	VH-04
8	2.4	888	8.08	0.71	9.19	681.9	2.913	31.7	1614.1	199.77	2.26	24.6	#	VH-05
9	14.1	3323	8.17	0.76	9.34	179.0	0.257	2.8	15.6	1.91	0.00	0.0	#	VH-06
10	8.7	1725	8.17	0.74	9.29	392.7	0.430	4.6	69.9	8.55	0.00	0.0	#	VH-07
11	5.9	571	8.05	0.72	9.21	735.3	1.153	12.5	561.3	69.73	0.52	5.6	#	VH-08
12	3.0	912	8.03	0.70	9.17	729.1	2.917	31.8	1767.7	220.13	2.30	25.1	#	VH-09
13	9.0	1215	8.08	0.74	9.22	638.2	0.767	8.3	273.2	33.81	0.20	2.2	#	VH-10
14	14.4	3880	8.18	0.78	9.30	185.6	0.247	2.7	15.4	1.88	0.00	0.0	#	VH-11
15	13.8	6996	8.22	0.78	9.38	123.2	0.197	2.1	8.3	1.01	0.00	0.0	#	VH-12
16	8.2	3840	8.13	0.73	9.29	198.1	0.253	2.7	17.3	2.12	0.00	0.0	#	VH-13
17	4.5	1595	8.13	0.71	9.22	461.4	0.477	5.2	87.0	10.70	0.02	0.2	#	VH-14
18	7.5	2473	8.18	0.74	9.30	308.0	0.450	4.8	44.4	5.43	0.00	0.0	#	VH-15
19	1.8	458	8.09	0.71	9.22	922.0	5.523	59.9	3821.5	472.38	4.77	51.7	#	VH-16
20	4.4	1036	8.13	0.73	9.30	514.7	0.553	5.9	136.5	16.79	0.74	8.0	#	VH-17
21	9.0	4661	8.15	0.75	9.27	214.2	0.280	3.0	19.2	2.36	0.00	0.0	#	VH-18
22	2.9	2623	8.11	0.72	9.21	549.4	0.563	6.1	143.6	17.71	0.08	0.8	#	VH-19
23	12.5	6063	8.16	0.74	9.36	165.9	0.253	2.7	12.4	1.52	0.00	0.0	#	VH-20
24	3.2	1000	8.03	0.71	9.17	776.5	4.677	51.0	3086.4	384.36	3.09	33.7	#	VH-21
25	7.2	2078	8.08	0.72	9.24	331.0	0.340	3.7	42.4	5.24	0.00	0.0	#	VH-22
26	10.5	3335	8.09	0.73	9.25	204.4	0.257	2.8	16.2	2.00	0.00	0.0	#	VH-23
27	9.9	2865	8.12	0.73	9.24	196.6	0.253	2.7	16.3	2.01	0.00	0.0	#	VH-24
28	9.9	3565	8.08	0.73	9.24	194.7	0.267	2.9	15.4	1.90	0.00	0.0	#	VH-25

Appendix 17: Data of tensile tests COHYRA

\# AEKI tensile tests summary file
\# date: 2004-2005
\# Project: Zr Cladding Oxidation in Hydrogen Rich Atmosphere (COHYRA)
\# Zr1%Nb ring samples
\#
\# ECR [%] equivalent oxidation on the basis of the measured mass gain
\# Hc [wppm] hydrogen content of the sample after the oxidation
\# D [mm] outer diameter
\# a [mm] width
\# v [mm] wall thickness
\# So [mm2] area of cross section
\# Fmax [N] maximum load
\# Rm [MPa] tensile strength
\# a1 [mm] width after the fracture
\# v1 [mm] wall thickness after the fracture
\# Su [mm2] area of its smallest cross section at the location of fracture
\# Z [%] reduction
\#
\#

#	No	ECR	Hc	D	a	v	So	Fmax	Rm	a1	v1	Su	Z		Sample
#															
	1	1.8	624.3	9.18	2.12	0.73	3.1	1507.1	486.9	2.01	0.7	2.81	9.09	#	PUM2-VH-1
	2	5.2	1253.4	9.26	2.13	0.73	3.11	648.1	208.4	2.1	0.72	3.02	2.76	#	PUM2-VH-2
	3	1.7	331.8	9.2	2.12	0.71	3.01	1470.5	488.5	1.88	0.63	2.37	21.31	#	PUM2-VH-3
	4	5.1	1412.3	9.23	2.15	0.73	3.14	684.8	218.2	2.08	0.73	3.04	3.26	#	PUM2-VH-4
	5	1.8	283.4	9.25	2.12	0.75	3.18	1456.5	458	1.92	0.68	2.61	17.89	#	PUM2-VH-5
	6	4.9	1443.7	9.22	2.15	0.73	3.14	390.6	124.4	2.15	0.73	3.14	0	#	PUM2-VH-6
	7	2	675.8	9.22	2.13	0.73	3.11	1365.7	439.2	1.6	0.68	2.18	30.03	#	PUM2-VH-7
	8	5.3	1235.6	9.28	2.17	0.75	3.26	562	172.7	2.15	0.73	3.14	3.56	#	PUM2-VH-8
	9	1.7	382.6	9.22	2.13	0.74	3.15	1402.9	445	1.56	0.65	2.03	35.67	#	PUM2-VH-9
	10	4.9	1009.3	9.27	2.17	0.74	3.21	683.8	212.9	2.17	0.74	3.21	0	#	PUM2-VH-10
	11	2.2	302.4	9.22	2.14	0.73	3.12	1372.6	439.3	1.6	0.68	2.18	30.35	#	PUM2-VH-11

12	4.8	696.4	9.26	2.18	0.72	3.14	877.5	279.5	2.16	0.72	3.11	0.92	#	PUM2-VH-12
13	2	159.4	9.19	2.14	0.72	3.08	1461.9	474.4	1.82	0.6	2.18	29.13	#	PUM2-VH-13
14	4.8	979.4	9.2	2.15	0.74	3.18	974.8	306.3	2.13	0.74	3.15	0.93	#	PUM2-VH-14
15	1.8	306.3	9.19	2.22	0.76	3.37	1455.3	431.3	1.88	0.65	2.44	27.57	#	PUM2-VH-15
16	5.5	1018.9	9.29	2.19	0.75	3.29	761.3	231.8	2.19	0.75	3.29	0	#	PUM2-VH-16
17	2	298.5	9.17	2.15	0.78	3.35	1475.8	440	2.01	0.7	2.81	16.1	#	PUM2-VH-17
18	5.7	1329.1	9.19	2.15	0.75	3.23	233.4	72.4	2.15	0.75	3.23	0	#	PUM2-VH-18
19	5.4	1497.4	9.25	2.14	0.74	3.17	417.3	131.8	2.14	0.73	3.12	1.35	#	PUM2-VH-19

Appendix 18: Data of ballooning tests COHYRA

Isothermal ballooning tests at linear pressure increase with Zr1%Nb tube specimens
date: 2004-2005
Project: Zr Cladding Oxidation in Hydrogen Rich Atmosphere (COHYRA)
dp/dt - pressure increase rate [bar/s]
T1 - temperature at burst [C]
p0 - initial pressure [bar]
p1 - pressure at burst [bar] (over pressure)
t - time to burst [s]
Pe0 - initial perimeter [mm]
v0 - initial wall thickness (nominal) [mm]
L0 - initial length [mm]
Pe1 - maximum perimeter after the burst
epsm - maximum deformation [%]
Atmo - atmosphere of the test
Preox - sample name at pre-oxidation tests
#
#
#

# No	p0	p1	t	dp/dt	T1	Pe0	v0	L0	Pe1	epsm		Atmo	Preox	Sample
#														
1	1	11.7	918	0.0127	1001.2	28.57	0.65	100	37	30	#	Ar	P1	Fuv-1
2	1	10.1	1261	0.008	999.3	28.57	0.65	100	35	23	#	Ar	P2	Fuv-2
3	1	10.9	1030	0.0106	1000.4	28.57	0.65	100	35	23	#	Ar	P3	Fuv-3
4	1	20.7	1432	0.0145	1000	28.57	0.65	100	35	23	#	Ar	P4	Fuv-4
5	1	15.6	2096	0.0074	998.9	28.57	0.65	100	35	23	#	Ar	P5	Fuv-5
6	1	12.2	1302	0.0094	1003.6	28.57	0.65	100	35	23	#	Ar	P6b	Fuv-6
7	1	9.9	662	0.015	1003.4	28.57	0.65	100	33	16	#	Ar	P7	Fuv-15
8	1	8.6	958	0.009	1001.6	28.57	0.65	100	40	40	#	Ar	_	Fuv-8

Appendix 19: Data of ballooning tests COHYRA

\# Isothermal ballooning tests at linear pressure increase with Zr1%Nb tube specimens
\# date: 2005-2006
\# Project: Zr Cladding Oxidation in Hydrogen Rich Atmosphere (COHYRA)
\# dp/dt - pressure increase rate [bar/s]
\# T1 - temperature at burst [C]
\# p0 - initial pressure [bar]
\# p1 - pressure at burst [bar] (over pressure)
\# t - time to burst [s]
\# Pe0 - initial perimeter [mm]
\# v0 - initial wall thickness (nominal) [mm]
\# L0 - initial length [mm]
\# Pe1 - maximum perimeter after the burst
\# epsm - maximum deformation [%]
\# Atmo - atmosphere of the test
\# Ppar - partial pressure of hydrogen [bar]
\# Hcal - calculated hydrogen content before the test [wppm]
\# Hc - measured hydrogen content of the sample after the test [wppm]
\#
\#

#	No	p0	p1	t	dp/dt	T1	Pe0	v0	L0	Pe1	epsm	Hcal	Hc		Atmo	Ppar	Sample
#																	
	1	1	9.70	657	0.0148	1003.4	28.57	0.65	100	37.40	30.9	2250.0	692.7	#	Ar-H	0.1000	FUV-16H6
	2	1	11.40	1086	0.0105	991.2	28.57	0.65	100	46.30	62.1	1350.0	1943.6	#	Ar-H	0.0358	FUV-19
	3	1	10.20	990	0.0103	1000.2	28.57	0.65	100	40.35	41.2	515.0	710.0	#	Ar-H	0.0052	FUV-20
	4	1	11.82	1153	0.0103	901.2	28.57	0.65	100	41.65	45.8	715.0	985.3	#	Ar-H	0.0050	FUV-21
	5	1	14.87	1463	0.0102	900.2	28.57	0.65	100	38.00	33.0	715.0	468.2	#	Ar-H	0.0050	FUV-22
	6	1	12.89	1232	0.0105	900.2	28.57	0.65	100	35.4	23.9	1100.0	1871.6	#	Ar-H	0.0119	FUV-23
	7	1	8.60	958	0.0090	1001.6	28.57	0.65	100	40	40.0	_	_	#	Ar	_	Fuv-8

Appendix 20: SEI images of the ballooning and compressed ring samples

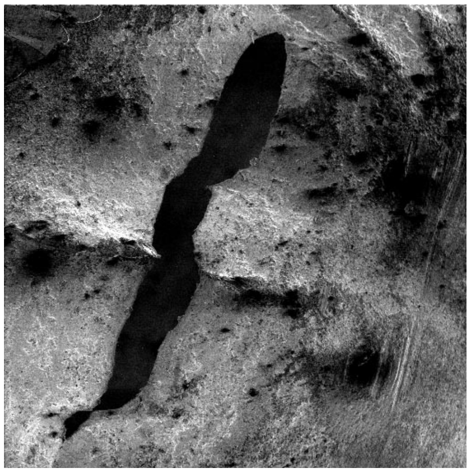
Fuv-1

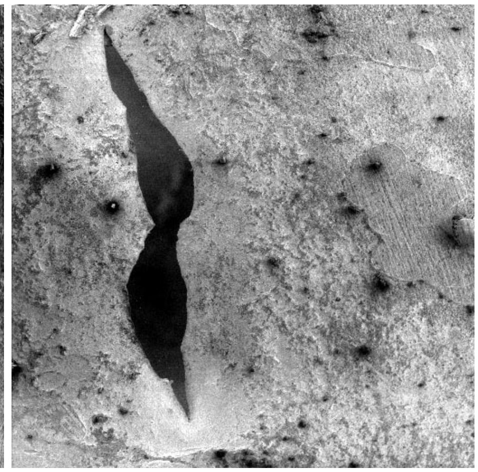
Fuv-3

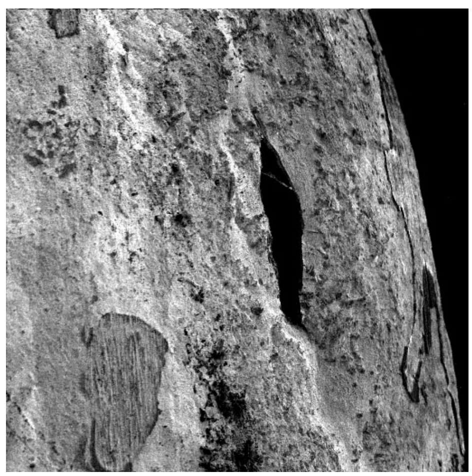
Fuv-5
4 mm x 4 mm

Figure 39. Typical SEI images of burst samples 1, 3, and 5, respectively

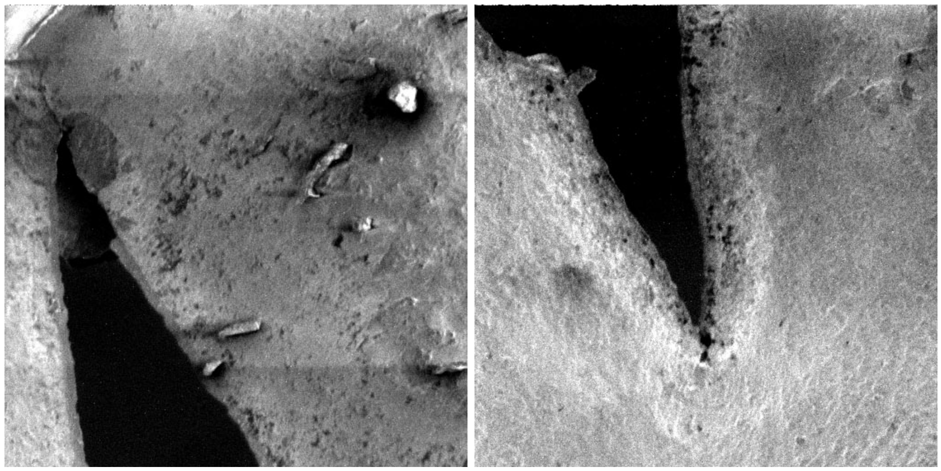

610 μm x 610 μm

Figure 40. Both ends of the opening up for sample Fuv-3

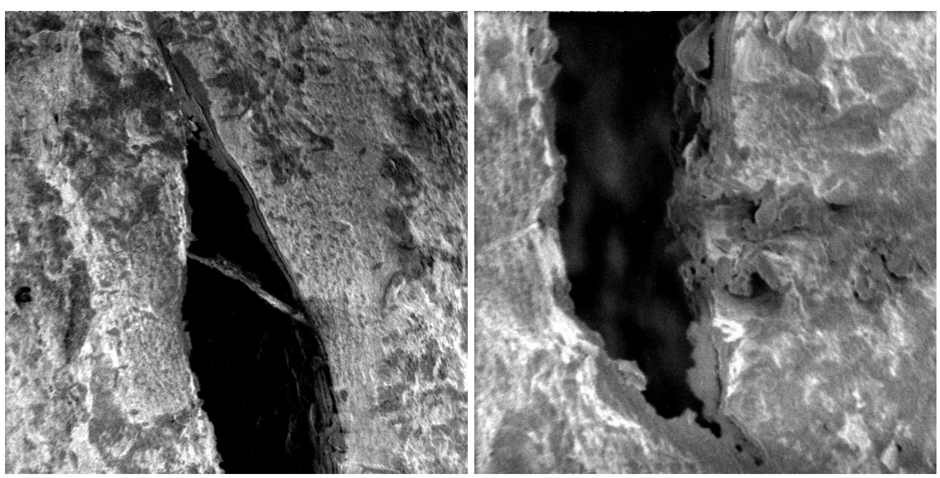

1.2 mm x 1.2 mm 610 μm x 610 μm

Figure 41. Both ends of the opening up for sample Fuv-5

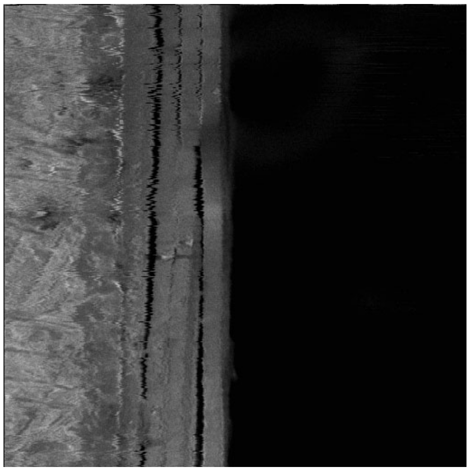

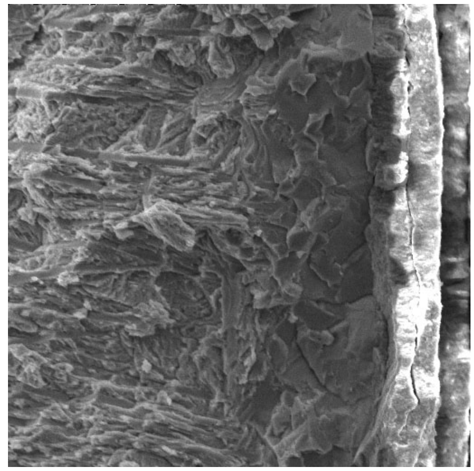

250 μm x 250 μm sample area

Sample PUM-VH-16 Sample PUM-VH-20

Figure 42. SEI images for compressed ring samples pre-oxidised at 900 ^{o}C for various times

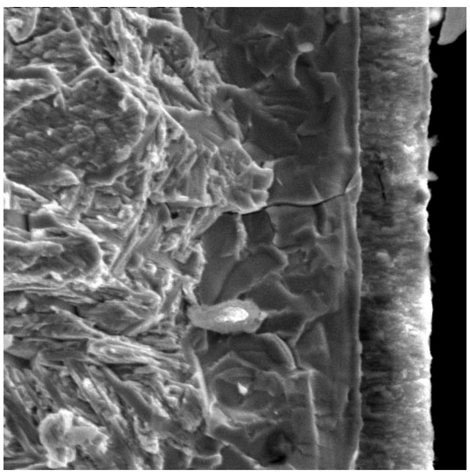

beta Zr alpha Zr oxide

120 μm x 120 μm sample area

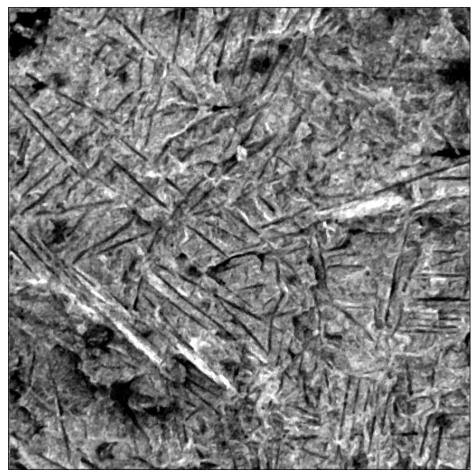

beta Zr, Widmanstätten lines

250 μm x 250 μm sample area

Figure 43. Typical SEI images for sample PUM-VH-16 showing the various structural elements

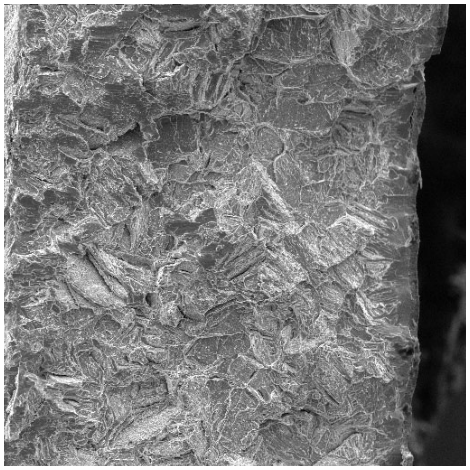

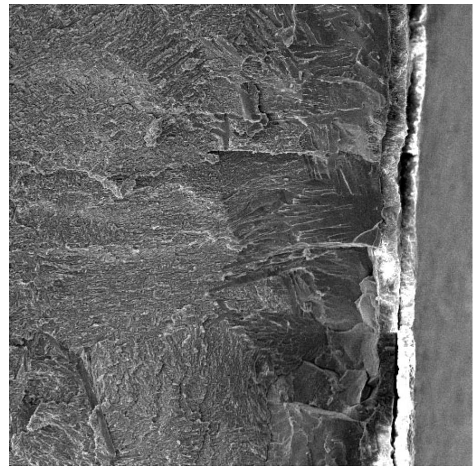

0.8 mm x 0.8 mm sample area

Sample PUM-VH-1
330s oxid. time, 357.9 ppm H_2

Sample PUM-VH-4
6600 s oxid. time, 2270.2 ppm H_2

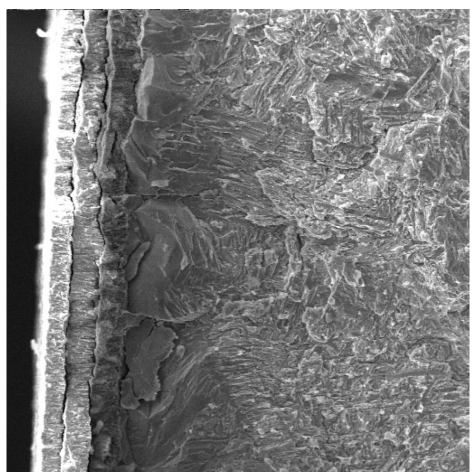

250 μm x 250 μm
Sample PUM-VH-12
3900s oxid. time, 4086.9 ppm H_2

Figure 44. SEI images of compressed ring samples pre-oxidised for various times at 1000 ^{o}C temperature

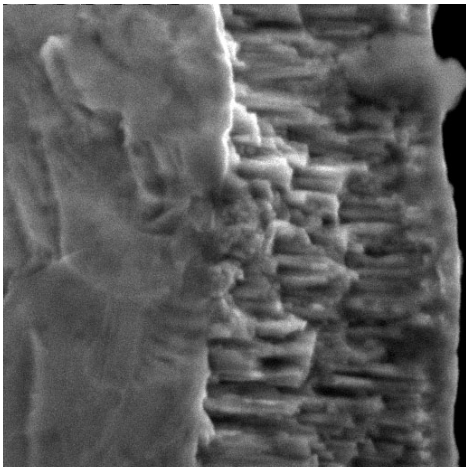

65 μm x 65 μm

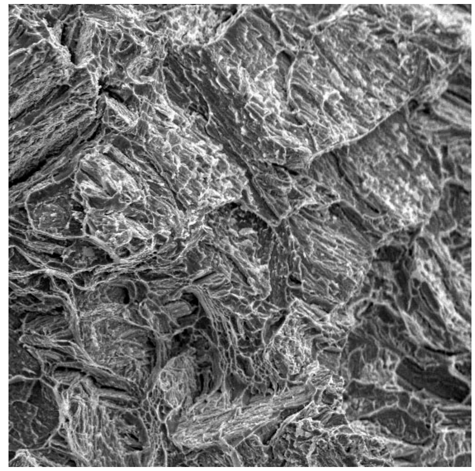

500 μm x 500 μm

Sample PUM-VH-1

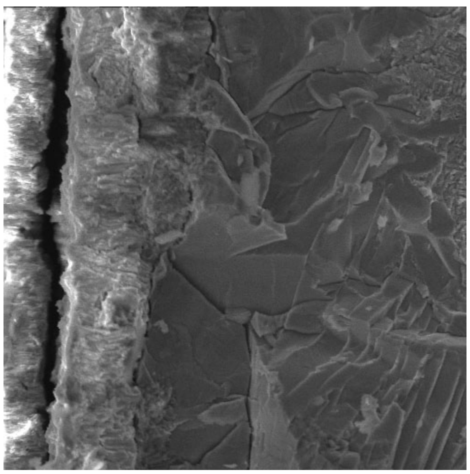

125 μm x 125 μm

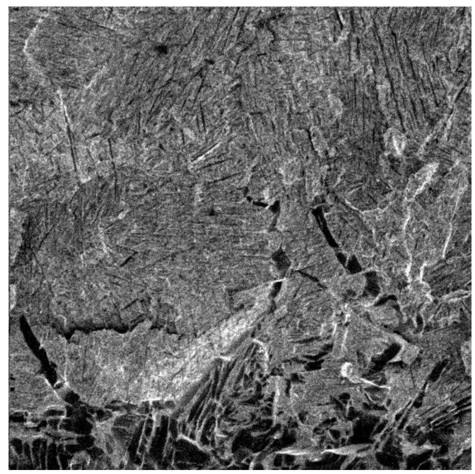

250 μm x 250 μm

Sample PUM-VH-4

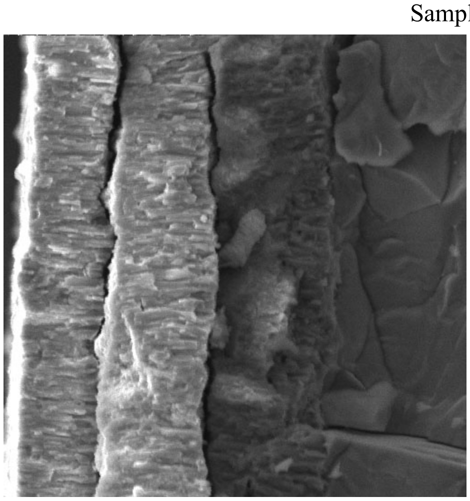

65 μm x 65 μm

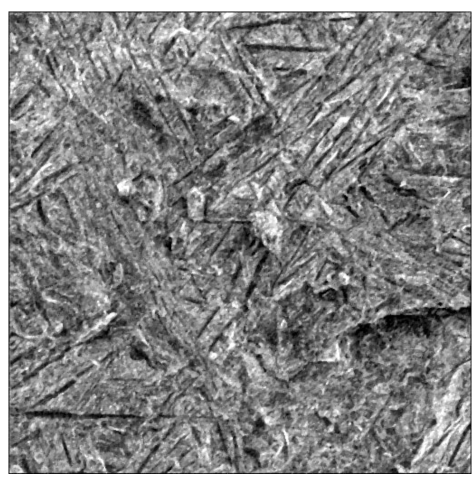

250 μm x 250 μm

Sample PUM –VH-12

Figure 45. Typical SEI images for samples pre-oxidised at 1000 ^{o}C

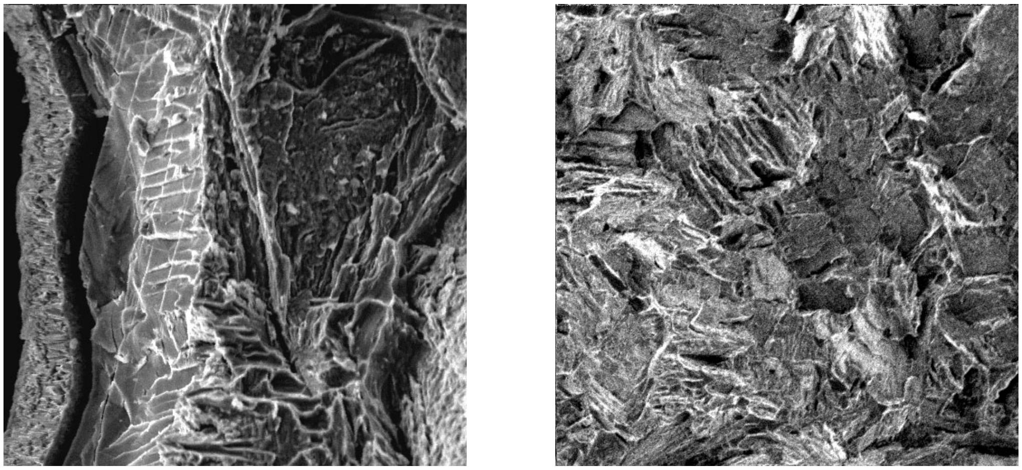

250 μm x 250 μm

Sample PUM-VH- 26

Oxid. time 300 s, 492.2 ppm H_2

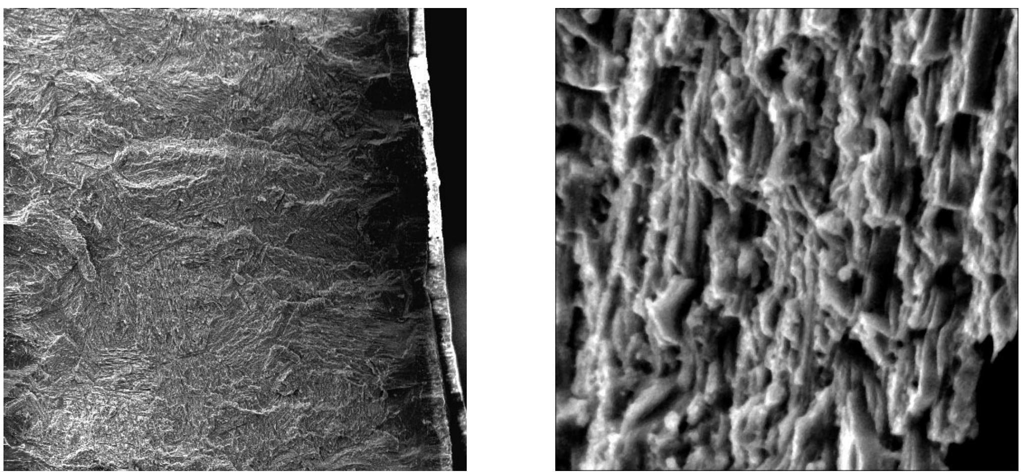

800 μm x 800 μm 65 μm x 65 μm

Sample PUM-VH-32

Oxid. time: 1140 s, 3330.4 ppm H_2

Figure 46. SEI images for compressed ring samples pre-oxidised at 1100 ^oC